DOCTORAL THESIS

In Vitro Methods for Predicting Leukoderma Caused by Quasi-Drug Cosmetics and Development of a New Skin Brightening Agent

Tokyo University of Technology

Graduate School of Bionics, Computer and Media Science

Bionics Program

Lihao Gu

March 2022

Contents

Abbreviation

ADH	Alcohol dehydrogenase
ARB	Hydroquinone-β-D-glucoside, Arbutin
BCA	Bicinchoninic Acid
B16	Mouse skin melanoma cell line
cAMP	Cyclic adenosine 3',5'-monophosphate
DHICA	5,6-dihydroxyindole-2-carboxylic acid
DMEM	Ulbecco's modified Eagle's medium
DMSO	2-mercaptoethanol, dimethyl sulfoxide
DNA	Deoxyribonucleic acid
EDTA	Ethylenediaminetetraacetic acid
GAPDH	Glyceraldehyde-3-phosphate dehydrogenase gene
H_2DCFDA	2',7'-dichlorodihydrofluorescein diacetate
HPF	Hydroxyphenyl fluorescein
HPLC	High-performance liquid chromatography
HWP	Hydrolyzed wheat protein
IC_{50}	Half maximal inhibitory concentration
LC–MS	Liquid chromatography–mass spectrometry
L-DOPA	3-(3,4-dihydroxyphenyl)-L-alanine
MC1R	Melanocortin 1 receptor
MITF	Microphthalmia-associated transcription factor
ML	2,2′-dihydroxy-5,5′-dipropyl-biphenyl, Magnolignan
4MS	4-methoxysalicylic acid
α-MSH	α-melanocyte-stimulating hormone
4MSK	4-methoxysalicylic acid potassium salt

NAD	Nicotinamide adenine dinucleotide
NAD^+	Nicotinamide adenine dinucleotide oxidized state
NADH	Nicotinamide adenine dinucleotide reduced state
NADPH	Nicotinamide adenine dinucleotide phosphate
NOXs	NADPH oxidase enzymes
PBS	Phosphate-buffered saline
Pmel17	Premelanosome protein 17
qPCR	Quantitative polymerase chain reaction
RD	4-(p-hydroxyphenyl)-2-butanol, Rhododendrol
RK	4-(p-hydroxyphenyl)-2-butanone, Raspberry ketone
RNA	Ribonucleic acid
RNS	Reactive nitrogen species
ROS	Reactive oxygen species
SBG	*Scutellaria baicalensis* Georgi
SD	Standard deviation
SDS	Sodium dodecyl sulfate
TEM	Transmission Electron Microscopy
Tris	2-amino-2-hydroxymethyl-1,3-propanediol
Triton X-100	2-[4-(2,4,4-trimethylpentan-2-yl)phenoxy]ethanol
TYR	Tyrosinase
TYRP1	Tyrosinase-related protein 1
TYRP2	Tyrosinase-related protein 2
UV	Ultraviolet
4BR	4-n-butylresorcinol
4PB	4-phenyl-2-butanol

Chapter I Introduction

1.1. Skin

1.1.1. Skin Composition

Skin, which is the entrance to the organism and the largest organ in the body, plays a major role in protecting the organism from external stimuli and maintaining homeostasis. The skin that exerts the barrier function of the organism is roughly divided into three layers: the epidermis, the dermis, and the subcutaneous tissue. The epidermis is made up of stratum corneum (which made of stratum corneum cells and intercellular lipids, responsible for water retention function), stratum granulosum (which made of keratinocytes and lamellar granules), stratum spinosum (the thickest layer in the epidermis, which made of Langerhans cells, one of immune cells) and stratum basale (the layer where keratinocyte cell division which called keratinization is most active). The dermis, which occupies most of the skin and can be said to be the "body" of the skin, is mainly made of blood vessels, lymph vessels, sweat glands, and hair follicle cells. It also contains a large amount of ingredients that are greatly related to the sagging and firmness of the skin such as collagen (which is a protein that controls strength), collagen fiber (which is mainly made of collagen), elastin (which is a protein that controls scalability and elasticity), elastic fibers (which is mainly made of elastin) and fibroblasts (which produces these biomaterials). The subcutaneous tissue, which plays the role of supporting the epidermis and dermis, is mainly made of subcutaneous fat and has the functions of cushioning external impact and maintaining body temperature [1–6].

1.1.2. Melanin and Melanocytes

Melanin, which is the main cause of darkening of the skin, is a major pigment present in the surface structure of vertebrates. It is formed as intracellular granules in

melanocytes, which are pigment cells present in the stratum basale, and transferred to epithelial cells via melanocytes and forms the major pigments in the hair and epidermis [7,8]. In the case of Asians such as Japanese and Chinese, a large amount of about 1,000 to 1,500 melanocytes is present per 1 mm^2 of human skin, especially present in high density on the face [1]. There are two types of melanin present in human epidermis and hair, one is eumelanin that is close to dark brown or black, and the other is pheomelanin that is close to brown or yellow [7]. Since melanin present in the skin and hair is a complex of these two types of melanin formed in different proportions, Asians and Africans with a high proportion of eumelanin in the epidermis appear darker than Europeans, and the hair color of Asians and Africans is close to black, while the hair color of Europeans is close to brown [1,7]. From the viewpoint of "brightening", bad melanocytes and melanin have many biological functions, one of which is that melanocytes activated by stimuli such as sunlight secrete a lot of melanin and play a role as a sunscreen to protect the skin from UV rays. It is known that damage caused by ultraviolet rays on the skin acts directly on DNA to cause damage, and also causes various effects such as erythema and pigmentation by generating reactive oxygen species via other light-absorbing substances [9]. For this reason, the darker the skin, the lower the risk of developing skin cancer due to UV rays [10–12]. However, some studies have shown that the Melanogenesis can lead to the generation of ROS, thereby inducing cytotoxicity and oxidative DNA damage [13–15].

1.1.3. Melanin Biosynthesis and Tyrosinase

Tyrosinase (EC.1.14.18.1), known as polyphenol oxidase, is a type of oxidoreductase that is widely distributed in nature and is a catalyst for the hydroxylation of monophenols and the two consecutive oxidations of diphenols. The o-quinone produced by this oxidation spontaneously polymerizes to synthesize various biopigments and biopolymers such as melanin [13]. Tyrosinase , which is one of the three pigment-specific enzymes present in melanosomes, acts as a catalyst for the two oxidations of tyrosine → dopa → dopaquinone, and is therefore also called a key enzyme in the

melanosomes formation pathway [16]. In addition to tyrosinase and the above-mentioned external stimuli, α-MSH (which raises intracellular cAMP and promotes melanin synthesis) and its receptor MC1R, TYRP1 (which involved in eumelanin production), TYRP2 (which involved in DHICA melanin production), MITF (transcription factor of TYR , TYRP1, TYRP2) , and Pmel17 (which involved in the membrane structure of melanosomes), are also significantly involved in melanin biosynthesis (Figure 1-1) [8,17].

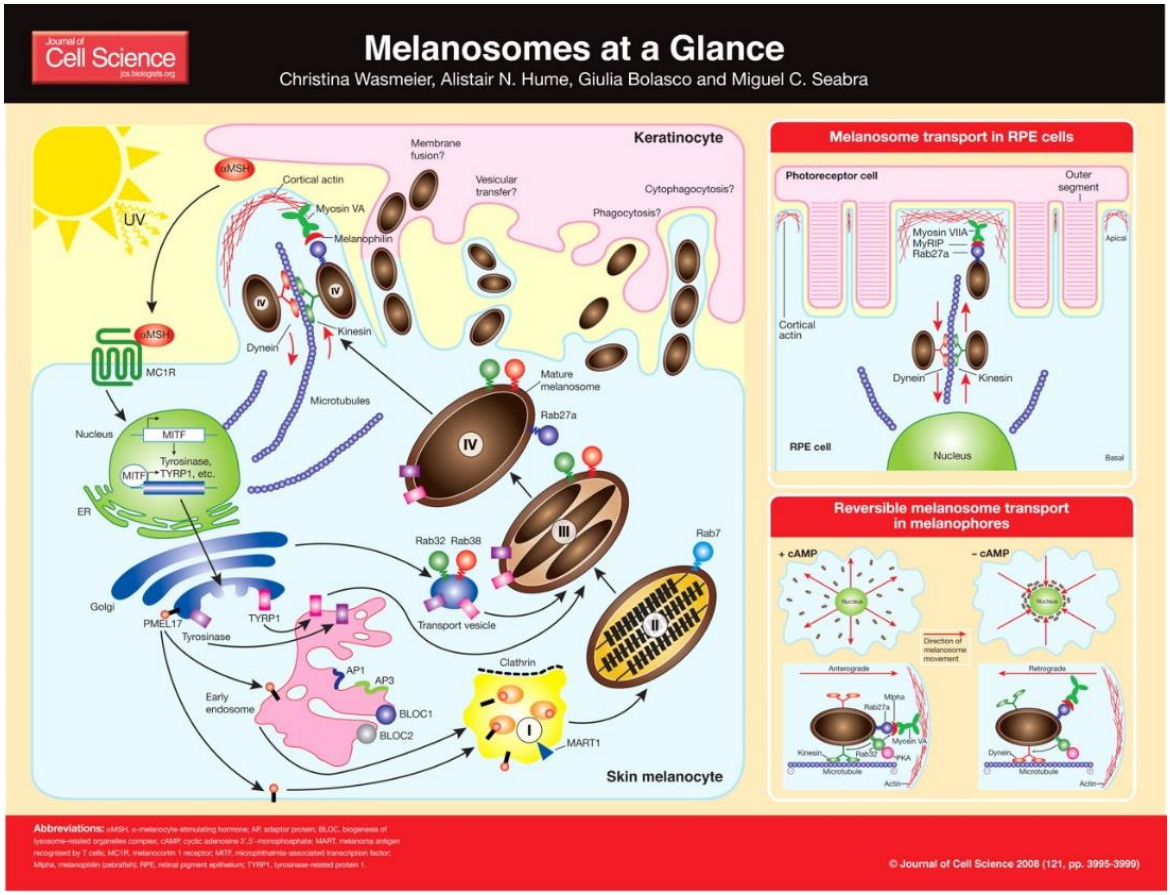

Figure 1-1. Melanosomes at a Glance [17].
From: Christina Wasmeier et al. J Cell Sci 2008, 121: 3995-3999.

1.1.4. Alcohol Dehydrogenase (ADH) and Nicotinamide Adenine Dinucleotide (NAD)

Alcohol dehydrogenase (ADH; EC 1.1.1.1 or EC 1.1.1.2), which is widely present in organisms, is an important enzyme involved in the biotransformation of alcohol. As the first enzyme discovered by humans, ADH is widely present in yeast, bacteria, plants,

and mammals. The isoenzymes of ADH are divided into several classes on the basis of differences in substrate specificity, sensitivity to inhibitors, localization, electrophoretic migration and immunological properties [18]. Today, 7 species of ADH have been found in mammals. Among them, 3 and 5 species of ADH have been found in mice [19,20] and human [19–25]. Western blot analysis and immunohistochemistry revealed that 3 species of ADH (I-III) have been located in human skin [26], and these ADHs mainly exist in the epidermis [26]. In addition to the skin, ADH is also present in the liver, lungs with a large amount, and in the kidneys and intestines with a small amount [22].

Nicotinamide Adenine Dinucleotide (NAD), a kind of coenzyme, exists in two forms: the oxidized form NAD^+, and the reduced form NADH. NAD^+ is the coenzyme of ADH and other dehydrogenase. ADH has a main function to oxidize alcohols to aldehydes or ketones, and can be subdivided into ADH (NAD^+) (EC 1.1.1.1) and ADH ($NADP^+$) (EC 1.1.1.2). The former can convert primary alcohols to aldehydes (Equation 1-1), or secondary alcohols into ketones (Equation 1-2), and the latter can convert primary alcohols to aldehydes (Equation 1-3).

$$\text{Primary alcohol} + NAD^+ = \text{Aldehyde} + NADH + H^+ \quad (1\text{-}1)$$

$$\text{Secondary alcohol} + NAD^+ = \text{Ketone} + NADH + H^+ \quad (1\text{-}2)$$

$$\text{Primary alcohol} + NADP^+ = \text{Aldehyde} + NADPH + H^+ \quad (1\text{-}3)$$

In metabolism, NAD participates in redox reactions, carrying electrons from one reaction to another. The balance between NAD^+ and NADH is called the NAD^+/NADH ratio. This ratio affects the redox state of a cell, so it is an important indicator reflecting the health of a cell. In the cell and in mammals, the ratio is higher than 1 [27,28]; the ratio is thus favorable for oxidative reactions. The decline of NAD^+ is often related to aging and disease [28–32]. Supplementing the precursor of NAD^+ through drugs, cosmetics, nutritional health products, etc. can often play a role in improving health

[33].

1.2. ROS and Oxidative Stress

1.2.1. ROS, RNS and Oxidative Stress

ROS (reactive oxygen species) is a by-product of aerobic metabolism includes superoxide anion (O^{2-}), hydrogen peroxide (H_2O_2), singlet oxygen ($^1O_2$), hydroxyl radical (·OH) and peroxyl radicals (ROO·). RNS (reactive nitrogen species) includes Nitric oxide radicals (NO·) and Nitrogen dioxide radical ($NO_2\cdot$). Both of ROS and RNS have inherent chemical properties and can react to different biological targets [34,35]. Oxidative stress was defined as the disturbance of balance between the occurrence of ROS/RNS and the organism's capacity to counteract their action by the antioxidative protection systems [36] or "a disruption in redox signaling and control" [37], and stems from over-generated ROS/RNS or decline in antioxidant capacity [38].

1.2.2. ROS Generation in Skin

The ROS generated in the skin is divided into endogenous ROS generated during normal metabolism and exogenous ROS caused by external factors. Endogenous ROS are generated through various enzymatic reactions. Superoxide anion ($O2^-$) produced by NADPH oxidation (via NOXs) or by mitochondria is converted to H_2O_2 by intracellular superoxide dismutases [35,39,40], and H_2O_2 can be converted to H_2O by oxidation of cysteine residues or by peroxiredoxins, glutathione peroxidase, and catalase [35,41]. Exogenous ROS are generated by external factors such as UV in sunlight or physical/chemical environment [42,43]. Different wavelengths of UV can induce the over-generation of ROS through different pathways [12,44], and substances directly applied to the skin, such as drugs or cosmetics, can also cause over-generation of ROS [43,45,46].

1.2.3. The Hazards of ROS

As one of the ubiquitous threats, the production of ROS can cause various damages and cause diseases to living organism. Over-generated ROS can disrupt the natural antioxidant defense system of cells and resulting in damage to major classes of biological macromolecules such as nucleic acids, proteins, carbohydrates and lipids, and also induce apoptosis [34]. The oxidative decay caused by ROS is irreversible, and after causing lipid peroxidation, DNA damage, protein denaturation, and enzyme inactivation, ROS can cause negative effects on the living organism, including impaired physiological functions, promote the occurrence of diseases and reduce life span [47]. The damage caused by free radicals in oxidative stress has been proven to cause more than 100 diseases including neurodegenerative conditions, cardiovascular diseases and cancers in living organisms [48–50]. As a biological organ that is always exposed to the external environment, ROS-induced skin diseases are often more than other ROS-induced diseases. For example, ROS produced excessively due to UV radiation will be recorded by mitochondria [51,52] and cause various diseases such as inflammation, photosensitive skin diseases and even skin cancer [12,44], and short-wavelength UVB is more likely to induce skin cancer [53]. In addition to UV radiation , topical drugs and cosmetics that people use in daily life can also cause over-generation of ROS in skin [46]. For example, titanium dioxide nanoparticles in sunscreen cosmetics can induce ROS-mediated genotoxicity in human epidermal cells [45]. At present, the main methods to deal with oxidative stress and oxidative damage in the skin are to use antioxidants, and promote the skin to produce more antioxidants like alpha-tocopherol and ascorbic acid [38,49].

1.3. Brightening

1.3.1. History of Brightening

In recent years, an increasing number of people are interested in cosmetology, regardless of age or gender. "Brightening care" cosmetics containing "brightening ingredients" that make the skin color look white are especially popular.

In Asian countries such as Japan and China, “white” is an important skin condition that expresses the attractiveness of women and has been emphasized by women since ancient times In Japan, there is a saying of "色の白いは七難隠す" (White skin hide seven faults), and in China, there is a saying of "一白遮百丑" (White skin hide hundred faults) with a similar expression. Although these two sayings have slightly different wording, surprisingly they express the same idea that "if the skin color is white, it looks beautiful even if there are defects." It is no coincidence that people in both countries break the language barrier and use similar expressions. The reason why "white" is preferred by people is that they do not engage in common labor such as cultivation and harvesting fruits that requires exposure to sunlight. There are several theories as to why white is preferred by people, including psychophysical theories such as white makes them look more noble and cleaner than ordinary people because the latter were stained with mud or dead insects due to poor sanitary conditions and had to work in the sun at that time, or religious reasons such as white being a sacred color. Although which of them is the main cause is still debated, it is certain that both countries have recommended fair skin since ancient times [1,54].

In recent years, as protests against racial discrimination have spread around the world, triggered by the incident in which a black man was killed by white police holding him by the neck (George Floyd incident), many cosmetic companies in Japan have gradually stopped using cosmetic advertising terms such as "whitening" due to concerns about racial discrimination, and a new term "brightening" has appeared instead. Today, the entire cosmetics industry, starting with major companies such as Kao and Shiseido,

has taken into consideration the diversity of skin tones and has taken measures such as product recalls and renewals, sealing off conventional terms such as "whitening" [55,56].

1.3.2. The Current Status of Brightening Cosmetics

Since most Asians have skin types II- III [57], they tend to darken due to sun exposure in daily life, so brightening cosmetics are very popular in the Japanese market. Brightening cosmetics used in Japan are generally classified according to their mechanism of action, such as promotion of melanin discharge, inhibition of melanocyte activation, melanin breakdown, inhibition of melanosomes, and inhibition of melanin synthesis. Cosmetic ingredients that are representative in various aspects are Adenosine monophosphate 2Na (promotion of melanin discharge), Tranexamic acid (inhibition of melanocyte activation), Ascorbic acid derivatives (melanin breakdown), Niacinamide (inhibition of melanosomes), and Arbutin (inhibition of melanin synthesis). Among them, inhibition of melanin synthesis is the most common mechanism for brightening cosmetics and it can be subdivided into inhibition of Tyrosinase and/or TYRP1 generation, reduction of Tyrosinase and/or TYRP1 activity, and promotion of Tyrosinase and/or TYRP1 decomposition.

Table 1-1. The Fitzpatrick skin types [57]

Skin type	Sunburn and tanning
I	Burns easily, never tans
II	Burns easily, tans minimally with difficulty
III	Burns moderately, tans moderately and uniformly
IV	Burns minimally, tans moderately and easily
V	Rarely burns, tans profusely
VI	Never burns, tans profusely

1.3.3. Quasi-drug Cosmetics

In Japan, cosmetics refer to the use of rubbing, spraying or similar methods on the human body to clean the body, beautify, enhance attractiveness, change the appearance or maintain the health of the skin and hair, and has a mild effect on human body. Quasi-drug cosmetic is a classification unique to Japan, which is between cosmetics and drugs. The difference between Quasi-drug cosmetics and cosmetics lies in functional ingredients and cosmetic materials. quasi-drug cosmetics have functional ingredients, and their effects can be declared as "effects brought about by functional ingredients". However, cosmetics only contain additives, so there are only 56 effects that cosmetics can claim [58]. Compared with cosmetics, quasi-drug cosmetics are more effective with relatively insecure [58,59]. In the field of brightening, approximately 20 active ingredients, including hydroquinone-β-D-glucoside (arbutin, ARB), 4-n-butylresorcinol (4BR), 3-*O*-ethyl ascorbic acid, tranexamic acid, and 4-methoxysalicylic acid potassium salt (4MSK), have been approved and used in quasi-drug cosmetics in Japan [60–64]. Product descriptions changed from “preventing dark spots and freckles due to sun damage” to “preventing dark spots and freckles by suppressing melanin production” or “preventing dark spots and freckles by suppressing melanin accumulation” in 2001. For products that inhibit tyrosinase, ingredients such as ARB, rhododendrol, magnolignan (2,2′-dihydroxy-5,5′-dipropyl-biphenyl; ML), 4BR, and 4MSK have been used as active ingredients of quasi-drug cosmetics in Japan.

1.4. Rhododendrol, Raspberry Ketone and leukoderma

1.4.1. Rhododendrol and Raspberry Ketone

Because bright skin looks cleaner, and for other reasons, East Asian countries have tried since ancient times to make skin brighter. Presently, brightening cosmetics are becoming more popular. Epidermal depigmentation products, such as brightening cosmetics, are typed according to their modes of action, which include promoting the excretion of melanin, melanin breakdown, inhibiting melanocyte activity, and inhibiting melanin synthesis by inhibiting tyrosinase, a key enzyme in the melanosome formation pathway [64].

Among products that inhibit tyrosinase, cosmetics containing 2% 4-(p-hydroxyphenyl)-2-butanol, or rhododendrol (RD) which was developed in 2008 as an active ingredient of approved by the Ministry of Health, Labour and Welfare under the Pharmaceutical Affairs Law in Japan, were voluntarily recalled after leukoderma was confirmed in consumers who had used them.

RD is a chiral compound containing (R)-RD and (S)-RD enantiomers, which can found in many plants like *Rhododendron*, *Acer nikoense*, *Betula platyphylla* et al. [65–69], and can also obtained via catalytic hydrogen reduction of 4-(p-hydroxyphenyl)-2-butanone, or raspberry ketone (RK), using a Raney nickel catalyst (Fig 1-2).

Fig 1-2. The reduction of RK to RD.

Raspberry ketone (RK) is not only found in raspberries, but also in fruits such as peaches and apples, and in bark from yew, maple, and pine [70]. As a safe compound, RK is often used in daily necessities such as food, health products, cosmetics, etc., so it has high economic value. Since it is very expensive to extract raspberry ketones from

raspberries or fruits containing RK, RK is often synthesized by chemical or biosynthesized methods. Some of them successfully developed a method to biosynthetic RK from RD by ADH [71–74].

The physicochemical properties of RD and RK are given in Table 1-2.

Table 1-2. Physiochemical properties of rhododendrol (RD) and raspberry ketone (RK).

	Rhododendrol	**Raspberry ketone**
Chemical Formula	$C_{10}H_{14}O_2$	$C_{10}H_{12}O_2$
Molecular Weight	166.22 g·mol^{-1}	164.20 g·mol^{-1}
Melting Point	68–71 °C	81–85 °C
Boiling Point	315.4±17.0 °C at 760 mmHg	292.2 ± 15.0 °C at 760 mmHg

1.4.2. Chemical Leukoderma

Skin depigmentation, such as vitiligo, has been reported to be due to impaired melanin production induced by damage to melanocytes at the exposed site. Among them, chemical leukoderma is defined as acquired hypopigmentation caused by repeated exposure to specific drugs that damage melanocytes [75–78]. The case of chemical leukoderma was first reported in 1939 [79]. Since then, multiple chemicals such as phenol, catechol, sulfhydryl, mercury, arsenic, cinnamon aldehyde, p-phenylenediamine, benzyl alcohol, azelaic acid, and corticosteroids, have been reported to cause leukoderma [75–78].

The structure of the chemicals that cause leukoderma is characteristic, especially 4-substituted phenols with a hydroxylated 1-position of the benzene ring, and alkyl groups with non-polar side chains at the 4-position. Many studies on leukoderma caused by 4-position-substituted phenols have been previously reported. After comparing the melanocyte cytotoxicity of 30 phenolic compounds, Smit et al. found that the 4-substituted phenols-induced melanocytes cytotoxicity is related to tyrosinase [80]. Further, in terms of the melanocytes cytotoxicity of 4-substituted phenols with different

chemical structures, the increase in chain length of 4-substituted phenols did not enhance the melanocytes cytotoxicity, 4-substituted phenols, but branching of the side chain seemed to increase the melanocytes cytotoxicity [80]. And in terms of the mechanism of 4-substituted phenols-induced melanocytes cytotoxicity, the melanocytes cytotoxicity is generally due to a) the 4-substituted phenols as a substrate to react with tyrosinase to produce quinone derivatives, and cause oxidative damage to melanocytes. However, the mechanism of b) self-oxidation or other ways to produce quinone derivatives, and cause oxidative damage to melanocytes; and c) induce apoptosis through other ways, have also been reported [81–86].

Here, some 4-substituted phenols and other compounds that have been reported to induce leukoderma and their mechanisms of inducing melanocytes cytotoxicity are listed, as shown in Table 1-3.

Table 1-3. 4-substituted phenols and other compounds causing chemical leukoderma and their mechanisms of inducing melanocytes cytotoxicity. The mechanism has been abbreviated as, a) reacts with tyrosinase as a substrate to produce quinone derivatives, and cause oxidative damage to melanocytes; b) self-oxidation or other ways to produce quinone derivatives, and cause oxidative damage to melanocytes; c) induce apoptosis through other ways, and -) there is not enough research to verify the mechanism. In addition to the reported mechanism, other potential mechanisms of inducing melanocyte cytotoxicity may also exist.

Phenol/catechol derivatives	Mechanisms	Reference
Hydroquinone	b	[81,82,87]
p-benzyloxyphenol	a	[81,83,84,88]
p-methoxyphenol	a	[81,89,90]
p-ethoxyphenol	-	[85]
p-phenoxyphenol	a	[81]
p-octylphenol	-	[91]
p-hexyloxyphenol	a	[81]
p-benzylphenol	a	[81,89]
p-methylphenol	a	[81]
p-phenylphenol	a	[81]
p-*tert*-amylphenol	a	[81,90]
p-*tert*-butylphenol	c	[84,86,92]
p-nonylphenol	-	[91]

1.4.3. Rhododendrol-induced leukoderma

Brightening cosmetics containing 2% RD were recalled in 4 July 2013 for causing leukoderma after being sold in the Japanese market for five years. It was reported that depigmentation appeared on the user's neck, hands, and face after repeated application of cosmetics containing RD. Among them, the symptoms in 79% of patients showed signs of disappearance or improvement within 6 months after stopping the use of these products [93]. The investigation report by Kanebo Cosmetics on 10 Nov 2021 states that the confirmed cases of leukoderma is 19,607 as of 31 Oct 2021[94]. This means that about 2.4% of consumers have experienced symptoms of leukoderma [95]. Among them, 11,923 patients have recovered even if some still suffer from the disease even after 7 years [94,95].

RD-induced leukoderma refers to the symptoms of leukoderma after using cosmetics containing RD. The symptoms shown by RD-induced leukoderma patients are i) leukoderma appeared only on the site where cosmetics application, and the symptoms were gradually disappeared after stopping the application, even if without treatment; ii) leukoderma appeared only on the site where cosmetics application, and the symptoms were not disappeared after stopping the application, but were improved after treatment; iii) in addition to the site where cosmetics application, leukoderma sometimes expanding to other non-application sites [93]. These diversity of clinical features shows that RD-induced leukoderma may have multiple mechanisms.

After that, the mechanism of RD-induced leukoderma began to draw attention. In order to clarify it, researchers from cosmetic companies, institutions and universities have conducted many studies. Tanemura et al. suggest that basal hypo-pigmentation, melanin incontinence, and remaining melanocytes appeared in the skin lesions of patients with RD-induced leukoderma [96]. It means that RD-induced leukoderma may be caused by melanocyte damage. In a 2014 study [97], Sasaki et al. suggest that the cell viability of human melanocyte strains and mouse B16 melanoma cells was inhibited by RD, and the tyrosinase activity is essential for RD-induced melanocyte cytotoxicity. Kasamatsu et al. also confirmed this [98], and Goto et al. suggest that UVB

exposure increased the tyrosinase activity in melanocytes [99]. And After that, Sasaki et al. found that tyrosinase is able to oxidize RD [100,101]. In a higher concentration of tyrosinase, RD is easily oxidized to RD-quinone and metabolized into catechol such as RD-catechol, RD-cyclic catechol, RD-hydroxy catechol, and finally oxidized to quinone such as RD-cyclic quinone and RD-hydroxy-*p*-quinone [100–102], and UVB exposure increased the content of them via tyrosinase activity in melanocytes [99]. The scheme for the oxidation of RD by tyrosinase is shown in Figure 1-2.

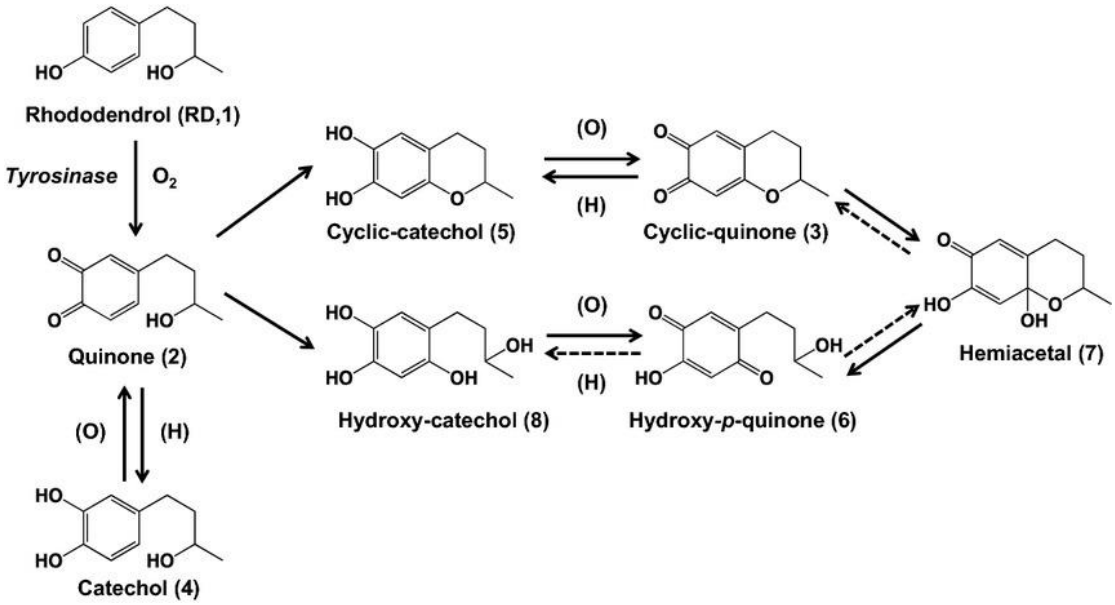

Figure 1-2. The scheme for the oxidation of RD by tyrosinase [100].
From: Ito, S. et al. *Pigment Cell & Melanoma Research* 2014, 27: 1149–1153,

Furthermore, some studies suggest that RD-induced melanocyte cytotoxicity seems to be related to endoplasmic reticulum stress and apoptosis [103–105], and UVB exposure may increase the RD-induced melanocyte cytotoxicity via the inducing endoplasmic reticulum stress [99]. Other studies have confirmed that ROS are generated during RD-oxidation by tyrosinase [106–110], and these ROS may induce the cytotoxicity through oxidative DNA damage [108]. The production of ROS may be related to the bind of RD metabolites (such as RD-quinone) with glutathione and cysteine (two essential cellular antioxidants) [101,102,111]. As shown in Figure 1-3, Inoue S. et al. summarized the mechanism underlying melanocyte-specific cytotoxicity induction by RD into a flow chart [112].

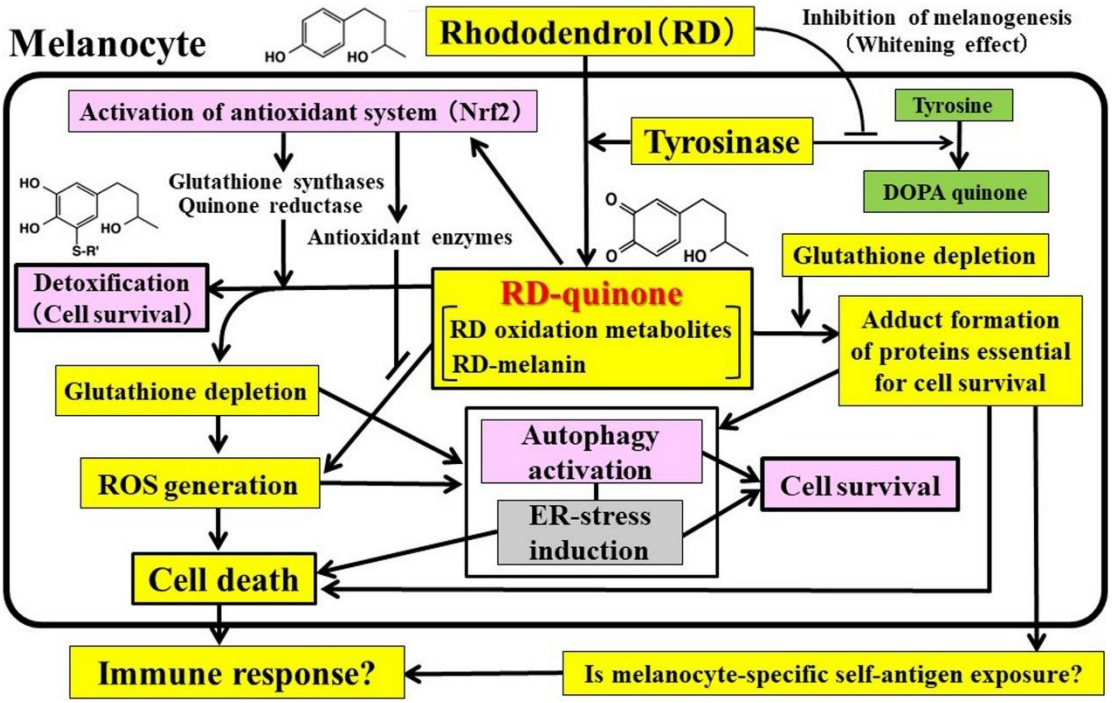

Figure 1-3. Mechanism underlying melanocyte-specific cytotoxicity induction by rhododendrol [112].

From: Inoue S. et al. *The Journal of Dermatology* 2021, 48: 969–978.

Further, Abe et al. developed a mouse model of RD-induced leukoderma using hairless mice, and this study suggests that after applying RD to the backs of mice 3 times a day, 85.7% of the mice suffered from leukoderma [113]. In addition, this study also suggests that the metabolites of 30% RD solution in mouse model include RD-quinone and RD-catechol, and induced the endoplasmic reticulum stress [113], and confirms the results of previous *in vitro* studies.

In addition to melanocytes, the immune system [114–116] and other cells like keratinocytes, resident memory T cells, innate lymphocytes, mast cells, and Langerhans cells may also be related to RD-induced leukoderma [112]. The reported mechanism of RD-induced leukoderma is shown in Table 1-4.

Table 1-4. The reported mechanism of RD-induced leukoderma.

The reported mechanism of RD-induced leukoderma	References
RD induces the cytotoxicity of melanocytes, and the RD-induced melanocytes cytotoxicity depends on tyrosinase.	[97,98]
In a higher concentration of tyrosinase, RD will be metabolized into RD quinone and other oxidized products such as RD catechol.	[100–102]
RD-induced melanocyte cytotoxicity seems to be related to endoplasmic reticulum stress and apoptosis.	[99,103–105]
ROS are generated during RD-oxidation by tyrosinase and may induce the cytotoxicity through oxidative DNA damage.	[106–110]
The production of ROS may be related to the bind of RD metabolites with glutathione and cysteine.	[101,102,111]
UVB exposure may increase the RD-induced melanocyte cytotoxicity via the inducing endoplasmic reticulum stress.	[99]

1.4.4. Raspberry Ketone-induced Leukoderma

As the raw material for the production of RD, RK has been reported to induce leukoderma 1988 study [117,118]. Three workers engaged in the production of RK were reported to have leukoderma, and two of them were not completely cured. One of them itchy after a few months with edema and erythema, followed by leukoderma on his hands and pigmentation on the back of his hands and around the leukoderma. He was treated and the leukoderma was alleviated to some extent, but it was not completely cured. Then another one itchy a few months later, developing edema and erythema, followed by pigmentation and vitiligo on his fingers and right wrist. Although the vitiligo on the face, neck and chest was mostly healed, some on the wrist remained [117]. It was reported that the cytotoxicity of RK is enhanced by the presence of tyrosinase, suggesting that leukoderma caused by RK is not due to the inhibition of melanin biosynthesis but the formation of toxic substances from RK by tyrosinase and

the resulting destruction of melanocyte [118]. Further, RK has also been reported to cause depigmentation in C57 black mice [119].

In addition, some recent studies suggests that RK-induced leukoderma is similar in mechanism to RD-induced leukoderma. For example, the RK-induced melanocyte cytotoxicity is similar to that of RD and appear to be mediated by apoptosis [104] and ROS generation [108,110,120]. The mechanism of ROS generation seems to be the same as that of RD, which is caused by the bind of metabolites (quinone compounds) with the thiol proteins [120]. Further, 3,4-dihydroxybenzalacetone, the oxidation product of RK, is also oxidized to dimeric and trimeric compounds by tyrosinase [121], and all of them can cause the generation of ROS, the depletion of cellular thiols, and reaction with cellular macromolecules [120,121]. This means that compounds exhibiting multiple redox reactions may have more complicated leukoderma induction mechanisms than simple quinone compounds.

1.5. Purpose of this study

Many Japanese cosmetics companies continue to develop new brightening actives and cosmetics to meet the growing demand for brightening. However, in the development process of new materials, R&D engineers often face a dilemma, whether to give priority to efficacy or safety? In the field of brightening cosmetics, the emergence of many materials explains this problem well. For example, ascorbic acid 2-O-α-glucoside and ascorbyl tetrahexyldecanoate are both derivatives of ascorbic acid. The former has better stability and safety with weak effects, while the latter has better effects with irritating and may cause allergies.

It is precisely because of the lack of attention to safety that causes the leukoderma incidents due to quasi-drug cosmetics containing RD. In addition to quasi-drug cosmetics containing RD, soap containing hydrolyzed wheat protein (HWP) has also experienced safety issues. In the fall of 2009, some consumers developed symptoms of wheat allergy after using soap containing HWP and the number of patients expanded to 1,147 in August 2012 [58,122].These cases suggests that the existing quasi-drugs and cosmetics safety evaluation system has loopholes, and Japanese consumers tend to treat quasi-drugs as cosmetics rather than drugs, so they pay more attention to its safety than effects. If cosmetics or quasi-drugs cosmetics have problems in terms of safety, in addition to consumer suffering, cosmetics companies will also lose a lot of manpower and material resources in terms of product recalls and compensation.

Based on this, this paper focuses on the following three problems:

(1) Whether the mechanism of RD-induced leukoderma has been clearly explained;

(2) What are the issues of the existing quasi-drug cosmetics evaluation system?

(3) It is possible to design a new set of evaluation methods for quasi-drug cosmetics based on the principle of RD-induced leukoderma.

In previous studies, Ito et al. found that RD is easily oxidized to oxides such as RD-quinone by tyrosinase, and the underlying mechanism of RD-induced leukoderma pathogenesis appears to be the catalysis of melanocyte tyrosinase to generate o-quinone from phenolic compounds, resulting in oxidative stress and cytotoxicity [96–111]. In

addition, Sugibayashi et al. have attempted to employ *in vitro* skin permeation experiments to study situations in which consumers apply cosmetics daily [123–125], but they have not analyzed the metabolites from the perspective of safety. Some of them have attempted to explain the penetration of RD on the skin through an infinite-volume test design, a scientifically incorrect method. Therefore, although previous studies have made a detailed explanation of the melanocyte metabolites of RD and the mechanism of RD-induced melanocyte cytotoxicity, the study on the skin metabolites of RD is still scarce.

Ito et al. designed a screening method to phenolic skin whitening tyrosinase inhibitors from leukoderma-inducing phenols by detecting the production rate of the corresponding quinone [126]. However, this method does not take into account the actual penetration of the substance into the skin.

Based on the above assumption and previous studies, this paper attempted to (a) further clarify the mechanism of leukoderma caused by 4-substituted phenols such as RD, (b) develop a new *in vitro* evaluation method to replace the existing one, and (c) find a new brightening material based on this method.

Chapter II

In Vitro Methods for Predicting Chemical Leukoderma Caused by Quasi-Drug Cosmetics

2.1. Introduction

As of 4 July 2013, quasi-drug cosmetics containing RD, which was an active ingredient approved by the Ministry of Health, Labour and Welfare under the Pharmaceutical Affairs Law in Japan were voluntarily recalled after leukoderma was confirmed in people who had used them. RD is a reduced form of raspberry ketone (RK), a 4-substituted phenol (*para*-phenol) that has been previously reported to cause leukoderma [117] and depigmentation in C57 black mice [119]. This information should have provided a warning signal; nevertheless, RD was approved as a quasi-drug cosmetics ingredient. The problem appeared to stem from the *in vitro* method used. Therefore, specific toxicity to melanocytes could not be evaluated.

The mechanism underlying the pathogenesis of leukoderma appears to be the toxicity of 4-substituted phenols to melanocytes. For example, occupational leukoderma caused by 4-tert-butylphenol, 4-octylphenol, and other 4-substituted phenols which has been reported to have occurred in resin, rubber, paint, and surfactant manufacturing plants since 1960 [91,92,127–131]. These phenols are detrimental to tyrosinase and its function in melanosomes or melanin-containing organelles. If the damaging effects are minimized, leukoderma could be reversed. However, in case of roughness, 4-substituted phenol levels may become elevated in the skin or become more toxic. Thus, over the long term, destruction of melanocytes could occur and the leukoderma may become permanent [91,92,128–130,132,133].

The purpose of this chapter was to develop an *in vitro* evaluation method for predicting the occurrence of leukoderma caused by the active ingredient in skin depigmentation quasi-drug cosmetics. Specifically, the method was designed to predict

the risk of leukoderma development and was based on mechanisms underlying melanocyte-specific toxicity, common to phenolic compounds that reportedly cause leukoderma. The risks of chemical leukoderma were predicted based on toxicity mechanisms, toxic concentrations, and percutaneous absorption rates. Since many skincare quasi-drug cosmetics are formulated with active ingredients for epidermal depigmentation and are intended to be used daily without limitations on usage or frequency, it is crucial that they do not cause leukoderma. The evaluation scheme developed in this chapter is proposed to be used as another appraisal tool to confirm that a skin depigmentation product poses little or no risk of causing leukoderma.

2.2. Materials and Methods

2.2.1. Materials

Rhododendrol (RD) was purchased from Wako Pure Chemical Industries, Ltd. (Osaka, Japan); Arbutin (ARB), 4-phenyl-2-butanol (4PB), and 4-n-butylresorcinol (4BR) were purchased from Tokyo Chemical Industry Co., Ltd. (Tokyo, Japan); Raspberry ketone (RK) and 4-methoxysalicylic acid (4MS) were purchased from Sigma-Aldrich Corp. (St. Louis, MO, USA); Magnolignan (ML) was purchased from Funakoshi Co., Ltd. (Tokyo, Japan). 4-methoxysalicylic acid potassium salt (4MSK) was used as the potassium salt of 4MS. Other reagents used were analytical grade and obtained from Wako Pure Chemical Industries, Ltd.

Melanocyte-specific toxicity of RD and RK, common to phenolic compounds that are known to cause leukoderma, were used as positive controls.

2.2.2. Measurements of Skin Concentrations of Test Ingredients

The octanol-water partition coefficients (*Ko*/*w*) of the test ingredients were measured [134] and skin permeability coefficients determined using Potts & Guy's skin permeation coefficient prediction equation (Equation (2-1)) [131]. The *in vitro* skin permeation rate was determined in frozen samples of excised skin of hairless mouse (Laboskin®, Hos:HR-1, male, 7 weeks of age, Hoshino Laboratory Animals, Inc., Ibaraki, Japan) in a diffusion cell using Fick's first law of diffusion (Equation (2-2)) [135] applied to a skin area of 1.5 cm^2 and then the rate was divided by wet skin weight to obtain the concentration in the skin. National guidelines were followed for the care and use of laboratory animals.

Potts & Guy's skin permeation coefficient prediction equation:

$$\text{Log } P \ (P \text{ in cm/s}) = -6.3 + 0.71 \times \log Ko/w - 0.0061 \times \text{MW} \quad (2\text{-}1)$$

Fick's first law of diffusion: $dQ/dt = PCv$ (2-2)

where abbreviations are as follows: MW, molecular weight; *Q*, amount permeated in skin (mg/cm^2); *t*, time of exposure; *Cv*, exposure concentration (mg/cm^3).

The octanol-water partition coefficient indicating the degree of lipid solubility (or water solubility) is generally proportional to the permeability coefficient [136,137]. Thus, the percutaneous absorption rate of 4MSK differs depending on the pH because the octanol-water partition coefficient (*Ko*/*w*) changes according to pH [138]. For 4MSK, pKa = 3.31 (25 °C), and according to the Henderson–Hasselbalch equation (Equation (2-3)), the pH of 4MSK can vary with the ratio of non-ionized molecules that are able to be absorbed percutaneously and ionized molecules that cannot. The aqueous phase was adjusted to pH 6.2 when the octanol-water partition coefficient was determined.

$$C_{union} + C_{ion} = C_{union} (1 + 10^{pH\text{-}pKa})$$

(2-3)

Where abbreviations are as follows: C_{union}, concentration (unionized); C_{ion}, concentration (ionized).

2.2.3. Measurements of Skin Permeation Rate

A lotion containing the test substance was formulated (contained in 100 g of lotion: glycerin, 4 g; 1,3-butanediol, 6 g; PEG-60 hydrogenated castor oil, 0.2 g; phenoxyethanol, 0.35 g; test ingredient, potassium hydroxide to adjust the pH to 6.2, with the remainder deionized water). In 100 g of lotion, the test ingredient was RD (2 g), ML (0.5 g), ARB (7 g), 4BR (0.3 g), or 4MSK (3 g).

The dorsal skin from hairless mice was mounted in a Franz diffusion cell (with 37 °C constant temperature circulating water), and 15 µL of lotion containing the test ingredient was applied to the skin (1.5 cm^2). The receptor chamber was stirred with a magnetic stirrer, and 100 µL of sample was taken every 20 min for up to 2 h. Samples were stored at −30 °C in the receptor chamber for later measurements of test ingredient concentration by HPLC. The conditions were as follows: CAPCELL PAK C18 (4.6 mmφ × 250 mm), column at 40 °C, flow rate (1.0 mL/min), and injection volume (10

μL). The detection wavelengths and mobile phase were 281 nm and acetonitrile:0.1% acetic acid (20:80) for RD, 290 nm and methanol:0.1% acetic acid (85:15) for ML, 285 nm and methanol:0.1% acetic acid (10:90) for ARB, 280 nm and methanol:0.1% acetic acid for 4BR (60:40), and 294 nm and methanol:0.1% acetic acid (85:15) for 4MS.

A 1-g skin sample was immersed overnight in chloroform: methanol (2:1) to remove the lipid fraction and then placed in a freeze dryer to remove the water, after which the skin dry weight was determined. The skin dry weight subtracted from the wet weight was defined as the solid fraction, and the rest was defined as the fraction in which the test ingredient was dissolved.

2.2.4. Measuring Cytotoxic Concentrations of Test Ingredients

The cloning of B16 melanoma cells (Cell Resource Center for Biomedical Research, Institute of Development, Aging and Cancer, Tohoku University, Sendai, Japan) was performed and cells with high tyrosinase activity and low tyrosinase activities were acquired. In 24-well plates (Thermo Fisher Scientific Inc., Waltham, MA, USA), 7×10^4 B16 melanoma cells with either high or low tyrosinase activity were incubated for 1 d with 500 μL of 10% bovine serum in Dulbecco's modified Eagle medium (DMEM, Thermo Fisher Scientific Inc.). The test ingredients with 10% bovine serum in DMEM were then added to the wells and incubated for 3 days. After replacing the culture medium, 50-μL samples were placed in a Cell Counting Kit-8 (Dojindo laboratories, Kumamoto, Japan), and 2 h later, the number of viable cells was determined by measuring 450 nm absorbance using a microplate reader (Multi-Detection Microplate POWERSAN HT, BioTek Instruments Inc., Winooski, VT, USA). The concentrations of RD, ML, ARB, 4BR, and 4MSK were based on previously determined percutaneous absorption amounts. The concentration of RK was the same as that of RD. In the 3-day exposure to the cells, final concentrations of the test ingredients in the wells were 600, 300, 150, 75, and 37.5 μmol/L (RD and RK); 40, 20, 10, 5, and 2.5 μmol/L (ML); 370, 185, 92.5, 46.25, and 23.125 μmol/L (ARB); 1940, 970, 485, 242, and 121 μmol/L (4MSK); 40, 20, 10, 5, and 2.5 μmol/L (4BR). In the 3-

hour-exposure to the cells, final concentrations of the test ingredients in the wells were 1200 μmol/L, 600 μmol/L, 300 μmol/L, 150 μmol/L, and 75 μmol/L (RD and RK), 40 μmol/L, 20 μmol/L, 10 μmol/L, 5 μmol/L, and 2.5 μmol/L (ML), 800 μmol/L, 400 μmol/L, 200 μmol/L, 100 μmol/L, and 50 μmol/L (ARB), 200 μmol/L, 100 μmol/L, 50 μmol/L, 25 μmol/L, and 12.5 μmol/L (4MSK), and 40 μmol/L, 20 μmol/L, 10 μmol/L, 5 μmol/L, and 2.5 μmol/L (4BR).

2.2.5. Measurements of Cytotoxicity of Test Ingredients in the Presence of Tyrosinase

In 24-well plates, 1×10^5 B16 melanoma cells were incubated for 1 d with 500 μL of 10% bovine serum in DMEM. 500 μL of 2% of bovine serum in DMEM with either test ingredient alone, or test ingredient with tyrosinase (mushroom 10 U/mL; Sigma-Aldrich) was then added and the cells incubated for 3 h. After replacing the culture medium, 50-μL samples were placed in a Cell Counting Kit-8, and 2 h later the number of viable cells was determined at 450 nm absorbance with the microplate reader.

2.2.6. Observations of Cell Morphology by Transmission Electron Microscopy (TEM)

The cultured cells were placed in 1.5% paraformaldehyde and 0.5% PBS at 4 °C for 1 h. After fixation, the cells were stirred and washed in PBS, centrifuged, post-fixed in 1% osmium tetroxide, centrifuged again, and the harvested cells were solidified in agar, which was finely sectioned. The samples were then dehydrated though an alcohol series and embedded in Epon epoxy resin to prepare blocks for electron microscopy. Toluidine-blue-stained specimens were prepared. After examination, one block per sample was selected for thin sectioning. The sections were examined using TEM (JEM-140, JEOL Ltd., Tokyo, Japan), and images were taken.

2.2.7. Measurements of Hydroxyl Radical (·OH)

In 96-well plates (Thermo Fisher Scientific Inc.), PBS (78 μL), test ingredient (2 μL), tyrosinase (mushroom 10 U/mL) (10 μL), and hydroxyphenyl fluorescein (HPF; 5 μmol/L, 10μL, Goryo Chemical, Inc., Sapporo, Japan) were added to each plate and allowed to react at 37 °C. The fluorescence intensity of the compound generated by ·OH (excitation, 485 nm; fluorescence, 528 nm) was measured every 30 min from 0 to 240 min using the fluorescent plate reader (POWERSAN HT). The test ingredient solution was initially 20 mmol/L (10 mmol/L for ML) and was serially diluted with an aqueous solution of 50% DMSO or DMSO 10 times.

2.2.8. Measurements of Hydrogen Peroxide (H_2O_2)

In 96-well plates, PBS (78 μL), test ingredient (2 μL), tyrosinase (mushroom 10 U/mL; 10 μL), and H_2DCFDA (5 mmol/L; 10 μL, Thermo Fisher Scientific Inc.) were added to each plate and allowed to react at 37 °C. The fluorescence intensity of the compound generated by H_2O_2 (excitation, 485 nm; fluorescence, 528 nm) was measured every 30 min from 0 to 240 min using the fluorescent plate reader (POWERSAN HT). The test ingredient solution was initially 20 mmol/L (10 mmol/L for ML) and was serially diluted in an aqueous solution of 50% DMSO or DMSO 10 times.

2.2.9. Effects of Chelator on ·OH Generation

In 96-well plates, test ingredient (2 μL), tyrosinase (mushroom 10 U/mL; 10 μL), and HPF (5 μmol/L; 10 μL) were added to each plate and with PBS alone, or PBS with Chelator (Kojic acid or D-Penicillamine) allowed to react at 37 °C. The fluorescence intensity of the compound generated by ·OH (excitation, 485 nm; fluorescence, 528 nm) was measured after 30 min using the fluorescent plate reader (POWERSAN HT). The test ingredient solution was initially 20 mmol/L.

2.2.10. Determination of ·OH Generation Sites

In four-chambered slides (AGC Techno Glass Co., Ltd., Shizuoka, Japan), 3 × 10^4 B16 melanoma cells were incubated for 1 d with 400 μL of 10% bovine serum in DMEM. RD (125 μmol/L) with 10% bovine serum in DMEM was then added, and the cells were incubated for 3 d. HPF (2μL of 5 μmol/L solution) was added and allowed to react at 37 °C for 1 h. After fixation in 4% paraformaldehyde in PBS, the cells were washed with PBS and blocked with 10% goat serum. The samples were stained with TYRP-1 using TMH-2 antibodies [139] and the Alexa Fluor 488-labeled anti-rat IgG goat polyclonal antibody. The samples were then observed using a fluorescence microscope, and images were taken.

2.2.11. Statistical Analytical Method

Tests for statistical significance between control and test ingredient were performed with unpaired two-tailed *t*-test in Excel, and $p < 0.05$ was considered significant.

2.3. Results

2.3.1. Octanol-Water Partition Coefficients (log *Ko/w*)

The determination of concentrations of test ingredients in the octanol and water phases indicate the octanol-water partition coefficients (log *Ko*/*w*) of RD, ML, ARB, 4BR, 4MS, 4MSK, and RK, as shown in Table 2-1. The skin permeability of chemical substances *in vivo* correlates well with their hydrophobicity and molecular weight. Therefore, log *Ko*/*w* and molecular weight are used to predict or determine the skin permeability of chemical substances. In addition, the accumulation of chemical substances *in vivo* is also related to hydrophobicity. Although the degree depends on the mode of action, toxicity becomes stronger as the hydrophobicity of the chemical substance increases. Furthermore, Potts & Guy's skin permeability coefficient prediction equation predicts that the skin permeability coefficient increases with an increase in log *Ko*/*w* and decreases with an increase in molecular weight [131]. Log *Ko*/*w* for the tested substances was ML > 4BR > 4MS > RK > RD > ARB > 4MSK, in increasing order. Molecular weight for the tested substances was RK < RD = 4BR < 4MS < 4MSK < ML < ARB, in ascending order.

Table 2-1. Octanol-water partition coefficients (log *Ko*/*w*).

Active Ingredient	RD	ML	ARB	4BR	4MS	4MSK	RK
log *Ko*/*w*	1.303	3.951	−1.485	2.399	1.744	−1.577	1.406
Ko/*w*	20.083	8927.841	0.033	250.336	55.416	0.026	25.495

ARB, arbutin; RD, rhododendrol; ML, magnolignan; 4BR, 4-n-butylresorcinol; 4MS, 4-methoxysalicylic acid; 4MSK, 4-methoxysalicylic acid potassium salt; RK, raspberry ketone.

2.3.2. Measurements of Skin Concentrations of Test Ingredients

Skin concentrations of test ingredients were determined from skin permeability coefficients calculated using the Potts & Guy's skin permeation coefficient prediction equation and Fick's first law of diffusion applied to a skin area of 1.5 cm^2 and divided by the skin wet weight (Table 2-2). As a reference, 7% ARB in lotion resulted in a skin

concentration of 0.008 mg/g, and 2% RD, 0.5% ML, and 0.3% 4BR in lotion resulted in concentrations of 0.335, 0.735, and 0.151 mg/g, respectively, all higher than the ARB reference. At pH 6.2, the concentration of the ionized form of 4MSK was calculated to be approximately 1×10^3 times greater than that of the unionized form; at this pH, the estimated skin concentration of 3% 4MSK lotion was low (0.004 mg/g), and almost no percutaneous absorption was observed. Wet skin (1 g) yielded 0.785 g of liquid phase when the dry weight was subtracted, and the skin concentrations of 7% ARB, 2% RD, 0.5% ML, 0.3% 4BR, and 3% 4MSK in lotion were determined to be 37.4, 2567, 3461, 1153, and 27.2 μmol/L, respectively, after considering the amount of test ingredients dissolved in the lipid–water fraction.

Table 2-2. Skin concentrations of test ingredients determined from Potts & Guy's skin permeation coefficient prediction equation.

Active Ingredient	RD	ML	ARB	4BR	4MSK
Molecular weight	166.22	270.37	272.25	166.22	206.24
Cosmetics formulation of active ingredient (mg/g)	20	5	70	3	30
Skin concentration (mg/g) *	0.335	0.735	0.008	0.151	0.004
Estimated skin concentration (μmol/L)	2567	3461	37.4	1153	27.2

* Skin concentrations of test ingredients were calculated from skin permeability coefficients determined using the Potts & Guy's skin permeation coefficient prediction equation and Fick's first law of diffusion applied to a skin area of 1.5 cm^2, divided by the skin wet weight. ARB, arbutin; RD, rhododendrol; ML, magnolignan; 4BR, 4-n-butylresorcinol; 4MSK, 4-methoxysalicylic acid potassium salt.

2.3.3. Number of Viable Cells after 3-Day-Exposure to Test Ingredients

The toxicity of the test ingredients to B16 melanoma cells with higher and lower tyrosinase activity after a 3-day exposure is shown in Figure 2-1. Upon treatment with RD and RK, the viability of high tyrosinase activity cells was lower than that of low tyrosinase activity cells. In the presence of 10% serum, a high degree of toxicity to both types of cells was observed for RD and RK concentrations higher than 150 μmol/L. Treatment with 20 μmol/L or 40 μmol/L ML and 10% serum resulted in a great decrease in viable cell count, with the number of viable cells being reduced to 10% of the starting

number. Toxicity was not observed in either the low or high tyrosinase activity cells for concentrations below 370 μmol/L ARB or 970 μmol/L 4MSK. For 4BR, toxicity was not observed in either the low or high tyrosinase activity cells at concentrations below 10 μmol/L.

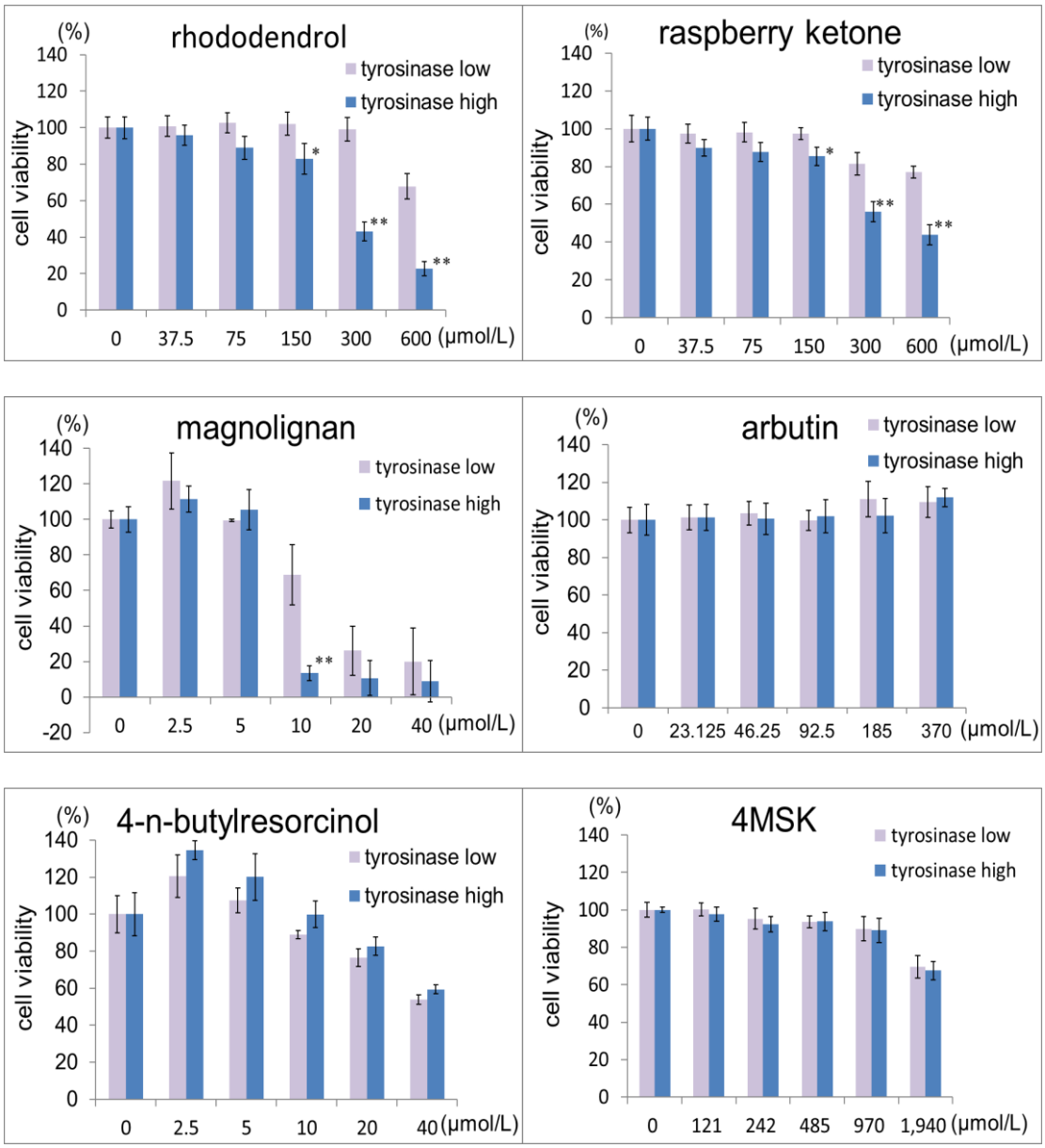

Figure 2-1. Effects of RD, RK, ML, ARB, 4BR, and 4MSK on the number of viable cultured B16 melanoma cells (3 days after addition). Viable cell numbers are shown, with the control set as 100%. Results are presented as the mean ± S.D. of three experiments. * $p < 0.05$, tyrosinase low vs. tyrosinase high at the same concentration; ** $p < 0.01$, tyrosinase low vs. tyrosinase high at the same concentration. RD, rhododendrol; RK, raspberry ketone; ML, magnolignan; ARB, arbutin; 4BR, 4-n-butylresorcinol; 4MSK, 4-methoxysalicylic acid potassium salt.

2.3.4. Number of Viable Cells after Exposure to Test Ingredients in the Presence of Tyrosinase

The toxicity of the test ingredients to B16 melanoma cells after a 3-h exposure in the presence or absence of tyrosinase is shown in Figure 2-2. In the presence of tyrosinase, treatment with RD or RK at 75–600 μmol/L with 2% serum resulted in a concentration-dependent decrease in viable cell counts. At 600 μmol/L, the viable cell number was reduced to approximately 20% of the control. Moreover, in the culture medium containing 2% serum, a concentration-dependent decrease in the number of viable cells was observed in cells treated with ML at concentrations above 20 μmol/L. In the presence of tyrosinase, the number of viable cells decreased after treatment with ML at concentrations above 5 μmol/L. The number of viable cells did not decrease on treatment with ARB, 4BR, 4MSK, or 4PB at any of the concentrations tested in the presence of tyrosinase.

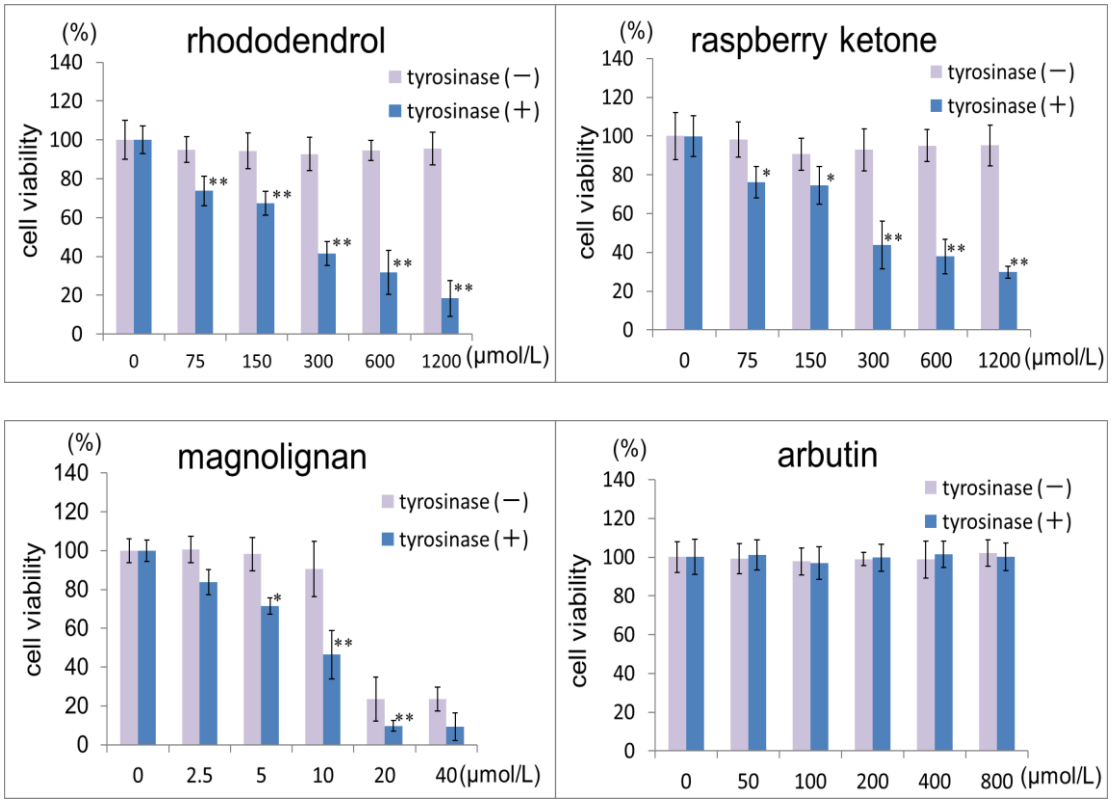

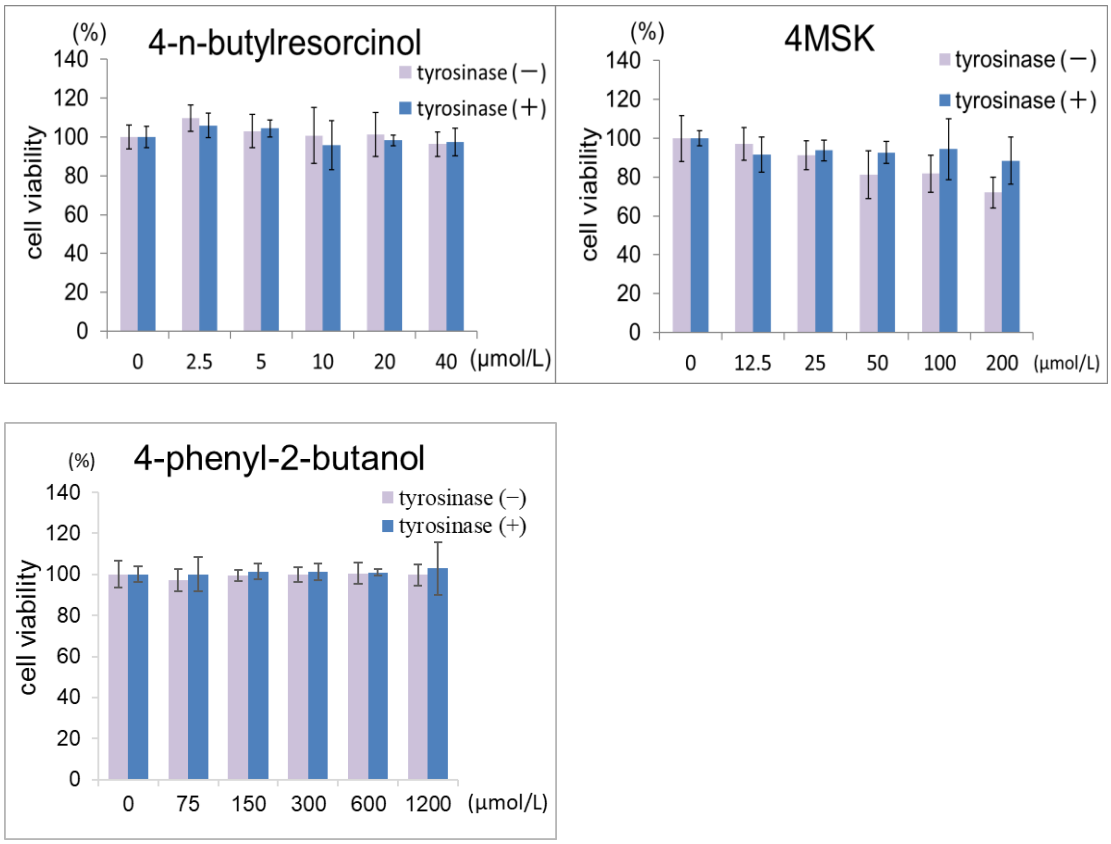

Figure 2-2. Effects of RD, RK, ML, ARB, 4BR, 4MSK, and 4PB in the presence of tyrosinase on viable cell numbers (3 h after addition). Viable cell numbers are shown, with the control set as 100%. Results are presented as the mean ± S.D. of three experiments. * $p < 0.05$, tyrosinase (−) vs. tyrosinase (+) at the same concentration; ** $p < 0.01$, tyrosinase (−) vs. tyrosinase (+) at the same concentration. RD, rhododendrol; RK, raspberry ketone; ML, magnolignan; ARB, arbutin; 4BR, 4-n-butylresorcinol; 4MSK, 4-methoxysalicylic acid potassium salt; 4PB, 4-phenyl-2-butanol.

The toxicity of RD or RK to pigment cells is shown in the micrographs in Figure 2-3. After 3 h, cells exposed to RD or RK at 75 μmol/L became spherical; at 600 μmol/L, toxic effects were noted as changes in cell shape occurred. Continued culturing of the cells resulted in spherical cells that peeled off the dish and floated in the medium.

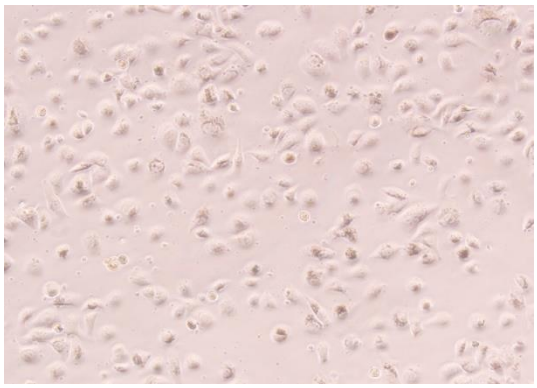

tyrosinase (−)

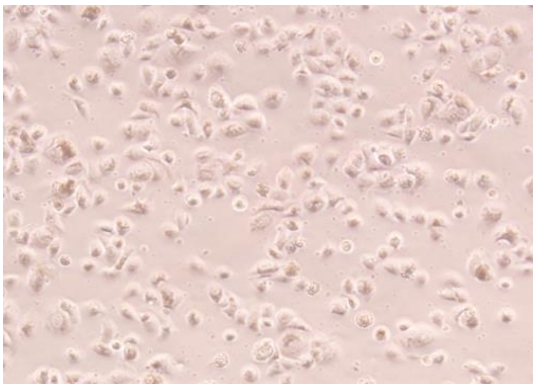

tyrosinase (+)

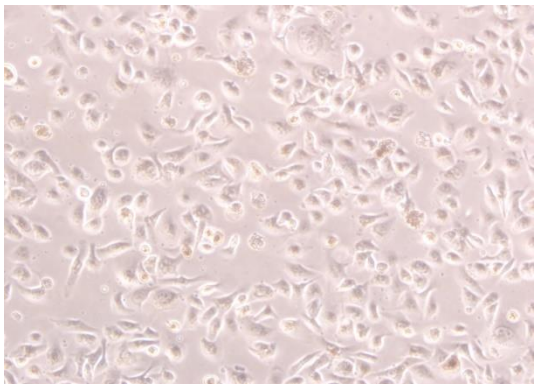

RD　75μmol/L

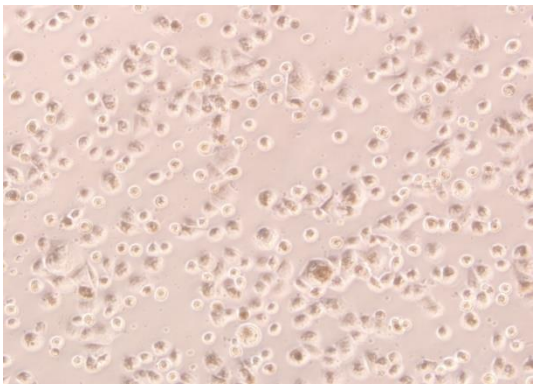

tyrosinase + RD　75μmol/L

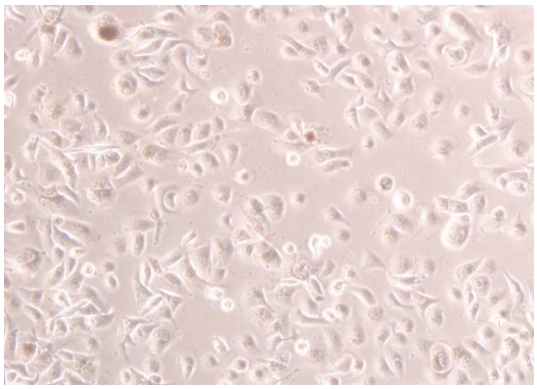

RK　75μmol/L

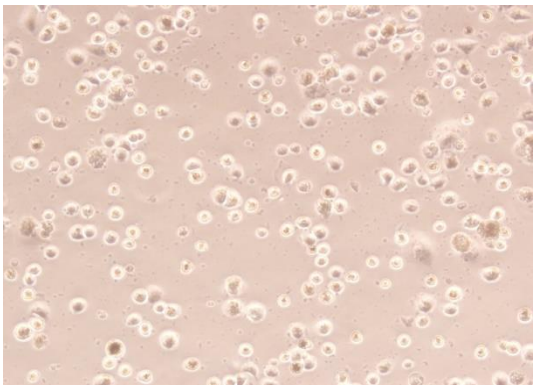

tyrosinase + RK　75μmol/L

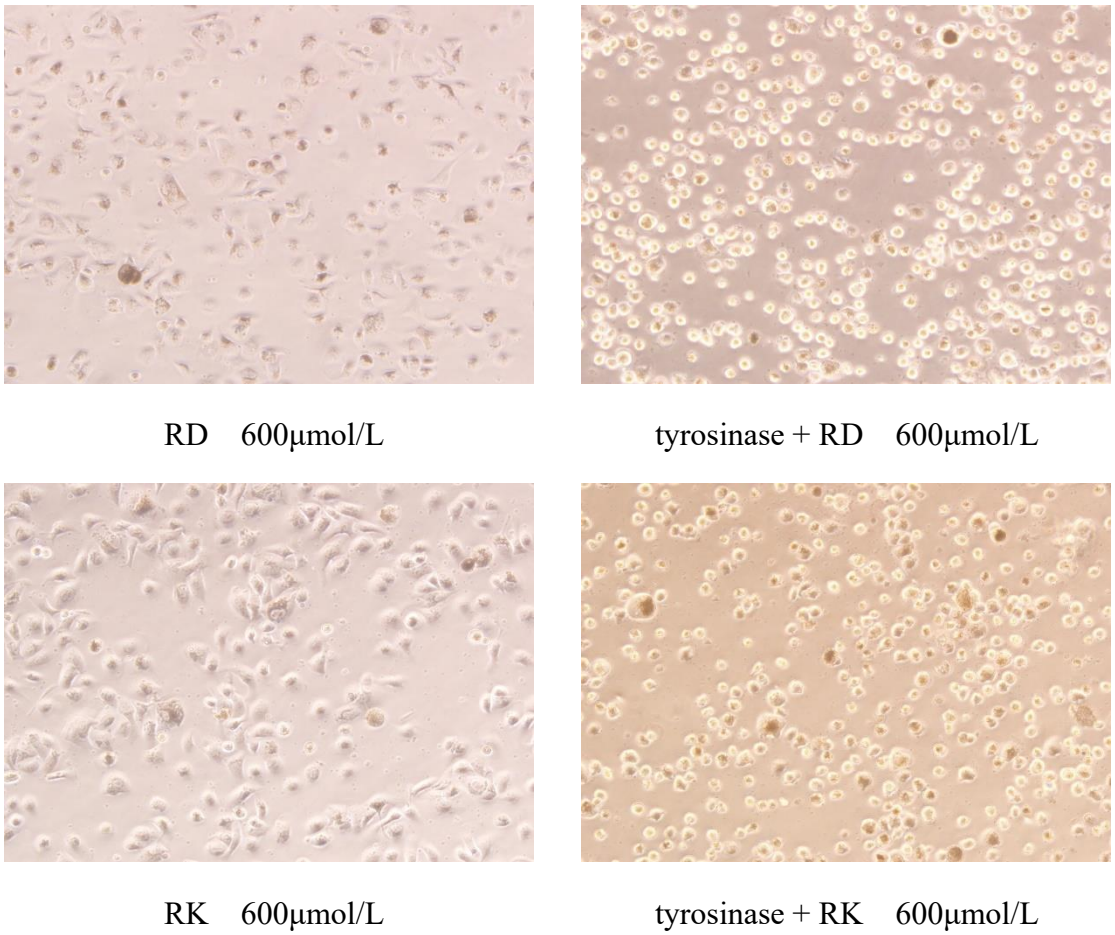

Figure 2-3. Micrographs of pigment cells showing cytotoxicity of RD and RK. Micrographs taken 3 h after RD (150 μmol/L) or RK (150 μmol/L), with or without tyrosinase added to the medium. RD, rhododendrol; RK, raspberry ketone.

2.3.5. Observation by TEM

Electron micrographs of pigment cells exposed to RD (125 μmol/L), RK (125 μmol/L), ML (25 μmol/L), and 4BR (50 μmol/L) are shown in Figure 2-4. Frequent vacuolization was noted as a cytotoxic feature caused by the accumulation of RD (125 μmol/L), RK (125 μmol/L), and ML (25 μmol/L). Pigment cells exposed to 4BR (50 μmol/L) were similar to the controls, and cytotoxic features were not observed.

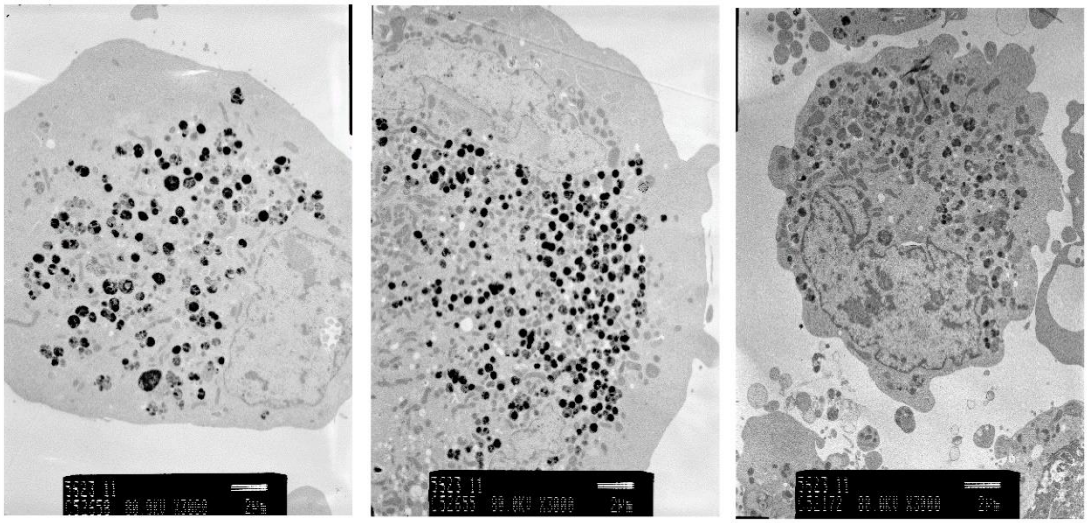

(**a**)

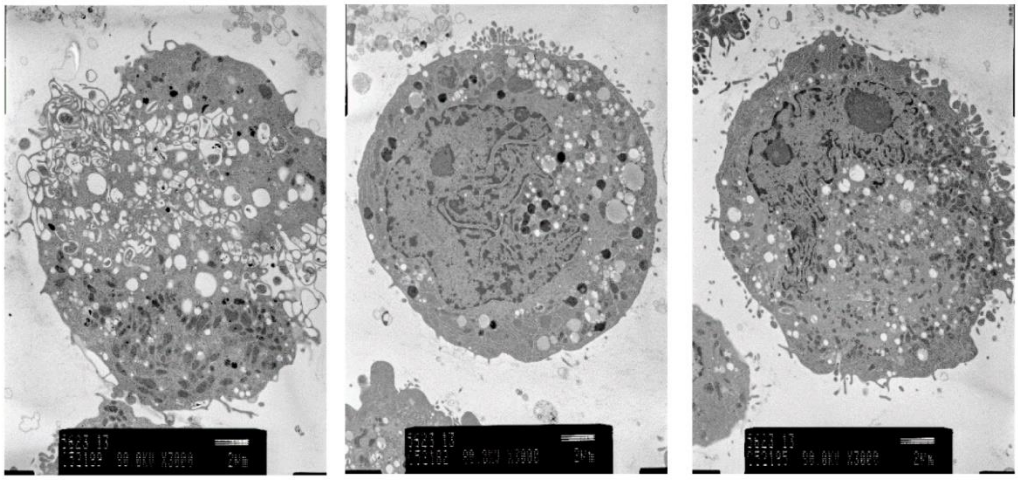

(**b**)

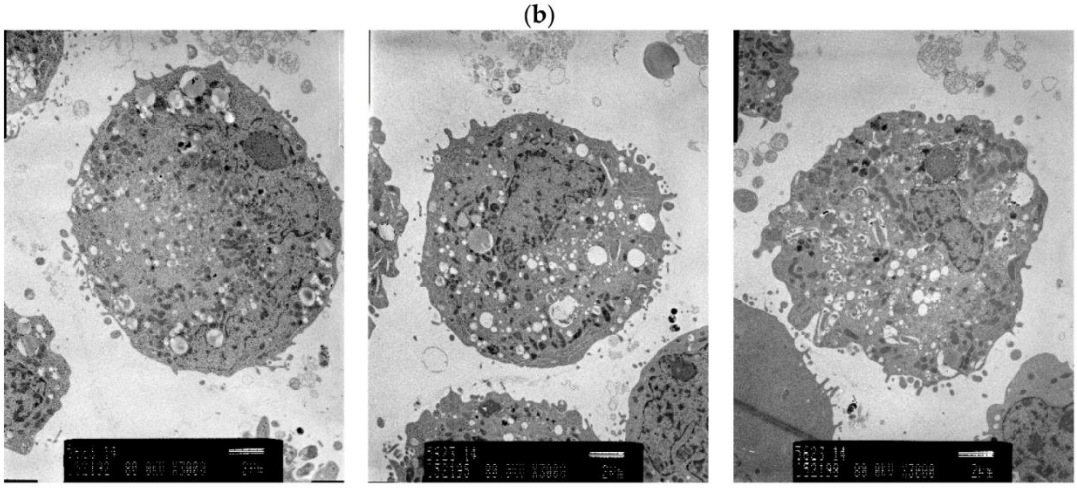

(**c**)

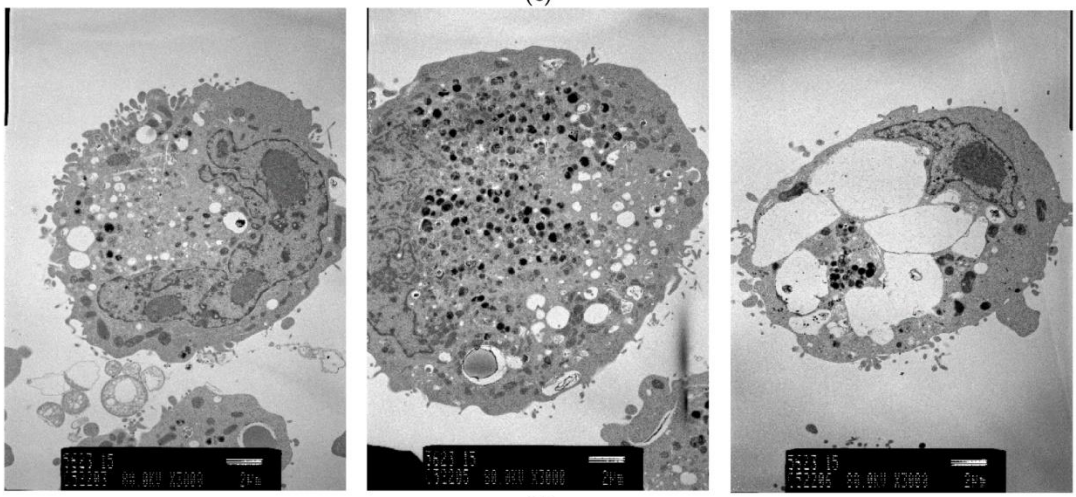

(**d**)

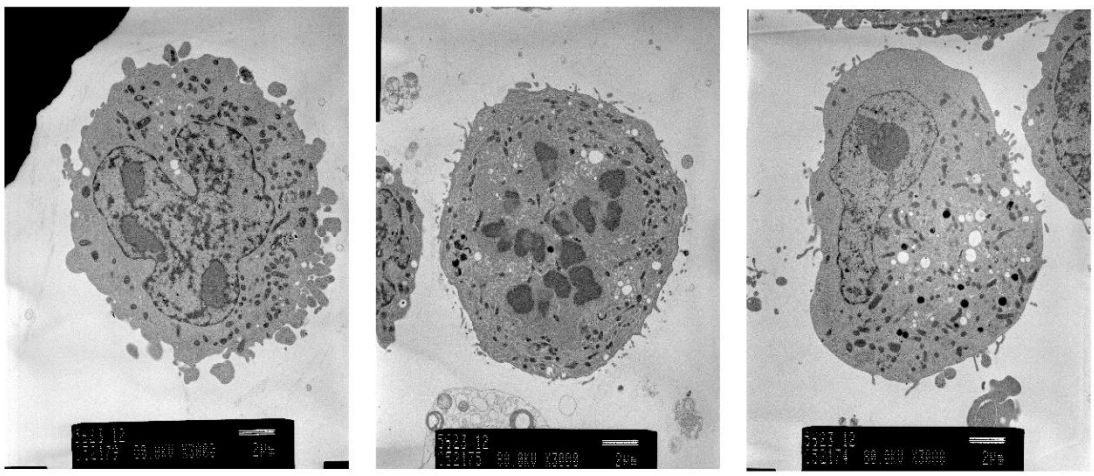

(**e**)

Figure 2-4. Electron micrographs (3000×) of pigment cells treated with RD (125 μmol/L), RK (125 μmol/L), ML (25 μmol/L), or 4BR (50 μmol/L) : (**a**) Control; (**b**) RD (125 μmol/L); (**c**) RK (125 μmol/L); (**d**) ML (25 μmol/L); (**e**) 4BR (50 μmol/L).

2.3.6. Hydroxyl Radical (·OH) Generation from Test Ingredients in the Presence of Tyrosinase

A graph comparing ·OH generation from test ingredients in the presence of tyrosinase after 30 min is shown in Figure 2-5. RD, RK, and ML were found to generate ·OH in a concentration-dependent manner in the presence of tyrosinase, peaking at 30 min and then remaining constant. Compared to controls, ·OH generation from 3 μmol/L RD was 5 times greater and that from 300 μmol/L was 10 times greater. RK and ML at 200 μmol/L also produced ·OH 10 times that in the controls. In addition, abundant ·OH generation was detected at concentrations lower than the estimated skin concentrations of RD (2567 μmol/L) and ML (3461 μmol/L). The ·OH generation from ARB at the estimated skin concentration (37.4 μmol/L) was small, approximately 2 times greater than that in the control. The ·OH generation was not observed at the estimated skin concentrations of 4BR (1805 μmol/L) or 4MSK (581 μmol/L). There is no risk of leukoderma by treatment with the lotions containing 7% ARB, 0.3% 4BR, or 3% 4MSK as determined by the amount of ·OH generated in the presence of tyrosinase at the estimated skin concentration (Table 2-3). However, there is a risk of leukoderma posed by treatment with the lotion containing 2% RD or 0.5% ML, as determined by the

amount of ·OH generated in the presence of tyrosinase at the estimated skin concentration (Table 2-3).

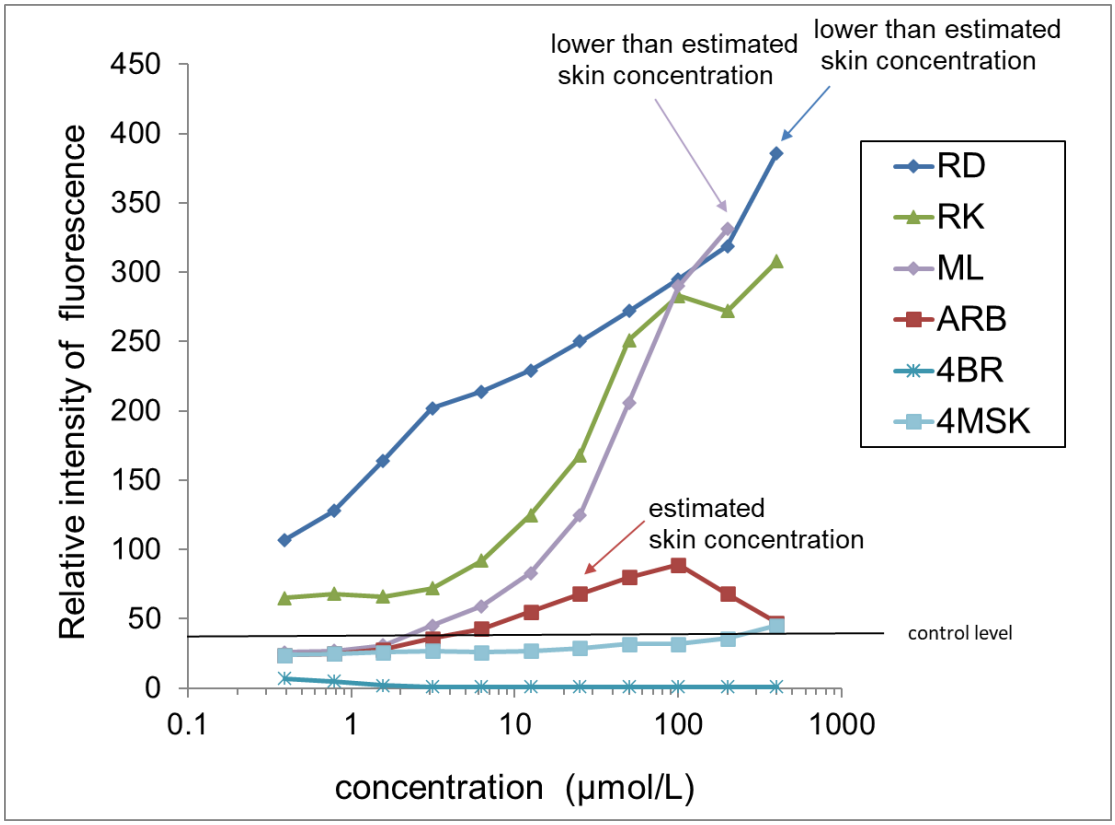

Figure 2-5. Comparison of ·OH generation by test ingredients in the presence of tyrosinase. Results are presented as the mean of three experiments. RD, rhododendrol; RK, raspberry ketone; ML, magnolignan; ARB, arbutin; 4BR, 4-n-butylresorcinol; 4MSK, 4-methoxysalicylic acid potassium salt.

2.3.7. Hydrogen Peroxide (H_2O_2) Generation by Test Ingredients in the Presence of Tyrosinase

A graph comparing H_2O_2 generation from test ingredients in the presence of tyrosinase after 240 min is shown in Figure 2-6. RK and RD generated abundant H_2O_2. H_2O_2 generation by RK was concentration dependent, with 50 μmol/L RK producing 13 times more H_2O_2 than controls and 400 μmol/L producing 21 times more. H_2O_2 generation by RD was concentration dependent, with 400 μmol/L RD yielding 9 times more H_2O_2 than the control. In the presence of tyrosinase, the amount of H_2O_2 generated from RK and RD began rising after reacting for 60 min, then increased

proportionally with reaction time. Only a small amount of H_2O_2 was generated by ARB, and no H_2O_2 generation was observed upon treatment with ML, 4BR, or 4MSK.

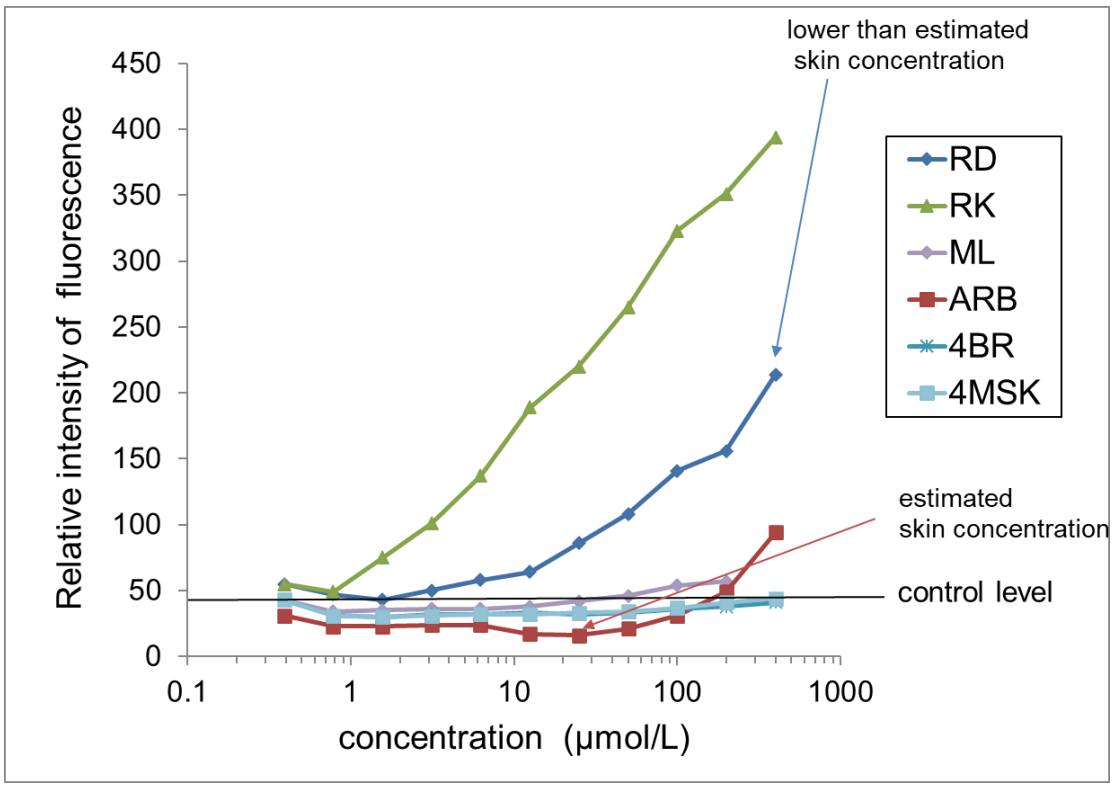

Figure 2-6. Comparison of H_2O_2 generation by test ingredients in the presence of tyrosinase. Results are presented as the mean of three experiments. RD, rhododendrol; RK, raspberry ketone; ML, magnolignan; ARB, arbutin; 4BR, 4-n-butylresorcinol; 4MSK, 4-methoxysalicylic acid potassium salt.

2.3.8. ·OH Generation from Test Ingredients with Tyrosinase in the Presence of Chelators

A graph comparing ·OH generation from test ingredients with tyrosinase in the presence or absence of chelators after 30 min is shown in Figure 2-7. The ·OH generation was not observed at all concentrations of RD and RK in the presence of chelators.

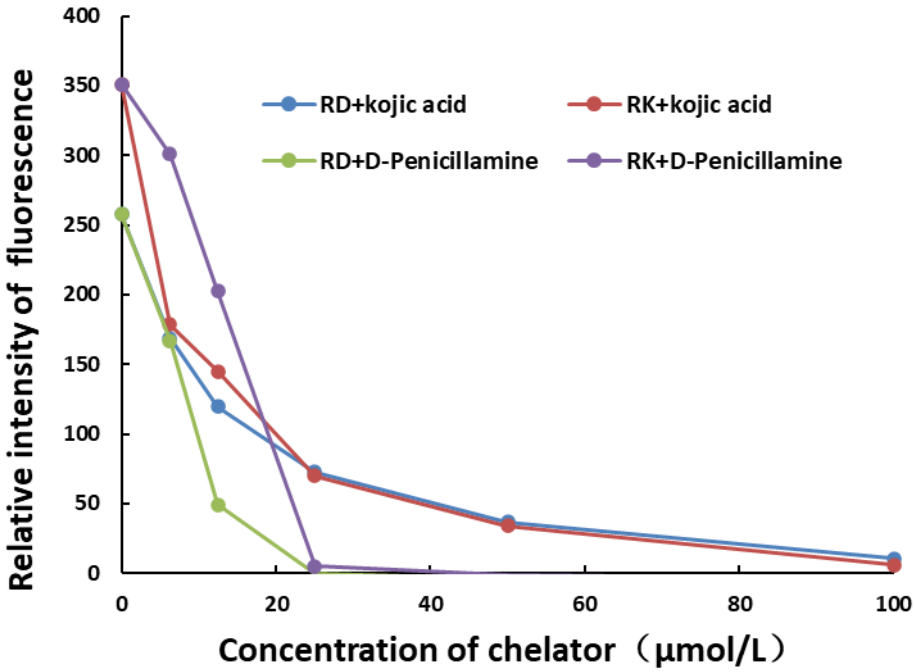

Figure 2-7. Comparison of ·OH generation from test ingredients with tyrosinase in the presence or absence of chelators. Results are presented as the mean of three experiments. RD, rhododendrol; RK, raspberry ketone.

2.3.9. Determination of ·OH Generation Sites

The sites of ·OH generation in B16 melanoma cells treated with RD are shown in Figure 2-8. Green fluorescently labeled ·OH co-localized with red anti-TYRP-1 antibody-stained melanosomes. ·OH generated from RD was confined to melanosomes, and large amounts of highly toxic ·OH were found where tyrosinase was present.

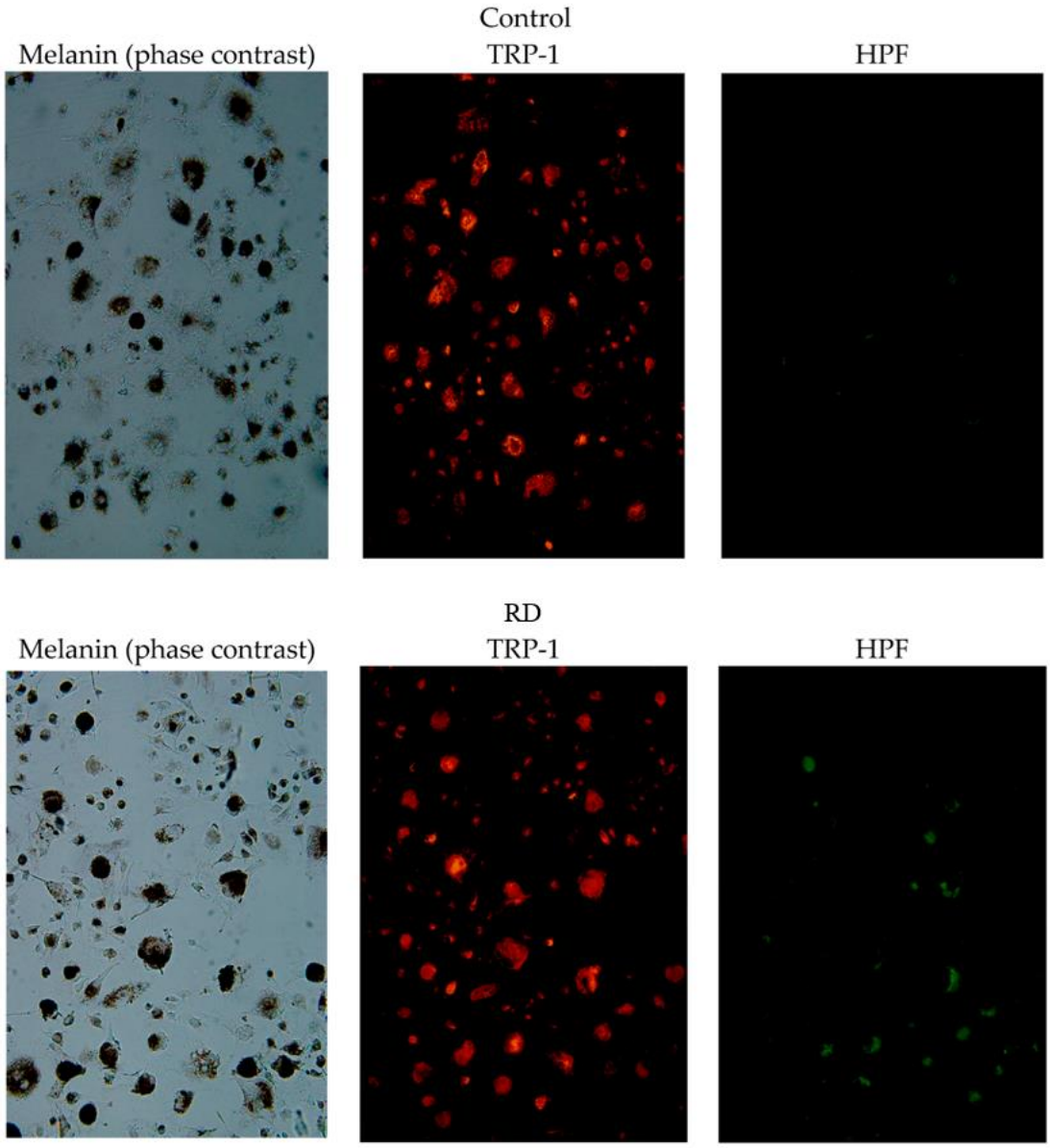

Figure 2-8. Hydroxy radical (·OH) generation sites in B16 melanoma cells treated with RD. Melanin (phase contrast); Red, anti-TYRP-1 antibody-stained melanosomes; Green, fluorescently labeled ·OH by HPF. RD, rhododendrol; TYRP-1, tyrosinase-related protein-1; HPF, hydroxyphenyl fluorescein.

2.3.10. *In Vitro* Factor of Safety and Factor of Effectiveness for Tested Substances

Using the skin permeability coefficient prediction of Potts & Guy, the estimated skin concentration was calculated at steady state, along with hydroxyl radical generation (Table 2-3). The *in vitro* factor of safety, calculated as B16 melanoma cytotoxic concentration/estimated skin concentration, for 7% ARB, 0.3% 4BR, and 3% 4MSK lotions were 25, 0.21, and 100, respectively. These values indicate a high degree of safety assurance for lotions formulated with 7% ARB or 3% 4MSK, and cytotoxic effects were not observed in the melanocytes. In contrast, the *in vitro* factor of safety for 2% RD and 0.5% ML was 0.13 and 0.07, respectively, indicating a very low degree of safety.

Table 2-3. *In vitro* B16 melanoma cytotoxicity concentration/estimated skin concentration and risk of hydroxyl radical generation.

Active Ingredient	RD	ML	ARB	4BR	4MSK
Cytotoxic concentration in B16 cells (μmol/L)	253	20	735	193	1940
Melanin inhibitory concentration in B16 cells (μmol/L)	253	20	92	10	970
Cytotoxic concentration in B16 cells/Estimated skin concentration	0.13	0.07	25	0.21	100
Estimated skin concentration/Melanin inhibitory concentration in B16 cells	7.98	13.61	0.32	92.77	0.02
Hydroxyl radical generation at the estimated skin concentration	High	High	Low	No	No

RD, rhododendrol; ML, magnolignan; ARB, arbutin; 4BR, 4-n-butylresorcinol; 4MSK, 4-methoxysalicylic acid potassium salt.

The *in vitro* factor of effectiveness, calculated as the estimated skin concentration/melanin inhibitory concentration in B16 cells, for 7% ARB and 0.3% 4BR lotions was 0.32 and 92.77, respectively. These values indicate a high degree of effectiveness for 0.3% 4BR and a moderate degree of effectiveness for 7% ARB. The inhibition of melanin production can also be expected with the application of lotion formulated with 7% ARB or 0.3% 4BR. However, the cytotoxicity concentration and melanin inhibitory concentration in B16 cells are equal to those of the lotion

formulated with the 2% RD and 0.5% ML, respectively, indicating a very low degree of effectiveness.

2.4. Discussion

In chemical leukoderma, premelanosomes are destroyed and melanocytes subsequently disappear, causing the symptom of skin depigmentation. A study of the mechanism of leukoderma reported that for RK in B16F10 melanoma cells expressing tyrosinase, the half maximal inhibitory concentration (IC_{50}), the concentration at which the cell viability is reduced to 50%, was 0.13 mmol/L. The IC_{50} of RK in HT1080 non-pigmented cells (a transformed human fibrosarcoma cell line) without tyrosinase was 1.56 mmol/L [118]. According to a previous study, the presence of tyrosinase increases the cytotoxicity of RK and the leukoderma caused by RK is not due to the inhibition of melanin biosynthesis, but rather the destruction of melanocytes by a toxic substance produced by RK with tyrosinase [118]. Similarly, skin depigmentation caused by topical application of 30% RD solution for 21 days may occur via selective melanocyte toxicity and re-pigmentation occurred approximately 50 days after the application was discontinued in black guinea pigs [140]. However, complete depigmentation was not accomplished because the max L* value was observed to be 46 and many melanocytes may have reproduced with hair growth and reproduction in that study [140], so re-pigmentation may have occurred in the guinea pigs. In this chapter, it has been proved that RD-induced leukoderma is not due to inhibition of melanin biosynthesis but rather due to the destruction of melanocytes by a toxic substance produced by RD with tyrosinase, and this result is also in line with the findings of Ito et al [100–102].

The structure of the chemical substance that causes leukoderma has been characterized as a 4-substituted phenol having an alkyl group with a nonpolar side chain attached to the 4-position and hydroxylated at the 1-position of the benzene ring. RD and its oxidized form, RK, which causes leukoderma, has strong ·OH-generating activity in the presence of tyrosinase. However, 4PB, the form obtained after removal of the hydroxyl group from the benzene ring of RD, did not show cytotoxicity at the

same concentration with RD, regardless of the presence of tyrosinase. It suggests that the melanocyte cytotoxicity of RD is dependent on the hydroxyl group on the benzene ring. Furthermore, it was found that ML also has strong ·OH-generating activity. These compounds are both 4-substituted phenols, indicating that there is structural similarity. On the other hand, ARB, which is a glycoside of hydroquinone, demonstrated weak ·OH-generating activity, while 4BR, which has resorcinol structure, did not.

The melanocyte-specific toxicity of 4-substituted phenols is caused by the *ortho*-quinone or *ortho*-quinone methide generated by the catalytic action of tyrosinase [141–146]. If RD is used as a substrate for tyrosinase, the reaction produces ·OH, which is a known melanocyte-specific toxin. This chapter results indicate that at least for RD and its oxidized form RK, previously reported to cause leukoderma, the generation of ·OH increases in the presence of tyrosinase.

The mechanism of ·OH production appears to be a Fenton reaction [107] occurring between the liberated H_2O_2 and Cu(I)−Cu(I) of tyrosinase, generating ·OH by the following reaction (Equation (3-4)):

$$\mathrm{Cu(I) - Cu(I) + \tfrac{1}{2}\, H_2O_2 \rightarrow Cu(II) - Cu(II) + \tfrac{1}{2}\, OH^- + \tfrac{1}{2}\, \cdot OH} \quad (3\text{-}4)$$

Muñoz-Muñoz et al. discussed the production of H_2O_2 from 4-substituted phenols in the presence of tyrosinase [147]. When C-1 of the hydroxyl group is bonded to Cu(II) of the tyrosinase catalytic site and an electron-withdrawing group of C-4 as in RK is present, the charge density of Cu(II) increases and affects the hydroxyl group of C-2, causing deprotonation of C-2 [147]. The protons are transferred to a tyrosinase catalytic site peroxide (OOH), generating H_2O_2. In contrast, if an electron donating group (e.g., COOH, NH_2) is present at C-4, as in tyrosine, which is the starting amino acid of melanin synthesis, the charge density of Cu(II) in the tyrosinase catalytic site decreases. In this case, the hydroxyl group protons of C-2 are transferred to a histidine residue of the enzyme, and H_2O_2 is not generated. The C-4 of RK is an electron-withdrawing group (3-oxobutyl), and the phenolic hydroxyl group of RK binds to the divalent copper Cu(II) of the catalytic site of tyrosinase, converting it to catechols. When oxidized to *ortho*-

quinones and released, divalent copper Cu(II) is reduced to monovalent copper Cu(I), and H_2O_2 is generated.

Cytotoxicity is observed with RD or its oxidized form RK, and both ·OH and H_2O_2 are generated in the presence of tyrosinase. Moreover, although cytotoxicity is observed with ML treatment in the presence of tyrosinase, ·OH but not H_2O_2 is generated. The results indicate that at least for RD, RK, and ML, the increased ·OH generation in the presence of tyrosinase, but not H_2O_2 production, is involved in the cytotoxicity. However, the ·OH generation was significantly reduced in the presence of chelators. A previous study suggests that the chelators were effective in reducing the generation of ROS by RK [107]. It is confirmed that the reduced ROS is ·OH in this chapter, which suggests that the mechanism of ·OH generation involves the Fenton reaction. Because H_2O_2 is not produced, it cannot be used to evaluate the potential of substances that cause chemical leukoderma in melanocytes; instead, ·OH generation should be used for such evaluations. The amounts of $^1O_2$ generated via RD and RD-catechol oxidations with mushroom tyrosinase were reported [109], and they were probably lower than that of $^1O_2$ exhibiting cytotoxicity [109]. The calculation of cell volume was erroneous in this previous report [109]; however, $^1O_2$ was produced by L-tyrosine and L-DOPA in the presence of tyrosinase. These findings suggest that $^1O_2$ generated via RD and RD-catechol oxidations with tyrosinase does not cause cytotoxicity.

Using the skin permeability coefficient prediction equation of Potts & Guy, the estimated skin concentration calculated at steady state and risk for developing leukoderma was determined. *In vitro* B16 melanoma cytotoxicity concentration/estimated skin concentration values for the ingredients RD and ML were less than 0.2, indicating a low degree of safety assurance. Cytotoxicity was observed at concentrations much lower than the minimum concentration to be used on the skin. At the skin concentrations tested, ·OH generation increased, and it is likely that the skin becomes lightened due to cytotoxicity to melanocytes. In contrast, the *in vitro* B16 melanoma cytotoxicity concentration/estimated skin concentration values for the

ingredients ARB and 4MSK were greater than 10, indicating a high degree of safety assurance. Cytotoxicity was not observed in pigment cells at the skin concentrations tested, and minimal ·OH generation was noted, indicating that the risk of causing leukoderma was low. 4MSK is ionized at pH 6.2; thus, its skin permeability is low, and the degree of safety assurance is high. The cytotoxic effects to pigment cells at the skin concentrations tested were minimal. Further, no ·OH generation was observed, suggesting that there was no risk of causing leukoderma.

Active ingredients in quasi-drug cosmetics in Japan must have a high degree of safety, and any detrimental effects must be minimized. Thus, an evaluation method that indicates the cytotoxicity of an ingredient at a given skin concentration may be useful. The results of this chapter suggest that, *in vitro*, the suppression of melanin production depends on the inhibition of tyrosinase activity and that concentrations that do not induce cytotoxic effects nor melanin production are required for product safety. ARB and 4MSK satisfied these conditions, but RD and ML did not. It is clear that RD and ML do not fulfill Japanese quasi-drug cosmetics standards for safety. The cytotoxicity of RD and ML was greater in the presence of 2% serum than in 10% serum. These molecules may bind to serum proteins, such that as the serum percentage increases, the availability of RD or ML decreases, thereby diminishing the toxic effect.

In the presence of tyrosinase, RD can be converted into catechols, which are reported as the main cause of cytotoxicity [97]. However, catechols seem to be responsible for approximately 1/10 of the effects observed in RD-treated samples. The cytotoxic effects of RD thus cannot be explained by catechol involvement alone. Furthermore, it can be seen from Figure 2-4B in the reference [97] that the cytotoxicity to melanocytes is 0.617 mmol/L, corresponding to 100 μg/mL, indicating that RD is cytotoxic to melanocytes at the skin concentration when it is applied at 2%.

This chapter confirmed that RD, RK, and ML react with tyrosinase substrate to generate high amounts of ·OH, thereby exerting toxic effects on melanocytes. Past reports have indicated that the first position in the benzene ring becomes hydroxylated, and 4-substituted alkyl phenols where an alkyl group of nonpolar side chains is attached

at the 4-position, are implicated in causing leukoderma. Leukoderma often appears after the occurrence of contact dermatitis. With skin irritation, percutaneous absorption increases and damage from leukoderma becomes more severe. RD is also a 4-substituted phenol; thus, it is expected to cause leukoderma. Melanocyte toxicity of 4-substituted phenols have been reported to be caused by ortho-quinones or ortho-quinone methides catalyzed by tyrosinase, but at low concentrations, tyrosinase enhances ·OH generation and this appears to be the main factor responsible for toxicity is the melanosome. However, Figure 2-6 shows that ·OH is not necessarily generated in all melanosomes of Stage IV cells, so the mechanism of generation/elimination of ·OH in melanosomes should be considered.

The skin depigmentation agents investigated in this chapter that produced high amounts of ·OH at the estimated skin concentrations are RD and ML. RD appears to cause leukoderma, and ML has a similar effect. Thus, caution is required in using these ingredients, taking into consideration the previous report concerning allergic contact dermatitis by ML [148–150]. Electron micrographs of B16 melanoma cells with leukoderma-causing RD, RK, and ML treatment show large numbers of vacuoles within cell melanosomes. Skin care cosmetics frequently contain whitening or lightening agents. They are routinely applied by adult women without limitations on usage or frequency. Thus, measures should be taken to prevent their adverse effects in the form of chemical leukoderma. Mild leukoderma may be cured. However, the concentrations of these agents in the skin are increased by roughness, resulting in marked toxicity. Prolonged exposure to these agents is cytotoxic to melanocytes, causing permanent leukoderma. Further, pigment cells cultured under conditions of high but not low tyrosinase activity demonstrated decreased viability when exposed to ingredients previously known to cause leukoderma. Thus, the *in vitro* evaluation method reported in this chapter may be used as an indicator of whether a given substance will cause leukoderma. B16 melanoma cells are generally used to support test validity and analyze the mechanism of quasi-drugs; they are also adopted as the approval test of the Ministry of Health, Labour and Welfare in Japan. However, together with the test result in a

normal human melanocyte in culture medium without phorbol myristate acetate or cholera toxin, it is necessary to consider the mechanism of leukoderma from now on.

2.5. Conclusion

In this chapter, the mechanisms of action and epidermal concentrations required of ingredients that are toxic to melanocytes, subsequently causing leukoderma have been further clarified. Loss of melanocytes can follow the destruction of premelanosomes by ·OH generated by tyrosinase-mediated reactions. The result is depigmentation of the skin, manifested clinically as leukoderma. This chapter suggests that the mechanism by which leukoderma onset occurs is the tyrosinase-mediated production of high amounts of ·OH; which damages melanosomes and in turn causes the apoptosis of melanocytes. The *in vitro* evaluation method developed here may be used to determine whether a given ingredient will cause leukoderma.

Chapter III

Detection of Raspberry Ketone After Percutaneous Absorption of Rhododendrol-containing Cosmetics and its Mechanism of Formation

3.1. Introduction

Given that skin-whitening products containing RD, which disabled due to caused leukoderma are applied to the skin many times a day, the concentration of RD in the skin might increase with repeated application and reach toxic levels; therefore, in this chapter we determined the amount of RD that is transepidermally absorbed at first. In addition, it has also been reported that (R)-Rhododendrol, contained in plants is converted to RK by alcohol dehydrogenase (ADH; EC 1.1.1.1) [71–73]. Alcohol dehydrogenase is an enzyme that exists widely in nature, and also exists in the skin of humans and animals, and plays a vital role in skin metabolism [26]; Therefore, the skin metabolites of RD-containing cosmetics were also be investigated in this chapter. Furthermore, there are individual differences in the onset of toxicity, and there is a possibility that the onset of toxicity will vary depending on the intensity of the metabolic activity of RD in the epidermis. Therefore, the purpose of this chapter was to clarify the conversion of RD to RK in the skin using the skin permeation test and to determine whether RK was also responsible for leukoderma caused by RD-containing cosmetics.

3.2. Materials and Methods

3.2.1. Materials

Glycerin was purchased from Sakamoto Yakuhin Kogyo Co., Ltd. (Osaka, Japan). PEG-60 hydrogenated castor oil (HCO-60) was purchased from Nippon Surfactant Industries Co., Ltd. (Tokyo, Japan). Squalene was purchased from Nikko Chemicals Co., Ltd. (Tokyo, Japan). Phenoxyethanol (PHE-S) was purchased from Yokkaichi Chemical Co., Ltd. (Mie, Japan). Sodium acrylate–sodium acryloyldimethyl taurate copolymer/isohexadecane/polysorbate 80 (SIMULGEL-EG) was purchased from SEPPIC SA (Courbevoie, France). RK was purchased from Sigma-Aldrich Co. LLC (St. Louis, MO, USA). RD was purchased from Tokyo Chemical Industry Co., Ltd. (Tokyo, Japan). Franz diffusion cell was purchased from Biocom Systems, Inc. (Fukuoka, Japan). Laboskin (4 cm × 7 cm; frozen dorsal full-thickness skin from Hos:HR-1 hairless mouse) was purchased from Hoshino Laboratory Animals Inc. (Ibaraki, Japan). Considering animal welfare, we used the minimum amount of laboskin necessary. Phosphate-buffered saline (PBS) was purchased from TaKaRa Bio Inc. (Shiga, Japan). Moreover, 1,3-butanediol, acetic acid, methanol, sodium pyrophosphate, NAD+, and alcohol dehydrogenase (ADH) from yeast with a specific activity of 390 international enzyme units per mg of protein were purchased from FUJIFILM Wako Pure Chemical Corporation (Osaka, Japan). Frozen human full-thickness skin (155 cm^2; abdomen skin from 30-year-old female donor) was purchased from Biopredic International Ltd. (Saint Gregoire, France).

3.2.2. Preparation of Test Solution

As shown in Table 3-1, three test solutions containing 2% RD (the concentration that is used in Kanebo Cosmetics and causes leukoderma) were prepared. Ultrasound (US-2R, AS ONE Corporation, Tokyo, Japan; high mode, 40°C–50°C, 20 min) was used to ensure uniform dissolution. The pH of all three solutions was adjusted to 6.2 using 1% potassium hydroxide solution.

Table 3-1. RD formulations used in this study

	Water	Lotion	Emulsion
RD	0.2	0.2	0.2
Glycerin	-	0.4	0.4
1,3-butanediol	-	0.6	0.6
PEG-60 hydrogenated castor oil	-	0.02	0.02
Phenoxyethanol	-	0.035	0.035
Squalene	-	-	1
Sodium acrylate–sodium acryloyldimethyl taurate copolymer/isohexadecane/polysorbate	-	-	0.25
Water	9.8	8.745	7.495

3.2.3. Measurement of Skin Permeability after Repeated Application of Solutions Containing RD

Laboskin from 7-week-old mice was thawed to room temperature and prepared into a circular shape with an area of approximately 1.5 cm^2 using surgical scissors. Experiments were conducted to determine the amount of skin penetration when the formulations were applied in the actual dosage form used. Specifically, laboskin was mounted in a Franz diffusion cell with circulating water at a constant temperature of 37 °C, and 15 mg of a 2% RD solution (2% RD, 98% water) was applied once to 1.5 cm^2 of laboskin, followed by a second application 10 min later and a third application 10 min later.

High-performance liquid chromatography (HPLC) was performed using Shimadzu HPLC system (Shimadzu Co., Kyoto, Japan), Capcell Pak C18 columns (4.6 × 250 mm; Shiseido Co. Ltd., Tokyo, Japan) at 35 °C, and an SPD-M20A photo diode array detector (Shimadzu Co., Kyoto, Japan) with the following conditions: flow rate, 1.0 mL/min; injection volume, 10 μL; detection wavelength, 210 nm; and mobile phase (methanol/water ratio, 30:70).

3.2.4. Measurements of Skin Permeation Rate with Different Cosmetic Formulations

Laboskin from 7-week-old mice was thawed to room temperature and prepared using surgical scissors into a circular shape with an area of approximately 1.5 cm^2. Laboskin was mounted in a Franz diffusion cell with circulating water at a constant temperature of 37 °C. Then, 15 mg of a test solution (water, lotion, or emulsion) was applied to the skin. The receptor chamber was filled with approximately 10 mL of PBS and stirred with a magnetic stirrer, and 100-μL samples were collected after 2, 4, 8, 12, and 24 h. The samples were stored at −30 °C for later analysis using HPLC.

After 24 h, the skin samples were immersed overnight in 300 μL of ethyl acetate. The extract was placed in an evaporator (Tokyo Rikakikai Co. Ltd., Tokyo, Japan) to remove the solvent. Once the extract was completely dried and stored at −30 °C for later analysis, the samples were dissolved in 200 μL of methanol before analysis using HPLC. The HPLC conditions were identical to those described in Section 3.2.3.

3.2.5. Analysis of Unknown Substance

After the samples were analyzed using HPLC, an unknown peak at 210 nm appeared on the chromatogram. To identify it, various possible substances, including RK and RD-quinone, were analyzed using HPLC. The detected absorption spectra were compared, and matching components were further verified using liquid chromatography–mass spectrometry (LC–MS).

The HPLC conditions were identical to those described in Section 3.2.3.

LC–MS was performed using a JMS-T100LC AccuTOF™ LC-TOFMS (JEOL DATUM Ltd., Tokyo, Japan) with Capcell Pak C18 columns (4.6 × 250 mm) at 35 °C with the following conditions: flow rate, 1.0 mL/min (approximately a quarter of the mobile phase was induced to the MS analyzer using a splitter); injection volume, 2 μL; detection wavelength, 210 nm; mobile phase (methanol/water ratio, 30:70); ionization, electrospray ionization (ESI) –; ionization voltage, –2000 V.

3.2.6. RK Generation by the Skin with Different Treatments

To investigate the mechanism of RK generation, a skin permeation test with the different treatments was performed, where 100-μL samples were collected after 24 h. The different experimental conditions included (1) heated skin, where laboskin was heated to 95 °C to deactivate the enzymes; (2) no skin, where laboskin was not mounted in a Franz diffusion cell and RD was added to PBS in the receptor chamber at the concentration that was in the receptor chamber after 24 h during the skin permeation test described in Section 3.2.4 (in water, in lotion, and in emulsion); and (3) normal laboskin as a control. Other experimental conditions were identical to those described in Section 3.2.4.

3.2.7. Conversion of RD to RK by ADH

The reaction solutions, which comprised a 9.18 mL sodium pyrophosphate buffer (10.9 mmol/L, pH 8.8), 9 mL ADH (0, 1, 10, and 100 U/mL), 0.09 mL NAD+ (10 mmol/L), and 0.09 mL RD (100 mmol/L), were allowed to react at 25 °C for 30, 60, or 120 min. 0.1 mL of 60% perchloric acid was added to 0.9 mL of sample, stirred, and left to stand for 30 minutes, then centrifuged to remove protein. The RD and RK concentrations were measured using HPLC. The experiment was repeated three times.

3.2.8. Skin Homogenate Analysis

Human skin was weighed, homogenized with homogenizer in PBS, to prepare 10% skin homogenate. Skin homogenate was centrifuged for 15 minutes (at a rotation with 3000×g) and the supernatant was collected and stocked. RD (100, 200, and 300 μg/mL) alone, or RD (100, 200, and 300 μg/mL) with NAD^+ (100 μmol/L) were added to 5 mL of supernatant and the solution was diluted to 10 mL with PBS. The reaction solutions were allowed to react and shake at 32 °C and 250 rpm for 24 h, and 100-μL samples were collected after 2, 4, 8, 12, and 24 h. Ten μL of 60% perchloric acid was added to 90 μL of sample, stirred, and left to stand for 30 minutes, then centrifuged to

remove protein. The samples were stored at −30 °C for later analysis using HPLC.

HPLC was performed using Shimadzu HPLC system (Shimadzu Co., Kyoto, Japan), Chiralcel OD-3R chiral columns (4.6 × 100 mm; Daicel Co. Ltd., Osaka, Japan) at 35 °C, and an SPD-M20A photo diode array detector (Shimadzu Co., Kyoto, Japan) with the following conditions: flow rate, 1.0 mL/min; injection volume, 10 μL; detection wavelength, 210 nm; and mobile phase (methanol/water ratio, 30:70).

3.2.9. Statistical Analysis

Numerical data were recorded in Excel (Microsoft, Redmond, WA, USA), and the means and standard deviations were calculated. The data shown in Table 3-2 were analyzed using two-way repeated measures analysis of variance and BellCurve Excel Statistics (Social Survey Research Information Co., Ltd., Tokyo, Japan). Tukey's test was used for multiple comparisons. For the data presented in Figure in Section 3.3.4, two-tailed *t*-test were performed. A p value of <0.05 was considered statistically significant.

3.3. Results

3.3.1. Skin Permeability of RD-Containing Solutions after Repeated Application

The experimental results are shown in Figure 3-1. The cumulative skin penetration of RD after 8 h was 102.1 μg/cm^2 when applied once, 196.6 μg/cm^2 after 8 h when applied for a second time after 10 min, and 365.1 μg/cm^2 after 8 h when applied three times at 10-minute intervals. The amount of penetration into the skin increased in proportion to the number of applications. Therefore, we could conclude that the concentration of RD in the skin increased with an increased number of applications.

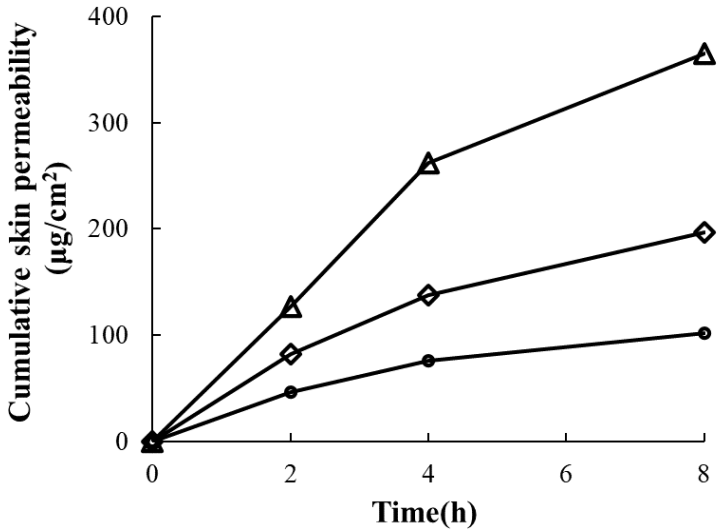

Figure 3-1. Repeated application of 2% RD solution increases skin permeability (circles, ○; one application, diamonds, ◇; two applications, and triangles, △; three applications). All data points are the mean of two experiments.

3.3.2. Skin Permeation Rate of Different Cosmetic Formulations

The skin permeation of RD in different dosage forms was studied using an *in vitro* skin permeation test. Samples collected after 2, 4, 8, 12, and 24 h and were quantified using HPLC. Then, the data were used to calculate the level of skin permeation, skin permeation rate, and recovery rate. After examining different types of HPLC columns,

types of mobile phase, detection wavelengths, etc., the best separation analysis possible under the conditions was described in the Materials and Methods section. The recovery ratios of RD in water, lotion, and emulsion formulations are shown in Table 3-2. The cumulative skin permeability, permeation rate, and apparent permeability coefficient are shown in Table 3-3. The skin permeation amounts and skin permeation rates are shown in Figure 3-2.

As shown in Table 3-2, the recovery ratio of RD from the receptor chamber was nearly 100% for the aqueous solutions and lotions, whereas the recovery ratio of RD was about 87% for the emulsions. As shown in Table 3-4, there was no significant difference in the permeation ratio of RD between the water and lotion formulations or between the lotion and emulsion formulations. However, there was a significant difference in the permeation ratio of RD between the water and emulsion formulations. Therefore, the penetration rate of RD in the aqueous solution was higher than that in the lotion and emulsion formulations (Figure 3-2). After finite dose treatment, the permeation rate exhibited a decreasing trend over time for all formulations (Figure 3-2). A multiple comparisons test for differences among the formulations revealed significant differences between the water and lotion formulations and between the water and emulsion formulations after 2 h (Table 3-5). Significant differences were observed only between the water and emulsion formulations after 4 h. However, no significant differences among the groups were observed after 8, 12, and 24 h (Table 3-5).

Table 3-2. RD recovery rate with different cosmetics formulations.

Formulation	RD Recovery Ratio in Receptor Chamber (%)	RD Recovery Ratio in Mice Skin (%)	Total RD Recovery Ratio (%)
Water	106.6 ± 6.3	0.480 ± 0.065	107.1 ± 6.4
Lotion	100.0 ± 3.2	0.331 ± 0.210	100.3 ± 3.4
Emulsion	87.0 ± 9.1	0.408 ± 0.104	87.4 ± 9.2

Table 3-3. Cumulative skin permeability, permeation rate, and apparent permeability coefficient of RD with different cosmetics formulations.

	Time (h)	Cumulative Skin Permeability (μg/cm²)	Permeation Rate (μg/cm²/h)	Apparent Permeability Coefficient #
Water	2	40.52	20.26	0.1013
	4	65.03	12.26	0.0613
	8	97.56	8.13	0.0406
	12	127.65	7.52	0.0376
	24	213.16	7.13	0.0356
Lotion	2	28.80	14.40	0.0720
	4	47.10	9.15	0.0457
	8	86.31	9.80	0.0490
	12	121.67	8.84	0.0442
	24	200.06	6.53	0.0327
Emulsion	2	24.36	12.18	0.0609
	4	35.94	5.79	0.0289
	8	59.32	5.84	0.0292
	12	89.55	7.56	0.0378
	24	173.91	7.03	0.0351

The apparent permeability coefficient was calculated by dividing the permeation rate by the initial amount of RD (μg/cm^2) applied to the skin.

Table 3-4. Comparison of RD permeation rates among the formulations.

Comparison between Formulations	*p* Value
Water vs. Lotion	0.3534
Water vs. Emulsion	0.0032
Lotion vs. Emulsion	0.0877

Table 3-5. Multiple comparisons test to evaluate differences in the RD permeation rates among the formulations based on time after application.

Time after Application	Comparison between Formulations	p Value
2 h	Water vs. Lotion	0.0239
	Water vs. Emulsion	0.0016
	Lotion vs. Emulsion	0.5471
4 h	Water vs. Lotion	0.3133
	Water vs. Emulsion	0.0118
	Lotion vs. Emulsion	0.2614
8 h	Water vs. Lotion	0.7070
	Water vs. Emulsion	0.5284
	Lotion vs. Emulsion	0.1600
12 h	Water vs. Lotion	0.8068
	Water vs. Emulsion	0.9999
	Lotion vs. Emulsion	0.8158
24 h	Water vs. Lotion	0.9569
	Water vs. Emulsion	0.9988
	Lotion vs. Emulsion	0.9696

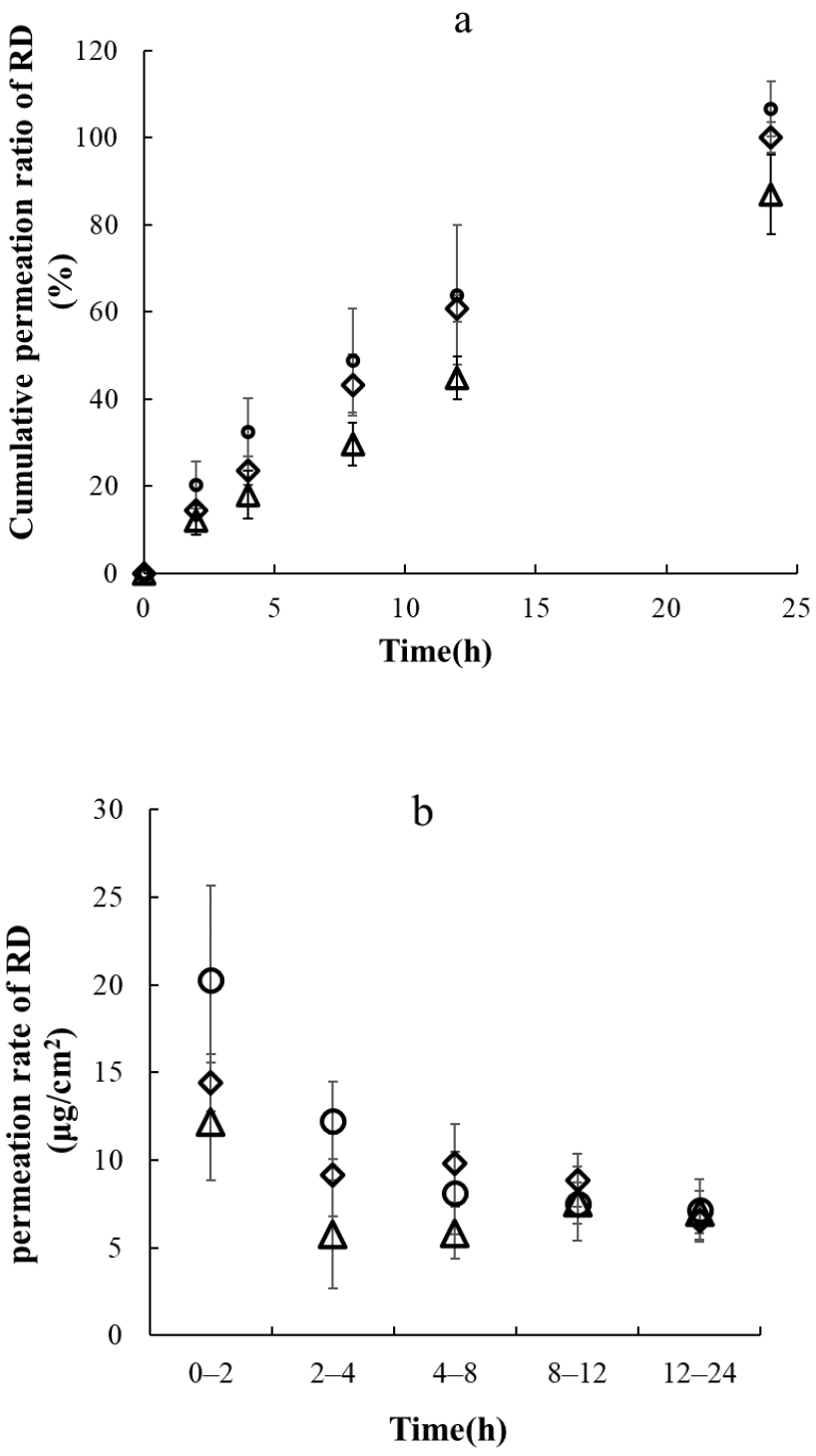

Figure 3-2. Cumulative rate of permeation of RD with different cosmetic formulations after different times (a) and permeation rates of RD with different cosmetic formulations in different time periods (b) under application of a 2% RD solution with a finite dose (○, water; ◇, lotion; and △, emulsion). Each point shows the mean ± standard deviation (n = 3).

3.3.3. Analysis of Unknown Substance

The 24-hours *in vitro* skin permeation study revealed an unknown peak at 210 nm in the HPLC chromatogram (Figure 3-3). To identify this peak, a variety of possible substances, including RK (m.w. 164.20 kD), was analyzed using HPLC. The detected chromatograms were compared, and the matching components were further confirmed using optimized LC–MS. As shown in Figure 3-3, the mass-to-charge ratio (*m/z*) of deprotonated anion for the authentic RK standard was 163.1 (Figure 3-4a). The same molecular ion peak with an *m/z* of 163.1 was detected in the sample (Figure 3-4b). Thus, LC–MS demonstrated that the unknown substance was RK.

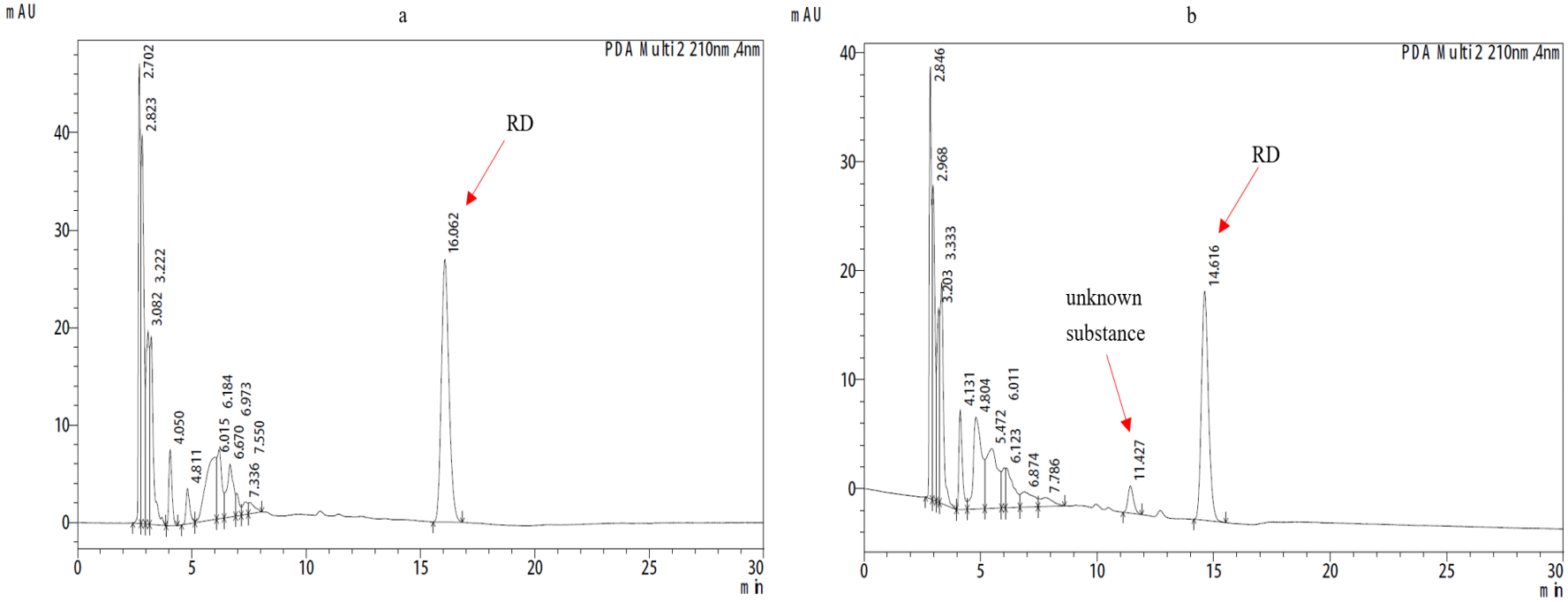

Figure 3-3. The unknown peak appearing at 210 nm on the HPLC chromatogram. (a), HPLC chromatogram of 4-h samples with water formulation; (b), HPLC chromatogram of 24-h samples with water formulation.

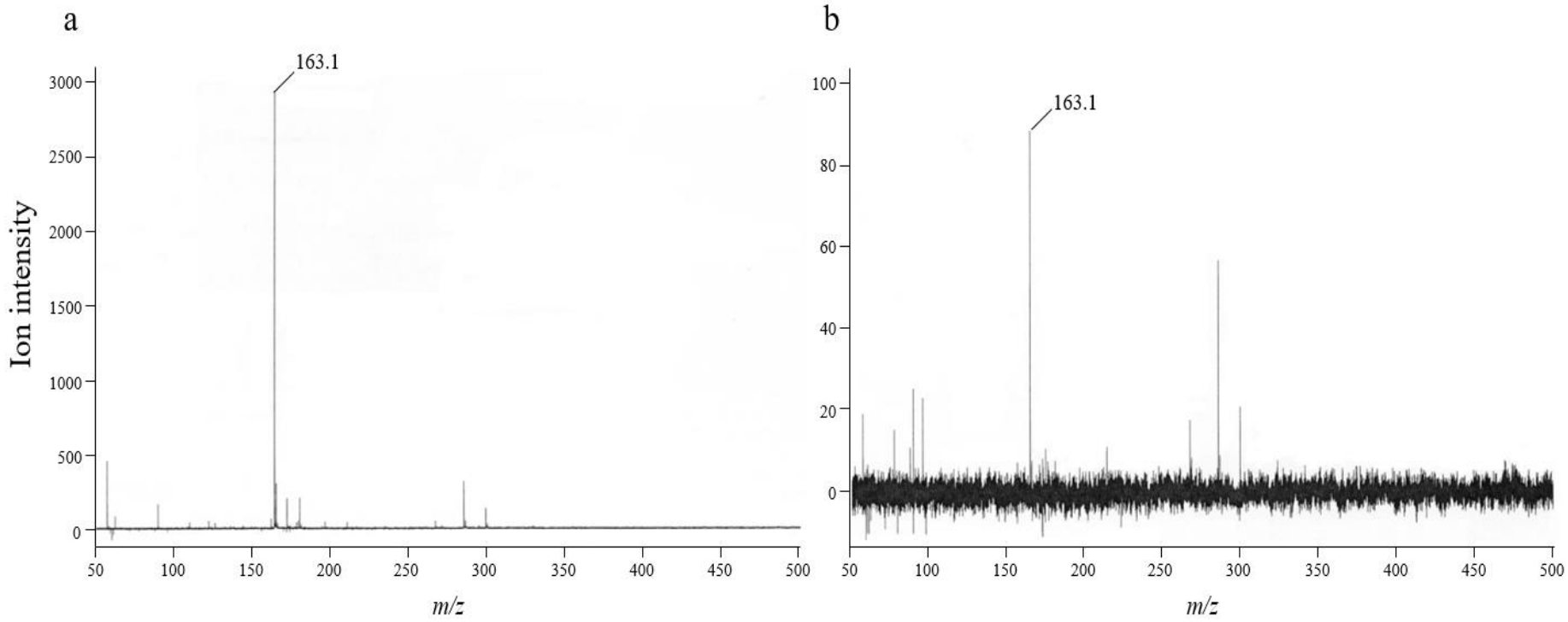

Figure 3-4. Mass spectra of different substances. Mass spectra of (a) RK standard and (b) RK in the sample.

3.3.4. RK Generation by the Skin with Different Treatments

RK generation after 24 hours in differently treated skin is shown in Table 3-6, and the graph comparing it is shown in Figure 3-5. Compared with the control, no RK production was observed in the aqueous or lotion formulations after heating the laboskin to 95 °C to deactivate the enzymes. RK production was observed in the emulsion formulation after heating the laboskin, but the amount produced was significantly lower than that in the control. No RK production was observed when the laboskin was not mounted in a Franz diffusion cell.

Table 3-6. RK concentration with differently skin treatment and cosmetics formulation.

Formulation	Skin treatment	RK concentration (μg/mL)		
		8h	12h	24h
Water	S	-	-	1.410±0.166
	NS	-	-	-
	HS	-	-	-
Lotion	S	-	-	1.469±0.412
	NS	-	-	-
	HS	-	-	-
Emulsion	S	-	-	2.118±0.258
	NS	-	-	-
	HS	-	-	0.324±0.110

* S, normal skin; NS, no skin; HS, heated skin.

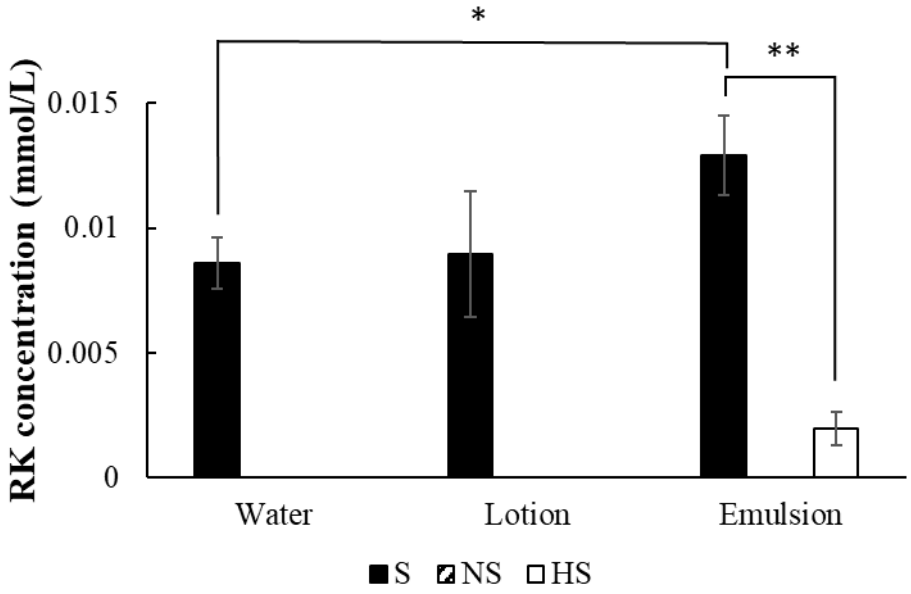

Figure 3-5. RK generation by the skin with different treatments. RK concentrations in 24-h samples are shown under application of a 2% RD solution with a finite dose (■, normal skin; ▨, no skin; and □, heated skin). *, $p < 0.05$, emulsion formulation vs. water formulation with the same normal skin; **, $p < 0.01$, heat treatment (−) vs. heat treatment (+) with the same emulsion formulation). RK concentrations of NS (water, lotion, and emulsion) and HS (water and lotion) were below the detection limit.

3.3.5. Conversion of RD to RK by ADH

As shown in Figure 3-6, the conversion of RD to RK after 30 min was not detected in the presence of any ADH dose, whereas partial conversion of RD to RK was observed after 60 min in the presence of ADH at ≥9.8 units/mL. Furthermore, after 120 min, RD was converted to RK in the presence of ADH at ≥0.98 units/mL. These results indicated that the effect was concen-tration- and time-dependent.

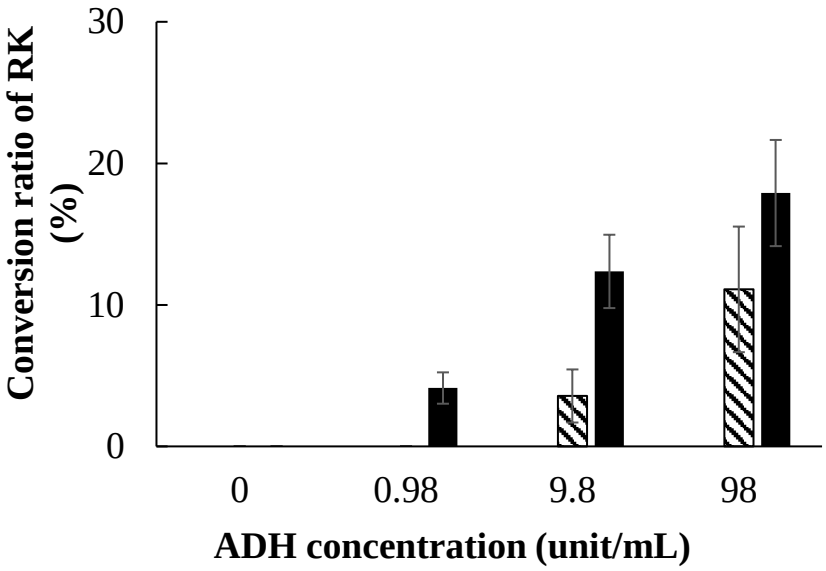

Figure 3-6. Conversion of RD to RK by alcohol dehydrogenase (ADH). The effect of different concentrations of ADH and different times on the RK conversion ratio is shown with the application of different doses of ADH (in final concentrations of 0, 0.98, 9.8, or 98 units/mL) after different times (□, 30 min; ▨, 60 min; and ■, 120 min). Data are presented as means ± standard deviation (n = 3). RK concentrations of 30 min (with the ADH concentration of 0, 0.98, 9.8, or 98 units/mL) and 60 min (with the ADH concentration of 0, 0.98 units/mL) were below the detection limit.

3.3.6. Metabolism of RD in Human Skin Homogenate

The metabolism of RD in human skin homogenates was examined at different concentration levels, which reflect the actual metabolism of RD in the skin after single and multiple applications of products containing 2% RD. The mass concentrations of RD and its metabolite RK in the skin homogenates at different times were obtained and the results are shown in Table 3-7 with Figure 3-7. In the control solution, no change in the concentration of RD was detected, whereas in the skin homogenate containing three different concentrations of RD at high, medium and low levels after 12 and 24 hours, there was decomposition of RD. The proportion of RD consumed appears to be independent of the concentration. In addition, higher concentrations of RK were detected in the NAD^+-containing group compared to the non-NAD^+-containing group. The above results suggest that the catabolism of RD was caused by the addition of skin

homogenates, i.e. there was metabolic catabolism of RD in the skin and the addition of NAD^+ promoted the metabolism of RD.

In addition, the consumption of RD-enantiomer was examined at different concentration levels in the presence or absence of 100 μmol/L NAD^+, and the results are shown in Table 3-7. The results showed that (S)-RD was more depleted than (R)-RD, regardless of the presence or absence of NAD^+. The consumption ratio of (S)-RD to (R)-RD in the skin homogenates with three different concentrations of RD at high, medium and low levels after 24 hours was a) 1.42, 1.63, 1.72; and b) 1.10, 1.88, 1.23.

Table 3-7. Comparison of the metabolism of RD to RK at different concentrations in human skin homogenate in the presence of NAD^+ after 12 h and 24 h.

	RD Concentration (μg/mL)	(S)-RD (%)	(R)-RD (%)	RK (%)	Consumption of (S)-RD (%)	Consumption of (R)-RD (%)	Consumption ratio of (S)-RD to (R)-RD
12h	100	50.24±0.80	49.76±0.80	-	-	-	-
	200	49.63±0.85	50.33±0.89	0.04±0.07	-	-	-
	300	49.10±0.60	50.83±0.57	0.07±0.08	-	-	-
12h NAD^+	100	43.51±0.61	44.86±0.78	11.63±0.74	6.49	5.14	1.26
	200	41.71±2.31	42.55±1.72	16.56±3.77	8.29	7.45	1.11
	300	42.21±2.44	44.13±1.95	13.66±4.31	7.78	5.87	1.32
24h	100	44.11±2.71	45.85±3.77	10.04±1.28	5.89	4.15	1.42
	200	43.15±1.20	45.81±1.40	11.04±0.32	6.85	4.19	1.63
	300	43.78±1.66	46.38±0.84	9.85±2.13	6.22	3.62	1.72
24h NAD^+	100	35.34±1.76	36.64±1.23	28.01±1.04	14.66	13.36	1.10
	200	30.31±8.96	39.53±3.65	30.16±5.48	19.69	10.47	1.88
	300	35.41±5.32	37.72±5.84	26.87±3.71	13.40	10.92	1.23

*Note that the concentrations of (S)-RD, (R)-RD, and RK have been converted into percentage form for the sake of clarity. Data are presented as means ± standard deviation (n = 3). RD, rhododendrol; (S)-RD, (S)-rhododendrol; (R)-RD, (R)-rhododendrol; RK, raspberry ketone; -, below the detection limit.

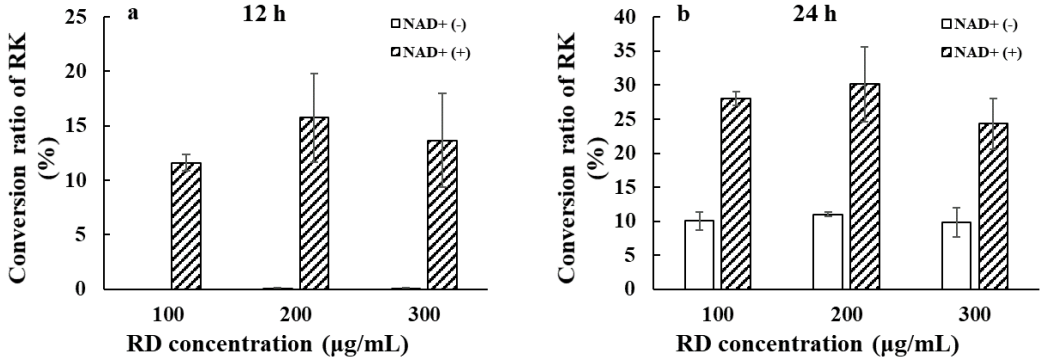

Figure 3-7. Comparison of the metabolism of RD to RK at different concentrations in human skin homogenate in the presence of NAD^+ after (a) 12 h; (b) 24 h. The RK conversion ratio is shown with the application of different doses (in final concentrations of 100, 200, 300 μg/mL) in the presence or absence of NAD^+ (□, NAD^+(-); ▨, NAD^+(+). Data are presented as means ± standard deviation (n = 3). Note that the concentrations of RK have been converted into percentage form for the sake of clarity. RD, rhododendrol; RK, raspberry ketone.

3.4. Discussion

As the living organism's boundary, the skin is the largest organ of the human body. It possesses key enzymes found in other tissues. Topically applied substances are metabolized in the skin and converted into medicinal or toxic substances [151]. Therefore, for drugs and cosmetics that are metabolized in the skin, the potential toxicity of the metabolites should be considered.

In this chapter, 15 mg of 2% RD solution was applied to 1.5 cm^2 of mouse skin—a dose of 10 mg/cm^2. Repeated applications increased the concentration of RD in the skin, which reflects the actual usage of the product. The tests reproduced the application of cosmetics, where the contact time with the skin is short. It is not scientifically correct to apply an infinite-volume test design, where a large amount of solution remains on the donor side, to a cosmetic product that evaporates after application. Moreover, as cosmetics, especially those aimed at brightening skin, are often applied at night before sleeping, the maximum duration for which they remain on the skin tends to exceed 8 hours. Therefore, it is scientifically appropriate to evaluate the safety of brightening cosmetics over an 8-hour duration. The 24-hour skin permeation test using finite-volume conditions revealed that some of the RD that penetrated the skin was oxidized to RK after the application of water and cosmetic formulations (lotion and emulsion) to the full-thickness dorsal skin from hairless mice. The emulsion formulation had a higher percentage of RD oxidized to RK compared with the lotion and water formulations.

In addition, in experiments evaluating the generation of RK in laboskin exposed to different formulations, it was found that any RD that did not penetrate the skin was not oxidized to RK when laboskin was not mounted in the Franz diffusion cell even when RD was added to PBS in the receptor chamber at 37°C. This result suggests that the oxidation of RD to RK is caused by skin and not by temperature. Furthermore, when the skin was heated to 95°C to deactivate skin enzymes, it was found that RD was not oxidized to RK in the water and lotion formulations. Some RD in the emulsion formulation was oxidized to RK, although significantly less than in the control (normal laboskin). This implies that enzymes in the skin may be involved in the oxidation of

RD to RK, and that some components in the emulsion formulation may also promote the oxidation of RD, which is supported by the fact that the oxidation ratio of RD was higher in the emulsion formulation than in the water formulation. In addition, the oxidation of RD to RK was also observed in the skin metabolism experiment using human skin homogenate. Therefore, the metabolism of RD to RK in the epidermis may be one of the mechanisms leading to increased susceptibility to leukoderma caused by cosmetics containing RD.

Some previous studies have suggested that RK has a risk of causing leukoderma [117,118]. According to a 1998 study, three workers engaged in RK generation suffered from leukoderma, and two of them were not completely cured [117,118]. RD-induced leukoderma appears to be due to the oxidation of RD by tyrosinase, and the quinone derivatives may cause melanocyte cytotoxicity through oxidative damage or induction of apoptosis [101,102,115]. RK-induced leukoderma appears to be due to destruction of melanocytes by the quinone derivatives of RK produced by the action of tyrosinase on RK [108,120], which is to a certain extent the same as the mechanism of RD-induced leukoderma. The metabolism from RD to RK, which is considered to be related to leukoderma, may also be another cause of leukoderma. Because RK has high economic value, many researchers try to oxidize RD in plants [66,67] to RK. It has been reported that RD is converted to RK by ADH [71–74] , or yeast or bacteria containing ADH [152,153]. As ADH is a ubiquitously expressed enzyme that is also present in human skin [25,26], it is possible that RD, a secondary alcohol, is oxidized to RK. Moreover, RD and RK are very similar compounds in terms of chemical structure and metabolic biosynthesis. Therefore, we investigated whether RD is converted to RK by ADH and confirmed that RD was converted to RK by ADH at a level of 0.98 unit/mL (3.27 nmol/mg protein/min) or higher. The reported ADH activity in the skin is 0.32–0.41 nmol/mg protein/min in humans and 1.07–1.21 nmol/mg protein/min in mice [20]. The above results indicating that RD is converted to RK by ADH in human skin, which is supported by the fact that RD was converted to RK after being metabolized by human skin, although the amount converted to RK was less than that of mouse skin. Further,

ADH activity has been reported to be lower in alcoholics/older people than in the general population/younger people [154]. It can therefore be assumed that RD is not readily metabolized to RK in alcoholics or the elderly.

Regarding the oxidative stability of the R- and S-enantiomers of secondary alcohols, it was reported that when a racemic mixture of secondary alcohols was added to the cultured cells of Catharanthus roseus, the S-enantiomer of the racemic mixture was rapidly oxidized to the ketone form; however, it was immediately, asymmetrically reduced to the R-enantiomer without being isolated, whereas the R-enantiomer was stable against the oxidation reaction [155]. There are many reports that the R- and S-enantiomers have different effects. For example, thalidomide was synthesized as a racemic mixture of equal amounts of R- and S-enantiomers; it was later reported that the R-enantiomer was harmless but the S-enantiomer was highly teratogenic and caused fetal abnormalities [156–160]. Ibuprofen is active only in the S-enantiomer; the R-enantiomer is converted to the S-enantiomer by enzymatic action in vivo [161–163]. These examples suggest the possibility that the S-enantiomer is more potent and toxic compared with the R-enantiomer. Therefore, chemically synthesized racemic mixtures should be thoroughly tested and carefully examined.

A previous study suggests that the R- and S-enantiomers of RD are substrates for tyrosinase, and the (S)-RD is more likely to be oxidized to quinone derivatives by human tyrosinase than the (R)-RD [100], and the oxidation rate of (S)-RD is about 1.5 times that of (R)-RD [100]. In the experiments in this chapter, it is also observed that the oxidation rate of (S)-RD is higher than that of (R)-RD, and the ratio is between 1 and 2. It was expected from the beginning of the development of cosmetics containing RD that if a product containing a 2% racemic mixture of RD is applied and the R-enantiomer is easily isomerized to the S-enantiomer in the skin, the effects and side effects of the product will be enhanced.

Finally, it was observed that as the NAD^+ concentration increases, more RD is metabolized to RK in the skin homogenate. NAD^+ is the coenzyme of ADH, and is involved in the metabolic conversion of secondary alcohols to aldehydes. It was

reported that aging leads to a decline in NAD^+ [31,32], and the NAD^+ in the skin of young adults (30-50 years) is more than twice that of middle age (51-70 years) [31]. It can therefore be assumed that RD is not readily metabolized to RK in the elderly.

In conclusion, it is confirmed that RD was partially metabolized to RK by mice skin and human skin, and the ADH in the skin may be the main reason for the appearance of this oxidation product in this chapter. Further, since RK was found to be less melanocyte cytotoxic than RD in chapter II, it can be assumed that the elderly and alcoholics are more likely to develop RD-induced leukoderma. This view is also confirmed by the third report of epidemiology based on a nationwide survey of rhododenol-induced leukoderma in Japan [164] that the majority of RD-induced leukoderma cases are in the elderly.

3.5. Conclusion

In this chapter, the mechanisms of RD-induced leukoderma have been further clarified. RD is partially metabolized to RK after cornified layer absorption, with enzymes in the skin appearing to be the cause. One such enzyme was found to be ADH. The intraepidermal oxidation of RD to RK may be one of the mechanisms of RD-induced susceptibility to leukoderma. Furthermore, the cosmetic ingredients of the emulsion formulation may promote the oxidation of RD to RK. In Chapter 2, RK was found to be less cytotoxic than RD, implying that the metabolism of RD in the skin may reduce the risk of RD-induced leukoderma.

Chapter IV

Inhibitory Effect and Mechanism of Scutellarein on Melanogenesis

4.1. Introduction

Scutellarein and baicalein (Figure 4-1) are bioactive flavones purified from the medicinal plant *Scutellaria baicalensis* Georgi (SBG) [165], which has been used for the treatment of various inflammatory diseases, hepatitis, tumors, and diarrhea in East Asian countries [166]. Low levels of scutellarein are observed in the aerial part of SBG; scutellarein exhibits high antioxidant activity [167], and is consequently used as a medicine to treat inflammation and neurological diseases [168]. Baicalein mainly accumulates in the roots of SBG and exhibits free radical-scavenging activity [169]. Additionally, studies have shown that SBG plant extracts inhibit melanogenesis [170]. However, there is no related research on the whitening effects of scutellarein and baicalein.

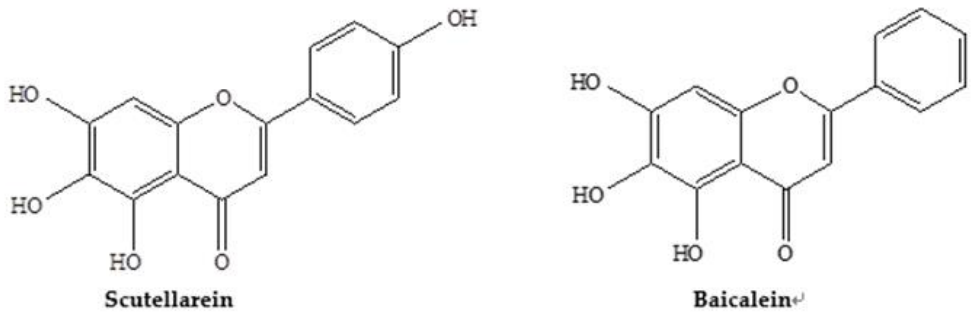

Figure 4-1. Chemical structure of scutellarein [5,6,7-trihydroxy-2-(4-hydroxyphenyl)-chromen-4-one] and baicalein (5,6,7-trihydroxy-2-phenyl-chromen-4-one) derived from SBG.

In this chapter, scutellarein and baicalein were used as experimental objects to explore their effects on melanin production in B16 cells. In the present study, 4-n-butylresorcinol was used as a positive control to examine the effect of scutellarein on the tyrosinase activity, cytotoxicity, and melanin content of B16 cells. The effects of

scutellarein on the expression of tyrosinase were also explored. Further, based on the *in vitro* method from the previous chapter, the potential of scutellarein to cause leukoderma was predicted by the measurement of the levels of hydroxyl radicals (·OH), as also its safety for use as a skin-lightening agent was evaluated.

4.2. Materials and Methods

4.2.1. Materials

Dulbecco's modified Eagle's medium (DMEM) + GlutaMAX^{TM} and 0.05% trypsin-ethylenediaminetetraacetic acid (EDTA) were purchased from Gibco (Thermo Fisher Scientific, Waltham, MA, USA). Phosphate-buffered saline (PBS) was purchased from TaKaRa Bio (Shiga, Japan). Fetal bovine serum, α-melanocyte stimulating hormone (α-MSH), and mushroom tyrosinase were purchased from Sigma-Aldrich (St. Louis, MO, USA). The cell counting kit-8 was purchased from Dojindo Laboratories (Kumamoto, Japan) and 20% HCl, NaCl, NaOH, 2-amino-2-hydroxymethyl-1,3-propanediol (Tris), glycine, 3-(3,4-dihydroxyphenyl)-l-alanine (L-DOPA), sodium dodecyl sulfate (SDS), sodium deoxycholate, 2-mercaptoethanol, dimethyl sulfoxide (DMSO), and rhododendrol were purchased from FUJIFILM Wako Pure Chemical (Osaka, Japan). Scutellarein and 4-n-butylresorcinol were purchased from the Tokyo Chemical Industry (Tokyo, Japan), Triton X-100 and Tween 20 were procured from Bio-Rad Laboratories (Alfred Nobel Drive Hercules, CA, USA), and hydroxyphenyl fluorescein (HPF; 5 μmol/L) was procured from Goryo Chemical (Sapporo, Japan).

4.2.2. Preparation of Test Compound

Scutellarein and baicalein solutions and 4-butylresorcinol solution were prepared with DMSO as the experimental and positive control groups, respectively.

4.2.3. Cell Culture

B16 mouse melanoma cells were cultured in DMEM containing 10% fetal bovine serum at 37 °C in a 5% CO_2 incubator. The cells were harvested using trypsin-EDTA.

4.2.4. Melanin Content Assay

B16 cells were cultured in a 100-mm dish (AGC Techno Glass, Shizuoka, Japan) at a concentration of 2.5 × 10^5 cells/mL for 24 h, then treated with the specific test compound and 20 ng/mL α-MSH at 37 °C in a 5% CO_2 incubator for 72 h. Cells were exposed to trypsin and shaken gently to remove all cells from the dish. The obtained solution was clarified by centrifugation at 10,000 rpm for 10 min, the supernatant was removed, and the pellet was dissolved in an NaOH solution per the number of cells. Absorbance of the cell suspension was measured at 475 nm using the multi-detection microplate reader.

4.2.5. Cellular Viability Assay

B16 cells were cultured in a 24-well microplate (Corning Coster, Corning, NY, USA) at a concentration of 1.25 × 10^5 cells/mL for 24 h and treated with the specific test compound at 37 °C in a 5% CO_2 incubator for 48 h. Cell counting kit-8 solution was added and the absorbance of the water-soluble formazan dye after 0 h and 2 h was measured at 450 nm using a multi-detection microplate reader. Cell viability was expressed as the difference between the two absorbance values.

4.2.6. Tyrosinase Activity Assay

B16 cells were cultured in a 96-well microplate (Corning Coster, Corning, NY, USA) at a concentration of 1.0 × 10^5 cells/mL for 24 h and treated with the specific test compound at 37 °C in a 5% CO_2 incubator for 48 h. Triton X-100 (10 μL), 10 mM L-DOPA (10 μL) and PBS (80 μL) were added, then the absorbance of dopachrome after 0 h and 2 h was measured at 475 nm using a multi-detection microplate reader (PowerScan HT; DS Pharma Biomedical Co. Ltd., Osaka, Japan). Tyrosinase activity was expressed as the difference between the two absorbance values.

4.2.7. Mushroom Tyrosinase Activity Assay

PBS (79 μL), the test compound (1 μL), and 10 mM L-DOPA (10 μL) with 100 U/mL mushroom tyrosinase (10 μL) were added to each 96-well plate. The absorbance of dopachrome after 0 min and 10 min was measured at 475 nm using a multi-detection microplate reader. Mushroom tyrosinase activity was expressed as the difference between the two absorbance values.

4.2.8. Western Blotting Assay

B16 cells cultured in a 100-mm dish at a concentration of 2.5×10^5 cells/mL for 24 h were treated with the specific test compound at 37 °C in a 5% CO_2 incubator for 72 h. Cells were washed with phosphate-buffered saline (PBS) three times and lysed with 2% sodium dodecyl sulfate (SDS) and 1% sodium deoxycholate (0.5 mL). Supernatants were collected as whole-cell lysates, and protein concentrations were determined using the BCA protein assay reagent (Thermo Fisher Scientific, Rockford, MA, USA). Each sample was adjusted to the same protein concentration and heated to 95 °C for 5 min. Proteins were separated by SDS polyacrylamide gel electrophoresis (SDS-PAGE) using a 4–20% gel (TEFCO, Hachioji, Japan), and then transferred to polyvinylidene fluoride (PVDF) membranes (Merck Millipore, Cork, Ireland). The membrane was blocked with 5% skim milk in tris-buffered saline (TBS) at room temperature for 30 min, then incubated with a mouse anti-β-actin antibody (diluted 1:1000; Proteintech Group, Rosemont, IL, USA) and a final anti-rabbit serum recognizing the anti-tyrosinase antibody (diluted 1:1000; Thermo Scientific) or anti-rabbit serum recognizing the microphthalmia-associated transcription factor (MITF) antibody (diluted 1:1000; Proteintech Group) with TBS at room temperature for 1 h. The membrane was washed three times with tris buffered saline with tween 20 (TBST) for 30 min and then incubated with a peroxidase-labeled anti-mouse antibody (GE Healthcare, Marlborough, MA, USA) for 30 min at room temperature. The membrane was washed three times with TBST for 3 h, and a western blotting detection reagent

(GE Healthcare) was added; the membrane was then incubated for 5 min at room temperature. Finally, immunoreactive bands were visualized using a Lumino Graph (ATTO, Tokyo, Japan).

4.2.9. Reverse Transcription qPCR (RT-qPCR) Assay

B16 cells cultured in 35-mm dishes at a concentration of 1.5×10^5 cells/mL for 24 h were treated with the specific test compound at 37 °C in a 5% CO_2 incubator. RNA was extracted from cells after 6, 12, and 24 h. Total RNA was prepared using the RNeasy Protect Mini Kit (QIAGEN, Hilden, Germany) according to the manufacturer's protocol. Total RNA was reverse transcribed to cDNA using the One Step TB Green™ PrimeScript™ RT-PCR Kit II (TaKaRa Bio) and oligo (dT) primers (QIAGEN). Real-time PCR was performed using the QuantStudio® 5 Real-Time PCR System (Applied Biosystems, Foster City, CA, USA). A reverse transcription reaction was carried out under the following conditions: 42 °C for 5 min and 95 °C for 10 s; PCR amplification: 95 °C for 5 s and 60 °C for 34 s; dissociation protocol: 95 °C for 15 s, 60 °C for 1 min, and 95 °C for 15 s. Expression levels of the tyrosinase gene were normalized to those of the glyceraldehyde-3-phosphate dehydrogenase gene (GAPDH). Relative changes in mRNA expression levels were calculated with the relative calibration method, and the levels were normalized to that of GAPDH. The experiment was performed in triplicate.

4.2.9. Measurements of Hydroxyl Radical (·OH)

PBS (78 μL), the specific test compound (2 μL), and HPF (5 μmol/L), with or without 100 U/mL mushroom tyrosinase (10 μL), were added to each 96-well plate and allowed to react at 37 °C. The fluorescence intensity of the compound generated by free hydroxyl radical (·OH) (excitation, 485 nm; fluorescence, 528 nm) was measured after 30 min using the multi-detection microplate reader.

4.2.10. Data Analysis

Data are expressed as mean ± standard deviation (SD). An unpaired *t*-test (two-tailed) was performed to compare the data of each test compound to the control data using an Excel for Microsoft Office Professional Plus 2016; $p < 0.05$ was considered statistically significant.

4.3. Results

4.3.1. Effects of Scutellarein and Baicalein on the Melanin Content of B16 Cells

When B16 cells were incubated with scutellarein and α-MSH, the cell pellet dissolved in the NaOH solution was visibly black. The color of the dissolved cell pellet was compared using NaOH at different concentrations, with the absorbance measured at 475 nm. Melanin content was significantly decreased in cells treated with 4-n-butylresorcinol and scutellarein compared with the untreated control; a clear dose-dependent decrease in cellular melanogenesis was observed (Figure 4-2a,b). To contrast, the color of the cell pellet dissolved in NaOH, corresponding to baicalein treatment at different concentrations, did not show any significant change, and there was no difference in absorbance (Figure 4-2c).

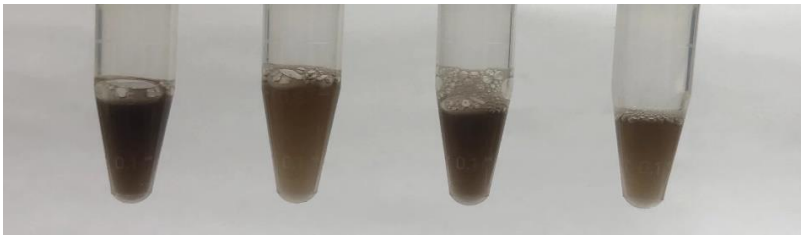

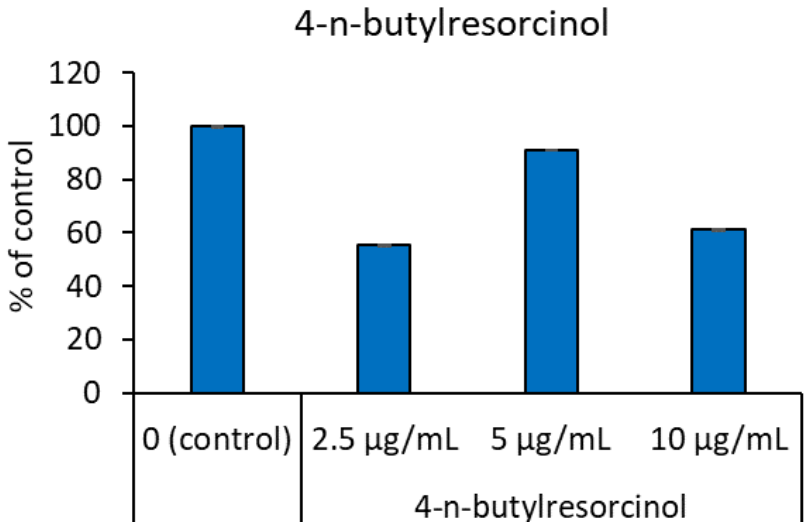

(a)

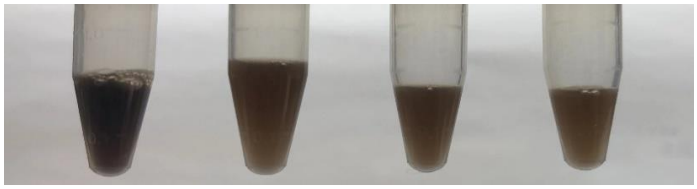

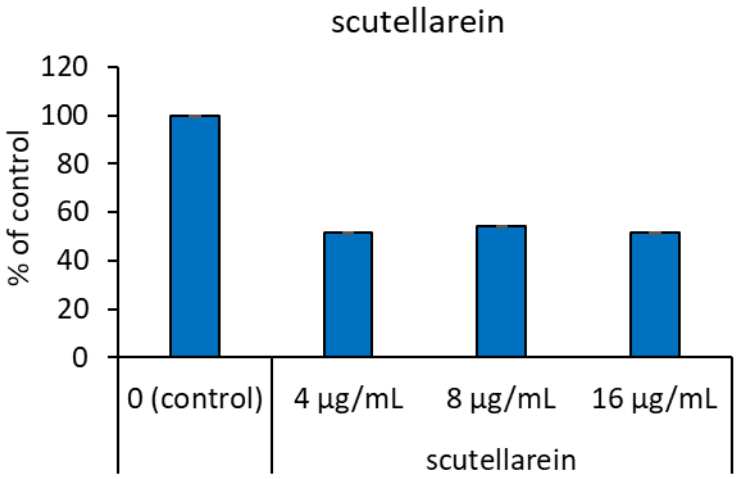

(b)

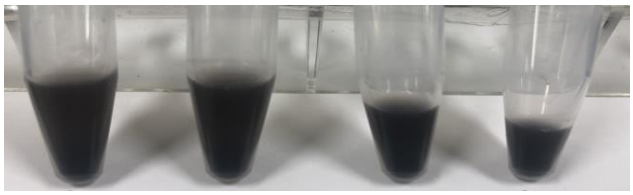

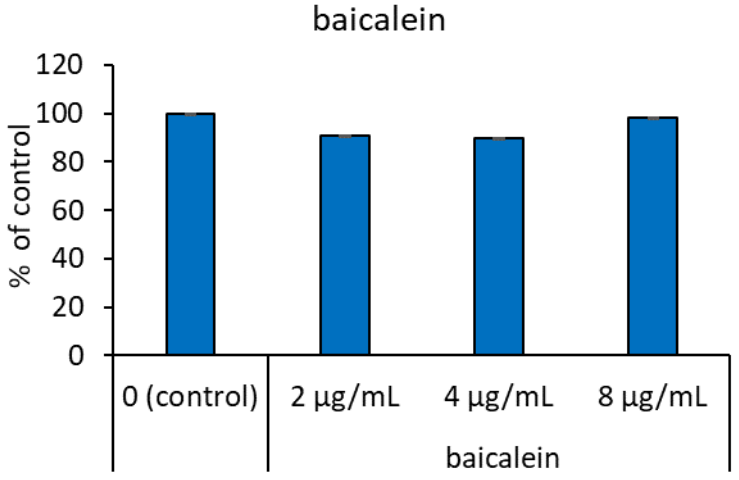

(c)

Figure 4-2. Effects of the tested compounds on the melanin content of B16 cells. The upper part of the figure shows the appearance of the cell suspension after the addition of the NaOH solution. The lower part of the figure represents the absorbance of the cell pellet dissolved in NaOH; absorbance was measured at 475 nm. Data are expressed as a percentage of the control. **(a)**: 4-n-butylresorcinol; **(b)**: scutellarein; **(c)**: baicalein.

4.3.2. Effects of Scutellarein on the Viability of B16 Cells

Cell viability was determined by reacting the cells with the cell counting kit-8 solution and measuring the absorbance of the water-soluble formazan dye at 450 nm. After cells were cultured in media containing different concentrations of 4-n-butylresorcinol or scutellarein for 48 h, there was no tendency toward a decreased cell viability, indicating that 4-n-butylresorcinol and scutellarein exhibited no cytotoxicity within the experimental concentration range (Figure 4-4a,b).

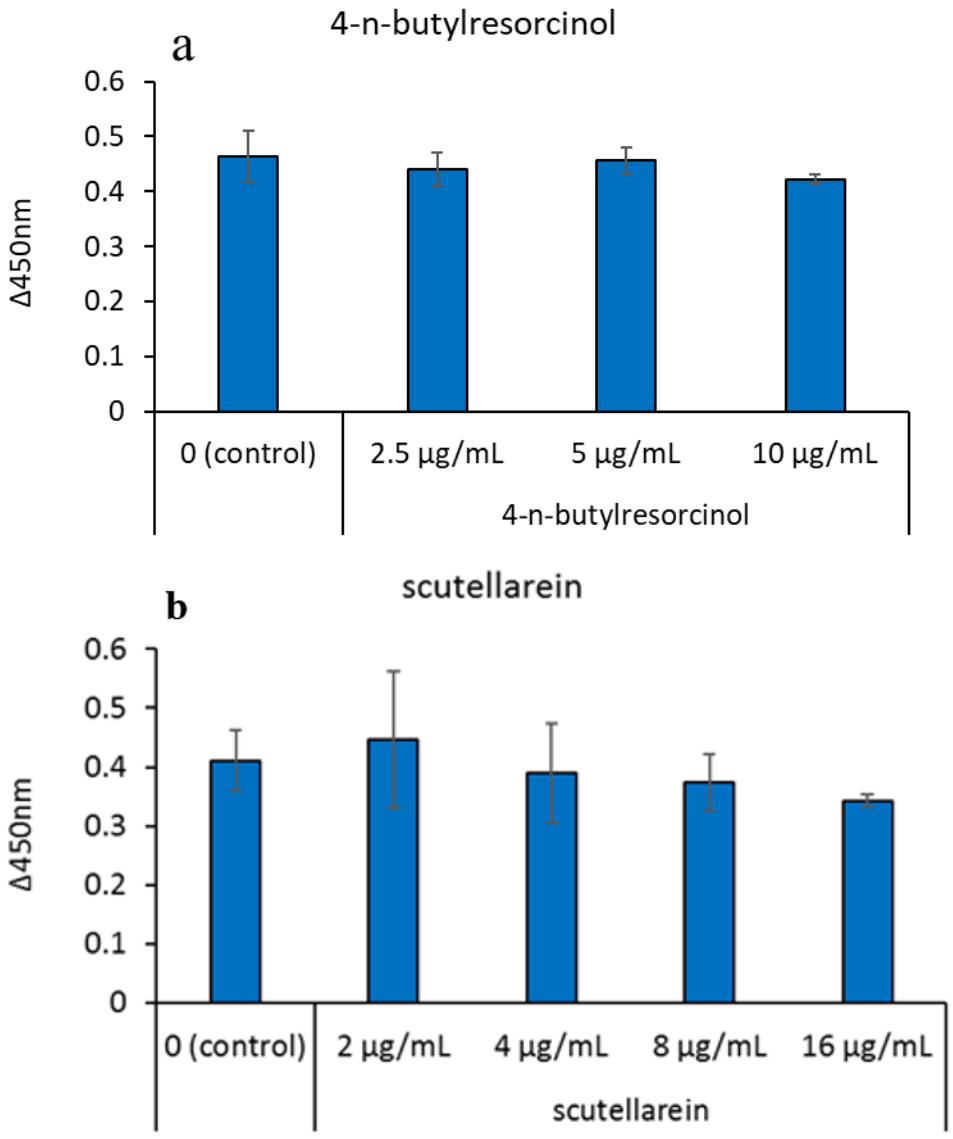

Figure 4-4. The effects of the tested compounds on the viability of B16 cells. Cell viability was determined by calculating the absorbance change rate in 2 h at 450 nm.

(a): 4-n-butylresorcinol; (b): scutellarein. Data are presented as the mean ± SD of experiments performed in triplicate.

4.3.3. Effects of Scutellarein on the Tyrosinase Activity in the Well

Tyrosinase is an important enzyme for melanin production, and its regulation is one of the factors affecting skin pigmentation [171]. Tyrosinase activity in the well was determined by adding L-DOPA to the cells and measuring absorbance of the produced dopachrome at 475 nm. In the positive control, 4-n-butylresorcinol dose-dependently inhibited tyrosinase activity at 2.5, 5, and 10 μg/mL (Figure 4-3a). Compared to the control group, when the concentration of scutellarein in the medium was 4 and 8 μg/mL, scutellarein dose-dependently inhibited tyrosinase activity (Figure 4-3b).

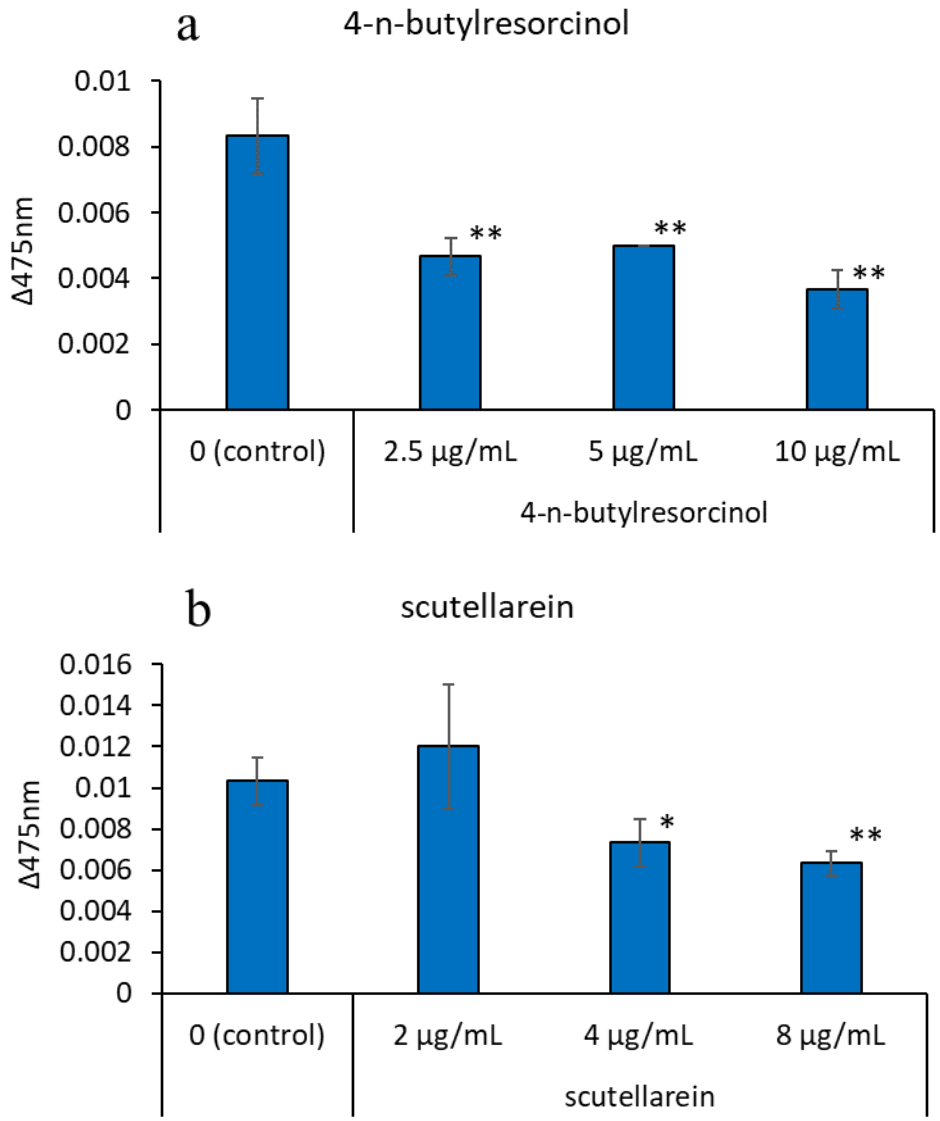

Figure 4-3. The effects of the tested compounds on the tyrosinase activity of B16 cells. Tyrosinase activity was determined by calculating the absorbance change rate in 2 h at 475 nm. (a), 4-n-butylresorcinol; (b): scutellarein. Data are presented as the mean ± SD of experiments performed in triplicate. * $p < 0.05$ compared to the control, ** $p < 0.01$ compared to the control.

4.3.4. Effects of Scutellarein and Baicalein on Mushroom Tyrosinase Activity

The inhibitory activity of scutellarein and baicalein on mushroom tyrosinase was investigated. 4-n-Butylresorcinol was used as a positive control. 4-n-Butylresorcinol showed a dose-dependent inhibitory effect, but scutellarein and baicalein did not inhibit the activity of mushroom tyrosinase (Figure 4-5).

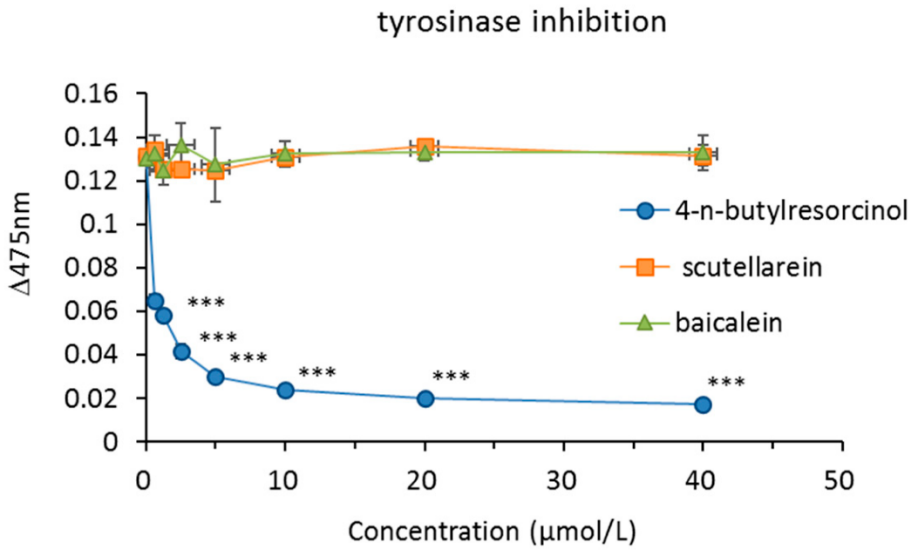

Figure 5. The effects of the tested compounds on mushroom tyrosinase activity. Mushroom tyrosinase activity was determined by calculating the absorbance change rate in 10 min at 475 nm. 4-n-butylresorcinol: 40 μmol/L (6.64 μg/mL), 20 μmol/L (3.32 μg/mL), 10 μmol/L (1.66 μg/mL), 5 μmol/L (0.83 μg/mL), 2.5 μmol/L (0.42 μg/mL), 1.25 μmol/L (0.21 μg/mL), 0.625 μmol/L (0.10 μg/mL). scutellarein: 40 μmol/L (11.44 μg/mL), 20 μmol/L (5.72 μg/mL), 10 μmol/L (2.86 μg/mL), 5 μmol/L (1.43 μg/mL), 2.5 μmol/L (0.72 μg/mL), 1.25 μmol/L (0.36 μg/mL), 0.625 μmol/L (0.18 μg/mL). baicalein: 40 μmol/L (10.8 μg/mL), 20 μmol/L (5.4 μg/mL), 10 μmol/L (2.7 μg/mL), 5 μmol/L (1.35 μg/mL), 2.5 μmol/L (0.68 μg/mL), 1.25 μmol/L (0.34 μg/mL), 0.625 μmol/L (0.17 μg/mL). * $p < 0.05$, ** $p < 0.01$, *** $p < 0.001$ compared to the control. Data are presented as the mean ± SD of experiments performed in triplicate.

4.3.5. Effects of Scutellarein on TYR and MITF Protein Expressions

To further elucidate the mechanism of scutellarein in melanogenesis, we focused on TYR and MITF protein expressions. Western blot analysis, using a specific antibody against tyrosinase, suggested that tyrosinase protein expression was inhibited in a dose-dependent manner when scutellarein concentration in the medium was 8 and 16 μg/mL ($p < 0.05$, $p < 0.05$, respectively; Figure 4-6a). Additionally, the expression of MITF also showed in a dose-dependent manner when scutellarein concentration in the medium was 4, 8, and 16 μg/mL ($p < 0.05$, $p < 0.05$, $p < 0.01$, respectively; Figure 4-6b).

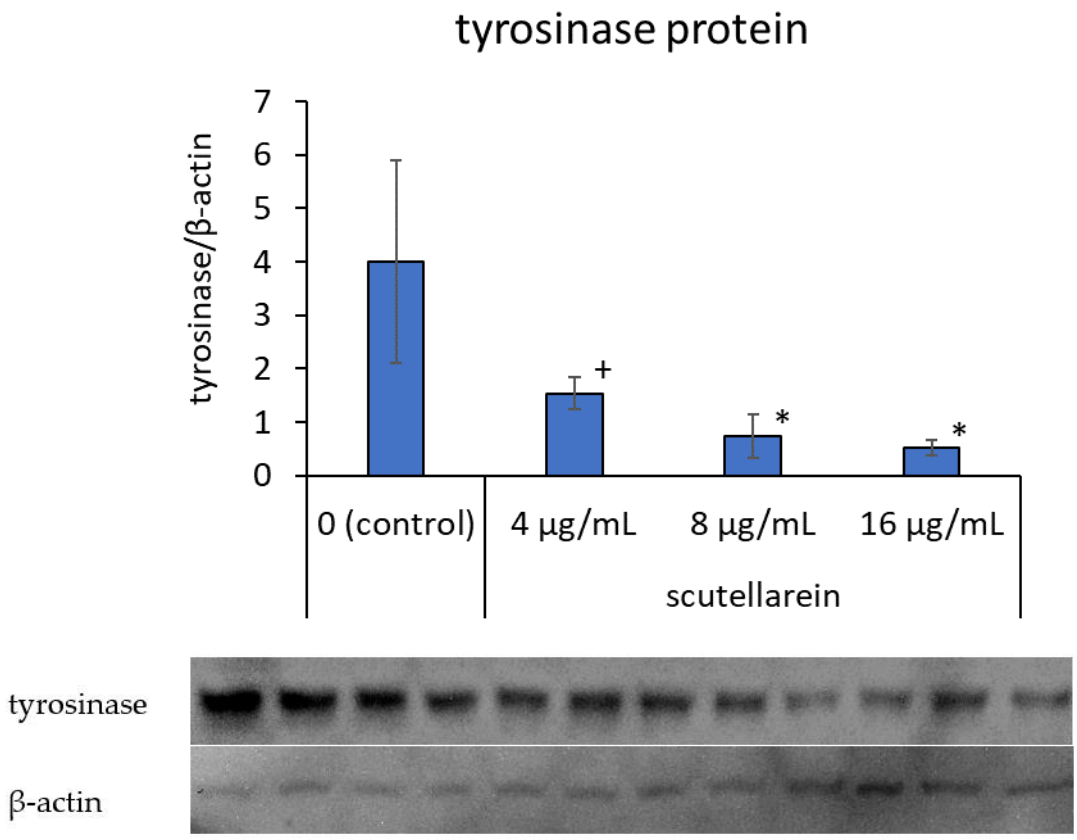

(a)

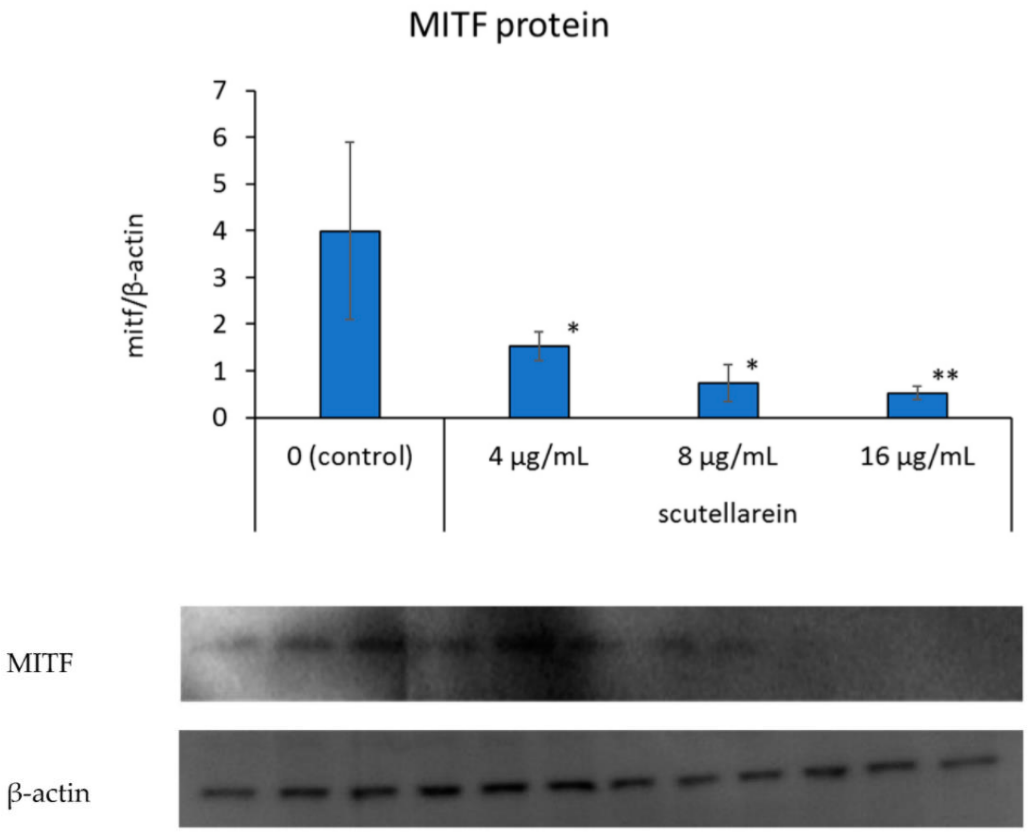

(b)

Figure 6. The effects of scutellarein on TYR protein (a) and MITF protein (b) expressions. B16 cells were treated with different concentrations of scutellarein for 48 h. Western blot analysis was then conducted using an anti-tyrosinase antibody or anti-MITF antibody; β-actin was used as a loading control. Fluorescence intensities of tyrosinase and β-actin were quantified using ImageJ. Band intensities were normalized to β-actin. Data are presented as the mean ± SD of experiments performed in triplicate. * $p < 0.05$ compared to the control. ** $p < 0.01$ compared to the control.

4.3.6. Effects of Scutellarein on Tyrosinase mRNA Expression

After adding scutellarein for 6, 12, and 24 h, tyrosinase mRNA expression in B16 cells was detected. However, quantitative analysis showed that after 6 and 12 h, tyrosinase mRNA expression in each concentration condition did not change significantly. After 24 h, tyrosinase mRNA levels were significantly downregulated at a concentration of 8 and 16 μg/mL ($p < 0.05$) in B16 cells, compared to the untreated control (Figure 4-7).

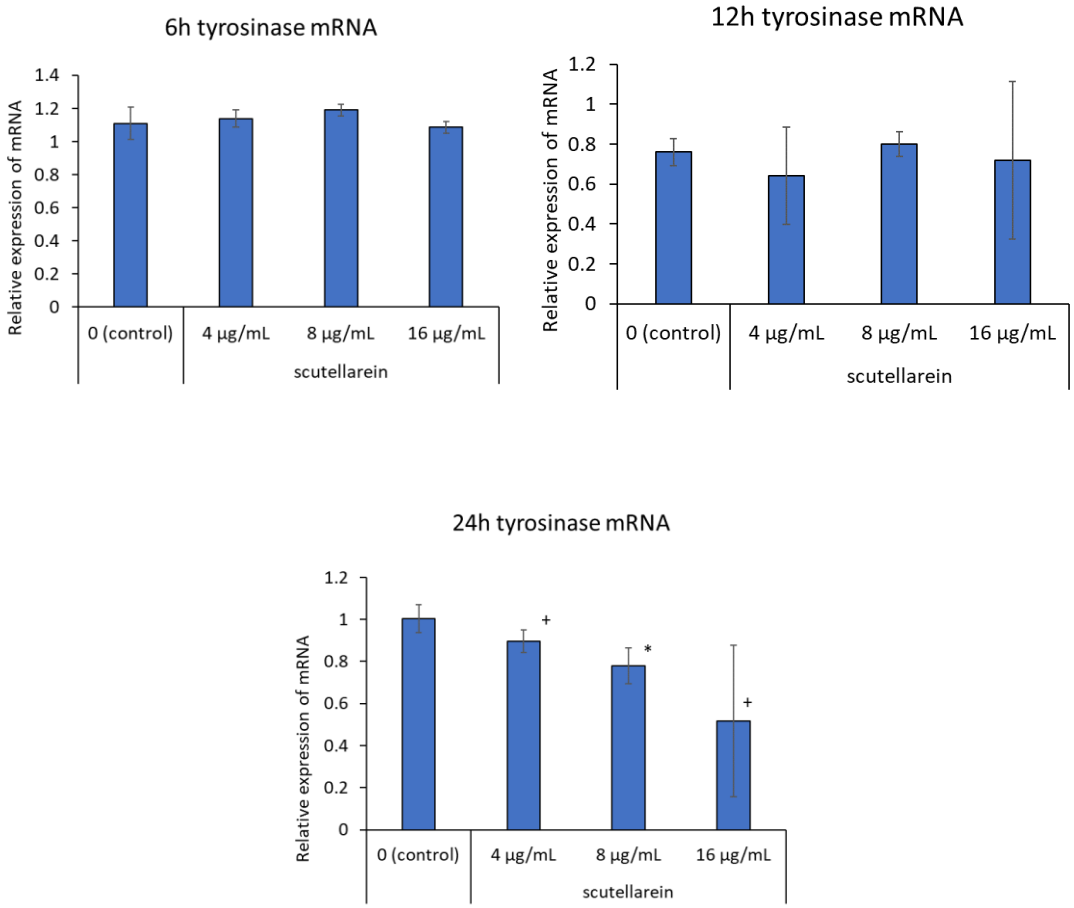

Figure 4-7. The effects of scutellarein on tyrosinase mRNA expression. B16 cells were treated with different concentrations of scutellarein for 6, 12, and 24 h. RT-qPCR analysis was then performed using the GAPDH as a loading control. Data are presented as the mean ± SD of experiments performed in triplicate. * $p < 0.05$ compared to the control.

4.3.7. Hydroxyl Radical(·OH) Generation from Scutellarein in the Presence of Tyrosinase

A comparison of the fluorescence intensity of the tested compounds in the presence of tyrosinase after 30 min is shown in Figure 4-8. The amount of free hydroxyl radicals (·OH) generated did not change in the absence of tyrosinase. Compared to the control group, RD was found to generate ·OH at 10 μmol/L (1.66 μg/mL), 100 μmol/L (16.6 μg/mL), and 1000 μmol/L (166 μg/mL). To contrast, the generation of ·OH at each concentration of scutellarein was significantly lower than the control level at 4 μg/mL

(14 μmol/L), 8 μg/mL (28 μmol/L), and 16 μg/mL (56 μmol/L) and, as the concentration increased, the levels of ·OH decreased.

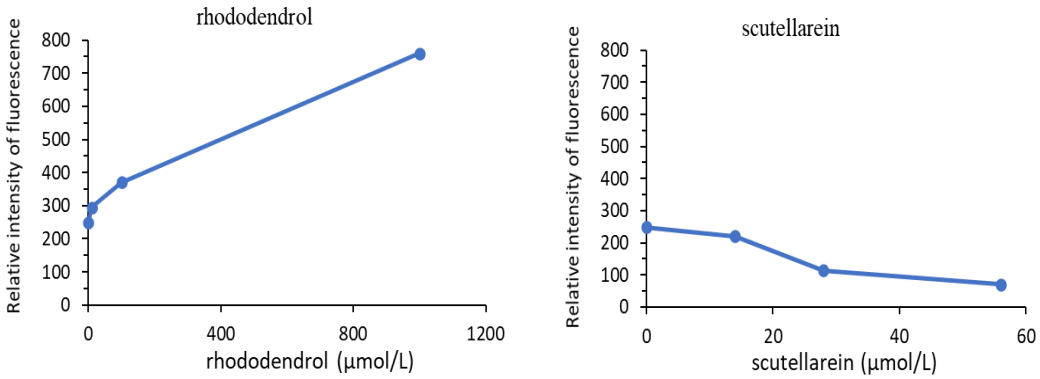

Figure 4-8. A comparison of ·OH generation by the tested compound in the presence of tyrosinase.

4.4. Discussion

As the molecular structure of melanin facilitates ultraviolet light absorption, it has the ability to resist ultraviolet light. Melanocytes are generally distributed in the hair, eyes, and skin [172]. Since the 21st century, researchers have discovered many whitening agents used in drugs for treating pigment diseases or skin-whitening cosmetics. Most whitening agents may be classified based on their different mechanisms of action, including the interference with melanin synthesis and transport and the acceleration of melanin decomposition [173].

Scutellarein and baicalein are flavones widely found in perennial herbs [174]. Presently, many scientists have confirmed that scutellarein has high anticancer activity and can be used as a drug for clinical treatment [175]. This chapter used three experiments assessing cytotoxicity, tyrosinase activity, and melanin content to explore the effects of baicalein and scutellarein on melanin production. We observed that scutellarein had an inhibitory effect on tyrosinase activity and showed no cytotoxicity at concentrations of 4 μg/mL, 8 μg/mL, and 16 μg/mL. In contrast, B16 cells treated with baicalein showed no change in tyrosinase activity per cell. The melanin content of B16 cells treated with scutellarein was significantly reduced after three days of culture; however, there was no change in the melanin content following baicalein treatment. Therefore, in subsequent experiments, baicalein was not used as the tested compound. The chemical structures of scutellarein and baicalein were compared, and it was found that scutellarein has a 4-hydroxyphenyl in the 2-position, which has a stronger reducibility than baicalein, which has a phenyl group at the 2-position. This may explain why baicalein did not show any melanin inhibitory effect. The 4-substituted phenolic (para-phenol) compounds were previously shown to be directly toxic to melanocytes in the presence of tyrosinase [80]. Measuring the amount of ·OH generated in the presence of tyrosinase is an *in vitro* method that predicts the risk of chemical leukoderma induce by a particular compound (Chapter II). Compared with RD, scutellarein showed no ·OH generation activity. Moreover, as the concentration of scutellarein increased, the ·OH generation activity showed a downward trend. Scutellarein has been reported to have

good antioxidant and anti-inflammatory effects, which may be one of the reasons for the inhibition of ·OH generation.

Additionally, the effect of scutellarein on tyrosinase expression was also tested. When scutellarein concentrations were 4 μg/mL, 8 μg/mL and 16 μg/mL, tyrosinase protein levels decreased. At the same time, tyrosinase mRNA levels decreased in a dose-dependent manner in the culture medium at concentrations of 4, 8, and 16 μg/mL. These results show that scutellarein affects melanin synthesis by inhibiting tyrosinase expression. However, in terms of gene expression, other factors that affect melanin production require further research.

In conclusion, the results revealed that scutellarein has an inhibitory effect on tyrosinase activity and melanin production at the concentration of any cytotoxicity; inhibition of ·OH generation was also observed. While investigating the mechanism of scutellarein's inhibition of melanin production, we found that tyrosinase expression was inhibited, which ultimately affected the synthesis of melanin in cells. To explore whether scutellarein could serve as a promising new skin-lightening agent, further experiments and research such as the cutaneous absorption experiment, concentration setting experiment, and clinical trials are needed.

4.5. Conclusion

In this chapter, scutellarein and baicalein were used as experimental objects to explore their effects on melanin production in B16 cells. After used three experiments assessing cytotoxicity, tyrosinase activity, and melanin content to explore the effects of baicalein and scutellarein, it was found that scutellarein has an inhibitory effect on tyrosinase activity, and shows no cytotoxicity at concentrations of 16 μg/mL or lower. In contrast, baicalein did not show an inhibitory effect on tyrosinase activity, and showed cytotoxicity. The reason may be the 4-hydroxyphenyl in the 2-position on structure of baicalein. Further, based on the *in vitro* method from the chapter II, the potential of scutellarein to cause leukoderma was predicted by the measurement of the levels of hydroxyl radicals (·OH), and scutellarein showed no ·OH generation activity. The above results indicate that scutellarein may be a safe brightening active ingredient with potential.

Chapter V Conclusion

Quasi-drug cosmetics containing RD, which was an active ingredient approved by the Ministry of Health, Labour and Welfare under the Pharmaceutical Affairs Law in Japan were voluntarily recalled after leukoderma was confirmed in people who had used them. This fact means that the existing quasi-drug cosmetics evaluation system has safety problems.

This study intends to develop an *in vitro* evaluation method for predicting the occurrence of leukoderma caused by the active ingredient in skin depigmentation quasi-drug cosmetics to replace the existing one.

In chapter II, the mechanisms of action and epidermal concentrations required of ingredients that are toxic to melanocytes, subsequently causing leukoderma have been further clarified. As a result, loss of melanocytes can follow the destruction of premelanosomes by ·OH generated by tyrosinase-mediated reactions, and the mechanism by which leukoderma onset occurs is the tyrosinase-mediated production of high amounts of ·OH; which damages melanosomes and in turn causes the apoptosis of melanocytes. Based on this result, an *in vitro* evaluation method for predicting the occurrence of leukoderma caused by the active ingredient in skin depigmentation quasi-drug cosmetics has been developed, and it was found that ARB and 4MSK has a high degree of safety, while RD, RK and ML has a very low degree of safety. It shows that RD and ML do not fulfill Japanese quasi-drug cosmetics standards for safety due to their risk of inducing leukoderma.

In chapter III, the skin permeation of RD in different dosage forms was studied using an *in vitro* skin permeation test, and an unknown skin metabolite was been found through the HPLC chromatogram. After using HPLC and LC–MS to characterize it, we found that the substance is RK, a raw material for production of RD. Since the emulsion formulation had a higher percentage of RD oxidized to RK compared with the lotion and water formulations, we wonder whether the cause of RK is the joint effect of skin

and formulation. For that, a skin permeation test again was been conducted after different treatments on skin (a, heated skin; b, no skin; and c, normal skin), to confirm whether temperature, enzymes in skin, or formulation is the cause of RK generation. As a result, it was found that both the enzymes in skin and the emulsion formulation caused the production of RK, and ADH in skin is the cause of RK generation. In addition, the oxidation of RD to RK was also observed in the skin metabolism experiment using human skin homogenate. Further, it was observed that as the NAD^+ concentration increases, more RD is metabolized to RK in the skin homogenate. This means that the deficiency of NAD^+ or ADH will reduces the metabolism of RD to RK. Based on the result that the melanocyte cytotoxicity of RD was higher than that of RK in Chapter II, it can be assumed that the metabolism of RD in the skin reduces its toxicity.

In chapter IV, scutellarein and baicalin, which has good anti-inflammatory effects has been selected to verify its brightening effect and safety. As a result, it was found that scutellarein has an inhibitory effect on tyrosinase activity, and shows no cytotoxicity at concentrations of 16 μg/mL or lower. In contrast, baicalein did not show an inhibitory effect on tyrosinase activity, and showed cytotoxicity. The 4-hydroxyphenyl in the 2-position on structure of baicalein may be the reason of it. Further, based on the *in vitro* method from the chapter II, compared with RD, scutellarein showed no ·OH generation activity. The above results indicate that scutellarein may be a safe brightening active ingredient with potential.

In summary, it is hoped that the study results can contribute to elucidating the mechanism of leukoderma induced by RD or other 4-substituted phenols. In addition, it is hoped that the new *in vitro* evaluation method can solve or reduce the safety issues of cosmetics.

References

1. Oguchi, K. Skin Function and Skin Care: Molecular Mechanisms of Melanin Production. *Life science* **2013**, 1–5.
2. Yoshikawa, kunihiro; Kawai, K. How the Skin Works and Its Function. *Journal of the Japan Reseach Association for textile end-uses* **1977**, *18*, 162–165, doi:10.11419/senshoshi1960.18.162.
3. Rawlings, A.V.; Harding, C.R. Moisturization and Skin Barrier Function. *Dermatologic Therapy* **2004**, *17*, 43–48, doi:10.1111/j.1396-0296.2004.04S1005.x.
4. Montagna, W.; Parakkal, P.F. 1 - An Introduction to Skin. In *The Structure & Function of Skin (Third Edition)*; Montagna, W., Parakkal, P.F., Eds.; Academic Press, 1974; pp. 1–17 ISBN 978-0-12-505263-4.
5. Montagna, W.; Parakkal, P.F. 2 - The Epidermis**With Contributions by Michael Im, Johns Hopkins Hospital, Baltimore. In *The Structure & Function of Skin (Third Edition)*; Montagna, W., Parakkal, P.F., Eds.; Academic Press, 1974; pp. 18–74 ISBN 978-0-12-505263-4.
6. Shimizu, H. Epidermis. In *New Dermatology (Third Edition)*; Nakayama Shoten, 2018; pp. 3–12 ISBN 978-4-521-74581-7.
7. Hunt, G.; Kyne, S.; Ito, S.; Wakamatsu, K.; Todd, C.; Thody, A.J. Eumelanin and Phaeomelanin Contents of Human Epidermis and Cultured Melanocytes. *Pigment Cell Research* **1995**, *8*, 202–208, doi:10.1111/j.1600-0749.1995.tb00664.x.
8. Riley, P.A. Melanin. *The International Journal of Biochemistry & Cell Biology* **1997**, *29*, 1235–1239, doi:10.1016/S1357-2725(97)00013-7.
9. Sinha, R.P.; Häder, D.-P. UV-Induced DNA Damage and Repair: A Review. *Photochem. Photobiol. Sci.* **2002**, *1*, 225–236, doi:10.1039/B201230H.
10. Pérez-Bernal, A.; Muñoz-Pérez, M.A.; Camacho, F. Management of Facial Hyperpigmentation. *Am J Clin Dermatol* **2000**, *1*, 261–268, doi:10.2165/00128071-200001050-00001.
11. Ito, S.; Wakamatsu, K. Quantitative Analysis of Eumelanin and Pheomelanin in Humans, Mice, and Other Animals: A Comparative Review. *Pigment Cell Research* **2003**, *16*, 523–531, doi:10.1034/j.1600-0749.2003.00072.x.
12. Swalwell, H.; Latimer, J.; Haywood, R.M.; Birch-Machin, M.A. Investigating the Role of Melanin in UVA/UVB- and Hydrogen Peroxide-Induced Cellular and Mitochondrial ROS Production and Mitochondrial DNA Damage in Human Melanoma Cells. *Free Radical Biology and Medicine* **2012**, *52*, 626–634, doi:10.1016/j.freeradbiomed.2011.11.019.
13. Ranadive, N.S.; Shirwadkar, S.; Persad, S.; Menon, I.A. Effects of Melanin-Induced Free Radicals on the Isolated Rat Peritoneal Mast Cells. *Journal of Investigative Dermatology* **1986**, *86*, 303–307, doi:10.1111/1523-1747.ep12285496.
14. Napolitano, A.; Panzella, L.; Monfrecola, G.; d'Ischia, M. Pheomelanin-Induced Oxidative Stress: Bright and Dark Chemistry Bridging Red Hair Phenotype and Melanoma. *Pigment Cell & Melanoma Research* **2014**, *27*, 721–733, doi:10.1111/pcmr.12262.
15. Smit, N.P.M.; Van Nieuwpoort, F.A.; Marrot, L.; Out, C.; Poorthuis, B.; Van Pelt, H.; Meunier, J.-R.; Pavel, S. Increased Melanogenesis Is a Risk Factor for Oxidative DNA

Damage— Study on Cultured Melanocytes and Atypical Nevus Cells†. *Photochemistry and Photobiology* **2008**, *84*, 550–555, doi:10.1111/j.1751-1097.2007.00242.x.
16. Fan, M.; Zhang, G.; Hu, X.; Xu, X.; Gong, D. Quercetin as a Tyrosinase Inhibitor: Inhibitory Activity, Conformational Change and Mechanism. *Food Research International* **2017**, *100*, 226–233, doi:10.1016/j.foodres.2017.07.010.
17. Wasmeier, C.; Hume, A.N.; Bolasco, G.; Seabra, M.C. Melanosomes at a Glance. *Journal of Cell Science* **2008**, *121*, 3995–3999, doi:10.1242/jcs.040667.
18. Holmes, R.S. Alcohol Dehydrogenases: A Family of Isozymes with Differential Functions. *Alcohol Alcohol Suppl* **1994**, *2*, 127–130.
19. Galter, D.; Carmine, A.; Buervenich, S.; Duester, G.; Olson, L. Distribution of Class I, III and IV Alcohol Dehydrogenase MRNAs in the Adult Rat, Mouse and Human Brain. *European Journal of Biochemistry* **2003**, *270*, 1316–1326, doi:10.1046/j.1432-1033.2003.03502.x.
20. Cheung, C.; Davies, N.G.; Hoog, J.-O.; Hotchkiss, S.A.M.; Smith Pease, C.K. Species Variations in Cutaneous Alcohol Dehydrogenases and Aldehyde Dehydrogenases May Impact on Toxicological Assessments of Alcohols and Aldehydes. *Toxicology* **2003**, *184*, 97–112, doi:10.1016/S0300-483X(02)00552-8.
21. Yin, S.-J.; Chou, C.-F.; Lai, C.-L.; Lee, S.-L.; Han, C.-L. Human Class IV Alcohol Dehydrogenase: Kinetic Mechanism, Functional Roles and Medical Relevance. *Chemico-Biological Interactions* **2003**, *143–144*, 219–227, doi:10.1016/S0009-2797(02)00167-9.
22. Smith, M.; Hopkinson, D.A.; Harris, H. Developmental Changes and Polymorphism in Human Alcohol Dehydrogenase. *Annals of Human Genetics* **1971**, *34*, 251–271, doi:10.1111/j.1469-1809.1971.tb00238.x.
23. Strömberg, P.; Höög, J.-O. Human Class V Alcohol Dehydrogenase (ADH5): A Complex Transcription Unit Generates C-Terminal Multiplicity. *Biochemical and Biophysical Research Communications* **2000**, *278*, 544–549, doi:10.1006/bbrc.2000.3837.
24. Höög, J.-O.; Brandt, M.; Hedberg, J.J.; Stromberg, P. Mammalian Alcohol Dehydrogenase of Higher Classes: Analyses of Human ADH5 and Rat ADH6. *Chemico-Biological Interactions* **2001**, *130–132*, 395–404, doi:10.1016/S0009-2797(00)00264-7.
25. Pyo, S.M.; Maibach, H.I. Skin Metabolism: Relevance of Skin Enzymes for Rational Drug Design. *SPP* **2019**, *4*, 283–294, doi:10.1159/000501732.
26. Cheung, C.; Smith, C.K.; Hoog, J.-O.; Hotchkiss, S.A.M. Expression and Localization of Human Alcohol and Aldehyde Dehydrogenase Enzymes in Skin. *Biochemical and Biophysical Research Communications* **1999**, *261*, 100–107, doi:10.1006/bbrc.1999.0943.
27. Zhang, Q.; Piston, D.W.; Goodman, R.H. Regulation of Corepressor Function by Nuclear NADH. *Science* **2002**, *295*, 1895–1897, doi:10.1126/science.1069300.
28. Lin, S.-J.; Guarente, L. Nicotinamide Adenine Dinucleotide, a Metabolic Regulator of Transcription, Longevity and Disease. *Current Opinion in Cell Biology* **2003**, *15*, 241–246, doi:10.1016/S0955-0674(03)00006-1.
29. Lin, Q.; Zuo, W.; Liu, Y.; Wu, K.; Liu, Q. NAD+ and Cardiovascular Diseases. *Clinica Chimica Acta* **2021**, *515*, 104–110, doi:10.1016/j.cca.2021.01.012.
30. Kim, H.-J.; Oh, G.-S.; Choe, S.-K.; Kwak, T.H.; Park, R.; So, H.-S. NAD+ Metabolism in Age-Related Hearing Loss. *Aging Dis* **2014**, *5*, 150–159, doi:10.14336/AD.2014.0500150.
31. Massudi, H.; Grant, R.; Braidy, N.; Guest, J.; Farnsworth, B.; Guillemin, G.J. Age-

Associated Changes In Oxidative Stress and NAD+ Metabolism In Human Tissue. *PLoS One* **2012**, *7*, e42357, doi:10.1371/journal.pone.0042357.
32. McReynolds, M.R.; Chellappa, K.; Baur, J.A. Age-Related NAD+ Decline. *Experimental Gerontology* **2020**, *134*, 110888, doi:10.1016/j.exger.2020.110888.
33. Fania, L.; Mazzanti, C.; Campione, E.; Candi, E.; Abeni, D.; Dellambra, E. Role of Nicotinamide in Genomic Stability and Skin Cancer Chemoprevention. *International Journal of Molecular Sciences* **2019**, *20*, 5946, doi:10.3390/ijms20235946.
34. Chandra, J.; Samali, A.; Orrenius, S. Triggering and Modulation of Apoptosis by Oxidative Stress. *Free Radical Biology and Medicine* **2000**, *29*, 323–333, doi:10.1016/S0891-5849(00)00302-6.
35. Schieber, M.; Chandel, N.S. ROS Function in Redox Signaling and Oxidative Stress. *Current Biology* **2014**, *24*, R453–R462, doi:10.1016/j.cub.2014.03.034.
36. Persson, T.; Popescu, B.O.; Cedazo-Minguez, A. Oxidative Stress in Alzheimer's Disease: Why Did Antioxidant Therapy Fail? *Oxidative Medicine and Cellular Longevity* **2014**, *2014*, e427318, doi:10.1155/2014/427318.
37. Jones, D.P. Redefining Oxidative Stress. *Antioxidants & Redox Signaling* **2006**, *8*, 1865–1879, doi:10.1089/ars.2006.8.1865.
38. López-Alarcón, C.; Denicola, A. Evaluating the Antioxidant Capacity of Natural Products: A Review on Chemical and Cellular-Based Assays. *Analytica Chimica Acta* **2013**, *763*, 1–10, doi:10.1016/j.aca.2012.11.051.
39. Lambeth, J.D. NOX Enzymes and the Biology of Reactive Oxygen. *Nat Rev Immunol* **2004**, *4*, 181–189, doi:10.1038/nri1312.
40. Brand, M.D. The Sites and Topology of Mitochondrial Superoxide Production. *Experimental Gerontology* **2010**, *45*, 466–472, doi:10.1016/j.exger.2010.01.003.
41. He, C.; Qureshi, A.A.; Han, J. Polymorphisms in Genes Involved in Oxidative Stress and Their Interactions with Lifestyle Factors on Skin Cancer Risk. *J Dermatol Sci* **2010**, *60*, 54–56, doi:10.1016/j.jdermsci.2010.07.003.
42. Rinnerthaler, M.; Bischof, J.; Streubel, M.K.; Trost, A.; Richter, K. Oxidative Stress in Aging Human Skin. *Biomolecules* **2015**, *5*, 545–589, doi:10.3390/biom5020545.
43. Bickers, D.R.; Athar, M. Oxidative Stress in the Pathogenesis of Skin Disease. *Journal of Investigative Dermatology* **2006**, *126*, 2565–2575, doi:10.1038/sj.jid.5700340.
44. Rünger, T.M. How Different Wavelengths of the Ultraviolet Spectrum Contribute to Skin Carcinogenesis: The Role of Cellular Damage Responses. *Journal of Investigative Dermatology* **2007**, *127*, 2103–2105, doi:10.1038/sj.jid.5700988.
45. Shukla, R.K.; Sharma, V.; Pandey, A.K.; Singh, S.; Sultana, S.; Dhawan, A. ROS-Mediated Genotoxicity Induced by Titanium Dioxide Nanoparticles in Human Epidermal Cells. *Toxicology in Vitro* **2011**, *25*, 231–241, doi:10.1016/j.tiv.2010.11.008.
46. Athar, M. Oxidative Stress and Experimental Carcinogenesis. *IJEB Vol.40(06) [June 2002]* **2002**.
47. Maulik, N.; McFadden, D.; Otani, H.; Thirunavukkarasu, M.; Parinandi, N.L. Antioxidants in Longevity and Medicine. *Oxidative Medicine and Cellular Longevity* **2013**, *2013*, e820679, doi:10.1155/2013/820679.
48. Cross, C.E.; Halliwell, B.; Borish, E.T.; Pryor, W.A.; Ames, B.N.; Saul, R.L.; McCORD, J.M.; Harman, D. Oxygen Radicals and Human Disease. *Ann Intern Med* **1987**, *107*, 526–

545, doi:10.7326/0003-4819-107-4-526.
49. Pisoschi, A.M.; Pop, A. The Role of Antioxidants in the Chemistry of Oxidative Stress: A Review. *European Journal of Medicinal Chemistry* **2015**, *97*, 55–74, doi:10.1016/j.ejmech.2015.04.040.
50. Chatterjee, N.; Walker, G.C. Mechanisms of DNA Damage, Repair, and Mutagenesis. *Environmental and Molecular Mutagenesis* **2017**, *58*, 235–263, doi:10.1002/em.22087.
51. Birch-Machin, M.A.; Swalwell, H. How Mitochondria Record the Effects of UV Exposure and Oxidative Stress Using Human Skin as a Model Tissue. *Mutagenesis* **2010**, *25*, 101–107, doi:10.1093/mutage/gep061.
52. Gniadecki, R.; Thorn, T.; Vicanova, J.; Petersen, A.; Wulf, H.C. Role of Mitochondria in Ultraviolet-Induced Oxidative Stress. *Journal of Cellular Biochemistry* **2001**, *80*, 216–222, doi:10.1002/1097-4644(20010201)80:2<216::AID-JCB100>3.0.CO;2-H.
53. Gruijl, F.R.D. P53 Mutations as a Marker of Skin Cancer Risk: Comparison of UVA and UVB Effects. *Experimental Dermatology* **2002**, *11*, 37–39, doi:10.1034/j.1600-0625.11.s.1.9.x.
54. Shimakura, H.; Sakata, K. The Effect of Brightness and Lightness on the Evaluation of Facial Skin Tone. *Journal of the Color Science Association of Japan* **2020**, *44*, 3, doi:10.15048/jcsaj.44.1_3.
55. Kao abolishes “whitening” expression Considering racial diversity discussion Available online: https://www.nikkei.com/article/DGXZQODZ25DD30V20C21A3000000/ (accessed on 7 September 2021).
56. “Whitening” cream and racism-cosmetics industry forced to change product name Available online: https://news.yahoo.co.jp/byline/mutsujishoji/20200702-00185818 (accessed on 7 September 2021).
57. Sachdeva, S. Fitzpatrick Skin Typing: Applications in Dermatology. *Indian J Dermatol Venereol Leprol* **2009**, *75*, 93, doi:10.4103/0378-6323.45238.
58. Tokunaga, H. Current Status and Prospects of Cosmetics and Quasi-Drugs. *Journal of Japanese Cosmetic Science Society* **2015**, *39*, 119–125, doi:10.11469/koshohin.39.119.
59. Inomata, S. Safety Assurance of Cosmetic in Japan: Current Situation and Future Prospects. *Journal of Oleo Science* **2014**, *63*, 1–6, doi:10.5650/jos.ess13501.
60. Maeda, K.; Fukuda, M. Arbutin: Mechanism of Its Depigmenting Action in Human Melanocyte Culture. *J Pharmacol Exp Ther* **1996**, *276*, 765–769.
61. Maeda, K.; Naganuma, M. Topical Trans-4-Aminomethylcyclohexanecarboxylic Acid Prevents Ultraviolet Radiation-Induced Pigmentation. *Journal of Photochemistry and Photobiology B: Biology* **1998**, *47*, 136–141, doi:10.1016/S1011-1344(98)00212-7.
62. Maeda, K.; Inoue, Y.; Nishikawa, H.; Miki, S.; Urushibata, O.; Miki, T.; Hatao, M. Involvement of Melanin Monomers in the Skin Persistent UVA-Pigmentation and Effectiveness of Vitamin C Ethyl on UVA-Pigmentation. *J. Jpn. Cosmet. Sci. Soc* **2003**, *27*, 257–268.
63. Kim, D.-S.; Kim, S.-Y.; Park, S.-H.; Choi, Y.-G.; Kwon, S.-B.; Kim, M.-K.; Na, J.-I.; Youn, S.-W.; Park, K.-C. Inhibitory Effects of 4-n-Butylresorcinol on Tyrosinase Activity and Melanin Synthesis. *Biological and Pharmaceutical Bulletin* **2005**, *28*, 2216–2219, doi:10.1248/bpb.28.2216.
64. Maeda, K. Advances in Development of Skin Whitening Agents. *Fragr. J.* **2008**, *36*, 65–67.

65. Kubo, M.; Inoue, T.; Nagai, M. Studies on the Constituents of Aceraceae Plants. III. Strucure of Acerogenin B from Acer Nikoense MAXIM. *Chemical & Pharmaceutical Bulletin* **1980**, *28*, 1300–1303, doi:10.1248/cpb.28.1300.
66. Parmar, V.S.; Vardhan, A.; Taneja, P.; Sinha, R.; Patnaik, G.K.; Tripathi, S.C.; Boll, P.M.; Larsen, S. Absolute Configuration of Epi-Rhododendrin and (–)-Rhododendrol [=(–)-Betuligenol] and X-Ray Crystal and Molecular Structure of Rhododendrin [= Betuloside], a Hepatoprotective Constituent of Taxus Baccata. *J. Chem. Soc., Perkin Trans. 1* **1991**, 2687–2690, doi:10.1039/P19910002687.
67. Srinivasa Reddy, P.; Jamil, K.; Madhusudhan, P.; Anjani, G.; Das, B. Antibacterial Activity of Isolates from Piper Longum and Taxus Baccata. *Pharmaceutical Biology* **2001**, *39*, 236–238, doi:10.1076/phbi.39.3.236.5926.
68. Fuchino, H.; Konishi, S.; Satoh, T.; Yagi, A.; Saitsu, K.; Tatsumi, T.; Tanaka, N. Chemical Evaluation of Betula Species in Japan. II. Constituents of Betula Platyphylla Var. Japonica. *Chemical & Pharmaceutical Bulletin* **1996**, *44*, 1033–1038, doi:10.1248/cpb.44.1033.
69. INOUE, T. Studies on the Constituents of Aceraceae Plants. I. Constituents in the Leaves and the Stem Bark of Acer Nikoense Maxim. *Chem Pharm Bull (Tokyo)* **1978**, *98*, 41–46.
70. Rao, S.; Kurakula, M.; Mamidipalli, N.; Tiyyagura, P.; Patel, B.; Manne, R. Pharmacological Exploration of Phenolic Compound: Raspberry Ketone—Update 2020. *Plants* **2021**, *10*, 1323, doi:10.3390/plants10071323.
71. Kosjek, B.; Stampfer, W.; Deursen, R. van; Faber, K.; Kroutil, W. Efficient Production of Raspberry Ketone via 'Green' Biocatalytic Oxidation. *Tetrahedron* **2003**, *59*, 9517–9521, doi:10.1016/j.tet.2003.10.019.
72. Becker, A.; Böttcher, D.; Katzer, W.; Siems, K.; Müller-Kuhrt, L.; Bornscheuer, U.T. An ADH Toolbox for Raspberry Ketone Production from Natural Resources via a Biocatalytic Cascade. *Appl Microbiol Biotechnol* **2021**, *105*, 4189–4197, doi:10.1007/s00253-021-11332-9.
73. Dumont, B.; Hugueny, P.; Belin, J.M. Preparation of Raspberry-like Ketones by Bioconversion 1996.
74. Musa, M.M. Enzymatic Production of Both Enantiomers of Rhododendrol. *Asian Journal of Chemistry* **2014**, *26*, 6719.
75. Ghosh, S. Chemical Leukoderma: What's New on Etiopathological and Clinical Aspects? *Indian J Dermatol* **2010**, *55*, 255–258, doi:10.4103/0019-5154.70680.
76. Bonamonte, D.; Vestita, M.; Romita, P.; Filoni, A.; Foti, C.; Angelini, G. Chemical Leukoderma. *Dermatitis* **2016**, *27*, 90–99, doi:10.1097/DER.0000000000000167.
77. O'Reilly K.E.; Patel U.; Chu J.; Patel R.; Machler B.C. Chemical leukoderma. *Dermatology Online Journal* **2011**, *17*, doi:10.5070/D36nc1w0nk.
78. Boissy, R.E.; Manga, P. On the Etiology of Contact/Occupational Vitiligo. *Pigment Cell Research* **2004**, *17*, 208–214, doi:10.1111/j.1600-0749.2004.00130.x.
79. Oliver, E.A.; Schwartz, L.; Warren, L.H. Occupational Leukoderma: Preliminary Report. *Journal of the American Medical Association* **1939**, *113*, 927–928, doi:10.1001/jama.1939.72800350003010a.
80. Smit, N.P.; Peters, K.; Menko, W.; Westerhof, W.; Pavel, S.; Riley, P.A. Cytotoxicity of a Selected Series of Substituted Phenols towards Cultured Melanoma Cells. *Melanoma Res* **1992**, *2*, 295–304, doi:10.1097/00008390-199212000-00002.

81. Kammeyer, A.; Willemsen, K.J.; Ouwerkerk, W.; Bakker, W.J.; Ratsma, D.; Pronk, S.D.; Smit, N.P.M.; Luiten, R.M. Mechanism of Action of 4-Substituted Phenols to Induce Vitiligo and Antimelanoma Immunity. *Pigment Cell & Melanoma Research* **2019**, *32*, 540–552, doi:10.1111/pcmr.12774.
82. Stratford, M.R.L.; Ramsden, C.A.; Riley, P.A. The Influence of Hydroquinone on Tyrosinase Kinetics. *Bioorganic & Medicinal Chemistry* **2012**, *20*, 4364–4370, doi:10.1016/j.bmc.2012.05.041.
83. van den Boorn, J.G.; Picavet, D.I.; van Swieten, P.F.; van Veen, H.A.; Konijnenberg, D.; van Veelen, P.A.; van Capel, T.; de Jong, E.C.; Reits, E.A.; Drijfhout, J.W.; et al. Skin-Depigmenting Agent Monobenzone Induces Potent T-Cell Autoimmunity toward Pigmented Cells by Tyrosinase Haptenation and Melanosome Autophagy. *Journal of Investigative Dermatology* **2011**, *131*, 1240–1251, doi:10.1038/jid.2011.16.
84. Hariharan, V.; Klarquist, J.; Reust, M.J.; Koshoffer, A.; McKee, M.D.; Boissy, R.E.; Caroline Le Poole, I. Monobenzyl Ether of Hydroquinone and 4-Tertiary Butyl Phenol Activate Markedly Different Physiological Responses in Melanocytes: Relevance to Skin Depigmentation. *Journal of Investigative Dermatology* **2010**, *130*, 211–220, doi:10.1038/jid.2009.214.
85. Frenk, E.; Ott, F. Evaluation of the Toxicity of the Monoethyl Ether of Hydroquinone for Mammalian Melanocytes and Melanoma Cells. *Journal of Investigative Dermatology* **1971**, *56*, 287–293, doi:10.1111/1523-1747.ep12261029.
86. Yang, F.; Sarangarajan, R.; Caroline Le Poole, I.; Boissy, R.E.; Medrano, E.E. The Cytotoxicity and Apoptosis Induced by 4-Tertiary Butylphenol in Human Melanocytes Are Independent of Tyrosinase Activity. *Journal of Investigative Dermatology* **2000**, *114*, 157–164, doi:10.1046/j.1523-1747.2000.00836.x.
87. SPENCER, M.C. Hydroquinone Bleaching: Submitted for Publication March 6, 1961. This Study Was Approved by the Veterans Administration Hospital, Danville, Ill. From the Department of Dermatology, Northwestern University Medical School, Chicago. *Archives of Dermatology* **1961**, *84*, 131–134, doi:10.1001/archderm.1961.01580130137022.
88. DORSEY, C.S. Dermatitic and Pigmentary Reactions to Monobenzyl Ether of Hydroquinone: Report of Two Cases. *A.M.A. Archives of Dermatology* **1960**, *81*, 245–248, doi:10.1001/archderm.1960.03730020081012.
89. Boyle, J.; Kennedy, C. t. c. Leucoderma Induced by Monomethyl Ether of Hydroquinone. *Clinical and Experimental Dermatology* **1985**, *10*, 154–158, doi:10.1111/j.1365-2230.1985.tb00544.x.
90. O'Sullivan, J.J.; Stevenson, C.J. Screening for Occupational Vitiligo in Workers Exposed to Hydroquinone Monomethyl Ether and to Paratertiary-Amyl-Phenol. *Occupational and Environmental Medicine* **1981**, *38*, 381–383, doi:10.1136/oem.38.4.381.
91. Ikeda, M.; Ohtsuji, H.; Miyahara, S. Two Cases of Leucoderma, Presumably Due to Nonyl- or Octylphenol in Synthetic Detergents. *Industrial health* **1970**, *8*, 192–196, doi:10.2486/indhealth.8.192.
92. James, O.; Mayes, R.W.; Stevenson, C.J. Occupational Vitiligo Induced by P-Tert-Butylphenol, a Systemic Disease? *The Lancet* **1977**, *310*, 1217–1219, doi:10.1016/S0140-6736(77)90451-2.
93. Nishigori, C.; Aoyama, Y.; Ito, A.; Suzuki, K.; Suzuki, T.; Tanemura, A.; Ito, M.; Katayama,

I.; Oiso, N.; Kagohashi, Y.; et al. Guide for Medical Professionals (i.e. Dermatologists) for the Management of Rhododenol-Induced Leukoderma. *The Journal of Dermatology* **2015**, *42*, 113–128, doi:10.1111/1346-8138.12744.

94. Homepage of Kanebo Cosmetics, Inc The Number of Checks of the White spots' Condition, and Recovery, a Reconciliation Situation/the Number of Object Recall. Available online: https://www.kanebo-cosmetics.jp/information/correspondence/ (accessed on 30 November 2021).
95. Kayoko, M.; Kayoko, S.; Tamio, S.; Yasuyuki, S.; Momoko, Y.; Shosuke, I.; Ichiro, K.; Akiko, Y.; Akiko, I.; Yukiko, M.; et al. Review Report 2018 on Rhododenol-Induced Leukoderma. *Jpn J Dermatol* **2018**, *128*, 2255–2267.
96. Tanemura, A.; Yang, L.; Yang, F.; Nagata, Y.; Wataya-Kaneda, M.; Fukai, K.; Tsuruta, D.; Ohe, R.; Yamakawa, M.; Suzuki, T.; et al. An Immune Pathological and Ultrastructural Skin Analysis for Rhododenol-Induced Leukoderma Patients. *Journal of Dermatological Science* **2015**, *77*, 185–188, doi:10.1016/j.jdermsci.2015.01.002.
97. Sasaki, M.; Kondo, M.; Sato, K.; Umeda, M.; Kawabata, K.; Takahashi, Y.; Suzuki, T.; Matsunaga, K.; Inoue, S. Rhododendrol, a Depigmentation-Inducing Phenolic Compound, Exerts Melanocyte Cytotoxicity via a Tyrosinase-Dependent Mechanism. *Pigment Cell & Melanoma Research* **2014**, *27*, 754–763, doi:10.1111/pcmr.12269.
98. Kasamatsu, S.; Hachiya, A.; Nakamura, S.; Yasuda, Y.; Fujimori, T.; Takano, K.; Moriwaki, S.; Hase, T.; Suzuki, T.; Matsunaga, K. Depigmentation Caused by Application of the Active Brightening Material, Rhododendrol, Is Related to Tyrosinase Activity at a Certain Threshold. *Journal of Dermatological Science* **2014**, *76*, 16–24, doi:10.1016/j.jdermsci.2014.07.001.
99. Goto, N.; Tsujimoto, M.; Nagai, H.; Masaki, T.; Ito, S.; Wakamatsu, K.; Nishigori, C. 4-(4-Hydroxyphenyl)-2-Butanol (Rhododendrol)-Induced Melanocyte Cytotoxicity Is Enhanced by UVB Exposure through Generation of Oxidative Stress. *Experimental Dermatology* **2018**, *27*, 754–762, doi:10.1111/exd.13555.
100. Ito, S.; Gerwat, W.; Kolbe, L.; Yamashita, T.; Ojika, M.; Wakamatsu, K. Human Tyrosinase Is Able to Oxidize Both Enantiomers of Rhododendrol. *Pigment Cell & Melanoma Research* **2014**, *27*, 1149–1153, doi:10.1111/pcmr.12300.
101. Ito, S.; Ojika, M.; Yamashita, T.; Wakamatsu, K. Tyrosinase-Catalyzed Oxidation of Rhododendrol Produces 2-Methylchromane-6,7-Dione, the Putative Ultimate Toxic Metabolite: Implications for Melanocyte Toxicity. *Pigment Cell & Melanoma Research* **2014**, *27*, 744–753, doi:10.1111/pcmr.12275.
102. Ito, S.; Okura, M.; Nakanishi, Y.; Ojika, M.; Wakamatsu, K.; Yamashita, T. Tyrosinase-Catalyzed Metabolism of Rhododendrol (RD) in B16 Melanoma Cells: Production of RD-Pheomelanin and Covalent Binding with Thiol Proteins. *Pigment Cell & Melanoma Research* **2015**, *28*, 295–306, doi:10.1111/pcmr.12363.
103. Arase, N.; Yang, L.; Tanemura, A.; Yang, F.; Suenaga, T.; Arase, H.; Katayama, I. The Effect of Rhododendrol Inhibition of NF-KB on Melanocytes in the Presence of Tyrosinase. *Journal of Dermatological Science* **2016**, *83*, 157–159, doi:10.1016/j.jdermsci.2016.05.002.
104. Lee, C.S.; Joo, Y.H.; Baek, H.S.; Park, M.; Kim, J.-H.; Shin, H.-J.; Park, N.-H.; Lee, J.H.; Park, Y.-H.; Shin, S.S.; et al. Different Effects of Five Depigmentary Compounds, Rhododendrol, Raspberry Ketone, Monobenzone, Rucinol and AP736 on Melanogenesis

and Viability of Human Epidermal Melanocytes. *Experimental Dermatology* **2016**, *25*, 44–49, doi:10.1111/exd.12871.

105. Yang, L.; Yang, F.; Wataya-Kaneda, M.; Tanemura, A.; Tsuruta, D.; Katayama, I. 4-(4-Hydroroxyphenyl)-2-Butanol (Rhododendrol) Activates the Autophagy-Lysosome Pathway in Melanocytes: Insights into the Mechanisms of Rhododendrol-Induced Leukoderma. *Journal of Dermatological Science* **2015**, *77*, 182–185, doi:10.1016/j.jdermsci.2015.01.006.
106. Okura, M.; Yamashita, T.; Ishii-Osai, Y.; Yoshikawa, M.; Sumikawa, Y.; Wakamatsu, K.; Ito, S. Effects of Rhododendrol and Its Metabolic Products on Melanocytic Cell Growth. *Journal of Dermatological Science* **2015**, *80*, 142–149, doi:10.1016/j.jdermsci.2015.07.010.
107. Nagata, T.; Ito, S.; Itoga, K.; Kanazawa, H.; Masaki, H. The Mechanism of Melanocytes-Specific Cytotoxicity Induced by Phenol Compounds Having a Prooxidant Effect, Relating to the Appearance of Leukoderma. *BioMed Research International* **2015**, *2015*, e479798, doi:10.1155/2015/479798.
108. Kim, M.; Baek, H.S.; Lee, M.; Park, H.; Shin, S.S.; Choi, D.W.; Lim, K.-M. Rhododenol and Raspberry Ketone Impair the Normal Proliferation of Melanocytes through Reactive Oxygen Species-Dependent Activation of GADD45. *Toxicology in Vitro* **2016**, *32*, 339–346, doi:10.1016/j.tiv.2016.02.003.
109. Miyaji, A.; Gabe, Y.; Kohno, M.; Baba, T. Generation of Hydroxyl Radicals and Singlet Oxygen during Oxidation of Rhododendrol and Rhododendrol-Catechol. *Journal of Clinical Biochemistry and Nutrition* **2017**, *60*, 86–92, doi:10.3164/jcbn.16-38.
110. Nagata, T.; Ito, S.; Itoga, K.; Kanazawa, H.; Masaki, H. Specific Cytotoxicities of Rhododenol and Raspberry Ketone on B16 Melanoma Cell by Increasing Intracellular Reactive Oxygen Species Levels. *Journal of Dermatological Science* **2016**, *84*, e82, doi:10.1016/j.jdermsci.2016.08.252.
111. Ito, S.; Okura, M.; Wakamatsu, K.; Yamashita, T. The Potent Pro-Oxidant Activity of Rhododendrol–Eumelanin Induces Cysteine Depletion in B16 Melanoma Cells. *Pigment Cell & Melanoma Research* **2017**, *30*, 63–67, doi:10.1111/pcmr.12556.
112. Inoue, S.; Katayama, I.; Suzuki, T.; Tanemura, A.; Ito, S.; Abe, Y.; Sumikawa, Y.; Yoshikawa, M.; Suzuki, K.; Yagami, A.; et al. Rhododendrol-Induced Leukoderma Update II: Pathophysiology, Mechanisms, Risk Evaluation, and Possible Mechanism-Based Treatments in Comparison with Vitiligo. *The Journal of Dermatology* **2021**, *48*, 969–978, doi:10.1111/1346-8138.15878.
113. Abe, Y.; Okamura, K.; Kawaguchi, M.; Hozumi, Y.; Aoki, H.; Kunisada, T.; Ito, S.; Wakamatsu, K.; Matsunaga, K.; Suzuki, T. Rhododenol-Induced Leukoderma in a Mouse Model Mimicking Japanese Skin. *Journal of Dermatological Science* **2016**, *81*, 35–43, doi:10.1016/j.jdermsci.2015.10.011.
114. Takagi, R.; Kawano, M.; Nakamura, K.; Tsuchida, T.; Matsushita, S. T-Cell Responses to Tyrosinase-Derived Self-Peptides in Patients with Leukoderma Induced by Rhododendrol: Implications for Immunotherapy Targeting Melanoma. *DRM* **2016**, *232*, 44–49, doi:10.1159/000441217.
115. Fujiyama, T.; Ikeya, S.; Ito, T.; Tatsuno, K.; Aoshima, M.; Kasuya, A.; Sakabe, J.; Suzuki, T.; Tokura, Y. Melanocyte-Specific Cytotoxic T Lymphocytes in Patients with Rhododendrol-Induced Leukoderma. *Journal of Dermatological Science* **2015**, *77*, 190–192, doi:10.1016/j.jdermsci.2015.01.017.

116. Nishioka, M.; Tanemura, A.; Yang, L.; Tanaka, A.; Arase, N.; Katayama, I. Possible Involvement of CCR4+CD8+ T Cells and Elevated Plasma CCL22 and CCL17 in Patients with Rhododenol-Induced Leukoderma. *Journal of Dermatological Science* **2015**, *77*, 188–190, doi:10.1016/j.jdermsci.2015.02.014.
117. Fukuda, Y.; Nagano, M.; Futatsuka, M. Occupational Leukoderma in Workers Engaged in 4-(p-Hydroxyphenyl)-2-Butanone Manufacturing. *Journal of Occupational Health* **1998**, *40*, 118–122, doi:10.1539/joh.40.118.
118. Fukuda, Y.; Nagano, M.; Tsukamoto, K.; Futatsuka, M. In Vitro Studies on the Depigmenting Activity of 4-(p-Hydroxyphenyl)-2-Butanone. *Journal of Occupational Health* **1998**, *40*, 137–142, doi:10.1539/joh.40.137.
119. Fukuda, Y.; Nagano, M.; Arimatsu, Y.; Futatsuka, M. An Experimental Study on Depigmenting Activity of 4-(p-Hydroxyphenyl)-2-Butanone in C57 Black Mice. *Journal of Occupational Health* **1998**, *40*, 97–102, doi:10.1539/joh.40.97.
120. Ito, S.; Hinoshita, M.; Suzuki, E.; Ojika, M.; Wakamatsu, K. Tyrosinase-Catalyzed Oxidation of the Leukoderma-Inducing Agent Raspberry Ketone Produces (E)-4-(3-Oxo-1-Butenyl)-1,2-Benzoquinone: Implications for Melanocyte Toxicity. *Chem. Res. Toxicol.* **2017**, *30*, 859–868, doi:10.1021/acs.chemrestox.7b00006.
121. Sugumaran, M.; Umit, K.; Evans, J.; Muriph, R.; Ito, S.; Wakamatsu, K. Oxidative Oligomerization of DBL Catechol, a Potential Cytotoxic Compound for Melanocytes, Reveals the Occurrence of Novel Ionic Diels-Alder Type Additions. *International Journal of Molecular Sciences* **2020**, *21*, 6774, doi:10.3390/ijms21186774.
122. Teshima, R. Allergies Due to Hydrolyzed Wheat. *Farumashia* **2013**, *49*, 116–120, doi:10.14894/faruawpsj.49.2_116.
123. Sugibayashi, K.; Todo, H.; Oda, A. Effect of Layered Application of Different Cosmeceutical Formulations Containing Rhododendrol. *Journal of Japanese Cosmetic Science Society* **2016**, *40*, 259–261, doi:10.11469/koshohin.40.259.
124. Arce, F.; Asano, N.; See, G.L.; Oshizaka, T.; Itakura, S.; Todo, H.; Sugibayashi, K. Prediction of Skin Permeation and Concentration of Rhododendrol Applied as Finite Dose from Complex Cosmetic Vehicles. *International Journal of Pharmaceutics* **2020**, *578*, 119186, doi:10.1016/j.ijpharm.2020.119186.
125. Arce, F.V.; Asano, N.; Yamashita, K.; Oda, A.; Uchida, T.; Sano, T.; Todo, H.; Sugibayashi, K. Effect of Layered Application on the Skin Permeation of a Cosmetic Active Component, Rhododendrol. *The Journal of Toxicological Sciences* **2019**, *44*, 1–11, doi:10.2131/jts.44.1.
126. Ito, S.; Wakamatsu, K. A Convenient Screening Method to Differentiate Phenolic Skin Whitening Tyrosinase Inhibitors from Leukoderma-Inducing Phenols. *Journal of Dermatological Science* **2015**, *80*, 18–24, doi:10.1016/j.jdermsci.2015.07.007.
127. Okmura, Y.; Shirai, T. Vitiliginous Lesions Occurring among Workers in a Phenol Derivative Factory. *Jpn J Dermatol* **1962**, *72*, 618.
128. Ebner, H.; Helletzgruber, M.; Höfer, R.; Kolbe, H.; Weissel, M.; Winker, N. Vitiligo from p-tert-butylphenol; a contribution to the problem of the internal manifestations of this occupational disease. *Derm Beruf Umwelt* **1979**, *27*, 99–104.
129. Budde, J.; Stary, A. Skin and systemic disease caused by occupational contact with p-tert-butylphenol. Case reports. *Derm Beruf Umwelt* **1988**, *36*, 17–19.
130. Rodermund, O.E.; Jörgens, H.; Müller, R.; Marsteller, H.J. Systemic changes in

occupational vitiligo. *Hautarzt* **1975**, *26*, 312–316.
131. Potts, R.O.; Guy, R.H. Predicting Skin Permeability. *Pharm Res* **1992**, *9*, 663–669, doi:10.1023/A:1015810312465.
132. Saruta, takao; Nakamizo, Y. Leukoplakia Due to Para-Tertiary Butyl Phenol. *Rinsho Derma (Tokyo)* **1974**, *16*, 161–170.
133. Yu, H. Study of Leukoplakia Due to Para-Tertiary Butyl Phenol. *The Japanese journal of dermatology* **1980**, *90*, 1129, doi:10.14924/dermatol.90.1129.
134. Leo, A.; Hansch, C.; Elkins, D. Partition Coefficients and Their Uses. *Chem. Rev.* **1971**, *71*, 525–616, doi:10.1021/cr60274a001.
135. Siddiqui, O. Physicochemical, Physiological, and Mathematical Considerations in Optimizing Percutaneous Absorption of Drugs. *Crit Rev Ther Drug Carrier Syst* **1989**, *6*, 1–38.
136. Cordero, J.A.; Alarcon, L.; Escribano, E.; Obach, R.; Domenech, J. A Comparative Study of the Transdermal Penetration of a Series of Nonsteroidal Antiinflammatory Drugs. *Journal of Pharmaceutical Sciences* **1997**, *86*, 503–508, doi:10.1021/js950346l.
137. Blank, I.H.; Scheuplein, R.J.; MacFarlane, D.J. 3. The Effect of Temperature on the Transport of Non-Electrolytes across the Skin. In *Mechanism of percutaneous absorption*; J. Investig. Dermatol., 1967; Vol. 49, pp. 582–589.
138. Oakley, D.M.; Swarbrick, J. Effects of Ionization on the Percutaneous Absorption of Drugs: Partitioning of Nicotine into Organic Liquids and Hydrated Stratum Corneum. *Journal of Pharmaceutical Sciences* **1987**, *76*, 866–871, doi:10.1002/jps.2600761204.
139. Tomita, Y.; Shibahara, S.; Takeda, A.; Okinaga, S.; Matsunaga, J.; Tagami, H. The Monoclonal Antibodies TMH-1 and TMH-2 Specifically Bind to a Protein Encoded at the Murine b-Locus, Not to the Authentic Tyrosinase Encoded at the c-Locus. *Journal of Investigative Dermatology* **1991**, *96*, 500–504, doi:10.1111/1523-1747.ep12470204.
140. Kuroda, Y.; Takahashi, Y.; Sakaguchi, H.; Matsunaga, K.; Suzuki, T. Depigmentation of the Skin Induced by 4-(4-Hydroxyphenyl)-2-Butanol Is Spontaneously Re-Pigmented in Brown and Black Guinea Pigs. *The Journal of Toxicological Sciences* **2014**, *39*, 615–623, doi:10.2131/jts.39.615.
141. Naish-Byfield, S.; Cooksey, C.J.; Latter, A.M.; Johnson, C.I.; Riley, P.A. In Vitro Assessment of the Structure-Activity Relationship of Tyrosinase-Dependent Cytotoxicity of a Series of Substituted Phenols. *Melanoma Res* **1991**, *1*, 273–287, doi:10.1097/00008390-199111000-00007.
142. Riley, P.A.; Cooksey, C.J.; Johnson, C.I.; Land, E.J.; Latter, A.M.; Ramsden, C.A. Melanogenesis-Targeted Anti-Melanoma pro-Drug Development: Effect of Side-Chain Variations on the Cytotoxicity of Tyrosinase-Generated Ortho-Quinones in a Model Screening System. *European Journal of Cancer* **1997**, *33*, 135–143, doi:10.1016/S0959-8049(96)00340-1.
143. Krol, E.S.; Bolton, J.L. Oxidation of 4-Alkylphenols and Catechols by Tyrosinase: Ortho-Substituents Alter the Mechanism of Quinoid Formation. *Chemico-Biological Interactions* **1997**, *104*, 11–27, doi:10.1016/S0009-2797(97)03763-0.
144. Bolton, J.L.; Pisha, E.; Shen, L.; Krol, E.S.; Iverson, S.L.; Huang, Z.; van Breemen, R.B.; Pezzuto, J.M. The Reactivity of O-Quinones Which Do Not Isomerize to Quinone Methides Correlates with Alkylcatechol-Induced Toxicity in Human Melanoma Cells. *Chemico-*

Biological Interactions **1997**, *106*, 133–148, doi:10.1016/S0009-2797(97)00066-5.
145. Sugumaran, M.; Bolton, J. Direct Evidence for Quinone-Quinone Methide Tautomerism during Tyrosinase Catalyzed Oxidation of 4-Allylcatechol. *Biochemical and Biophysical Research Communications* **1995**, *213*, 469–474, doi:10.1006/bbrc.1995.2155.
146. Thörneby-Andersson, K.; Sterner, O.; Hansson, C. Tyrosinase-Mediated Formation of a Reactive Quinone from the Depigmenting Agents, 4-Tert-Butylphenol and 4-Tert-Butylcatechol. *Pigment Cell Research* **2000**, *13*, 33–38, doi:10.1034/j.1600-0749.2000.130107.x.
147. Muñoz-Muñoz, J.L.; Garcia-Molina, F.; Varon, R.; Garcia-Ruíz, P.A.; Tudela, J.; Garcia-Cánovas, F.; Rodríguez-López, J.N. Suicide Inactivation of the Diphenolase and Monophenolase Activities of Tyrosinase. *IUBMB Life* **2010**, *62*, 539–547, doi:10.1002/iub.348.
148. Roberts, D.W.; Aptula, A.O. Allergic Contact Dermatitis Caused by a Skin-Lightening Agent, 5,5′-Dipropylbiphenyl-2,2′-Diol. A Comment. *Contact Dermatitis* **2012**, *66*, 357–359, doi:10.1111/j.1600-0536.2012.02098.x.
149. SUZUKI, K.; YAGAMI, A.; MATSUNAGA, K. Allergic Contact Dermatitis Caused by a Skin-Lightening Agent, 5,5'-Dipropylbiphenyl-2,2'-Diol. *Contact Dermatitis* **2012**, *66*, 51–52.
150. Yagami, A.; Suzuki, K.; Sano, A.; Takahashi, M.; Kobayashi, T.; Morita, Y.; Ando, A.; Iwata, Y.; Matsunaga, K. Rhododendrol-Induced Leukoderma Accompanied by Allergic Contact Dermatitis Caused by a Non-Rhododendrol Skin-Lightening Agent, 5,5′-Dipropylbiphenyl-2,2′-Diol. *The Journal of Dermatology* **2015**, *42*, 739–740, doi:10.1111/1346-8138.12878.
151. Hisatomi, A.; Kimura, M.; Maeda, M.; Matsumoto, M.; Ohara, K.; Noguchi, H. Toxicity of Polyoxyethylene Hydrogenated Castor Oil 60 (Hco-60) in Experimental Animals. *The Journal of Toxicological Sciences* **1993**, *18*, 1–9, doi:10.2131/jts.18.SupplementIII_1.
152. Fronza, G.; Fuganti, C.; Pedrocchi-Fantoni, G.; Serra, S.; Zucchi, G.; Fauhl, C.; Guillou, C.; Reniero, F. Stable Isotope Characterization of Raspberry Ketone Extracted from Taxus Baccata and Obtained by Oxidation of the Accompanying Alcohol (Betuligenol). *J. Agric. Food Chem.* **1999**, *47*, 1150–1155, doi:10.1021/jf980717u.
153. Paul, C.E.; Lavandera García, I.; Gotor Fernández, V.; Kroutil, W.; Gotor Santamaría, V.M. Escherichia Coli/ADH-A: An All-Inclusive Catalyst for the Selective Biooxidation and Deracemisation of Secondary Alcohols. *ChemCatChem* **2013**.
154. Seitz, H.K.; Egerer, G.; Simanowski, U.A.; Waldherr, R.; Eckey, R.; Agarwal, D.P.; Goedde, H.W.; Wartburg, J.P. von Human Gastric Alcohol Dehydrogenase Activity: Effect of Age, Sex, and Alcoholism. *Gut* **1993**, *34*, 1433–1437, doi:10.1136/gut.34.10.1433.
155. Takemoto, M.; Achiwa, K. Deracemization of Racemic 4-Pyridyl-1-Ethanol by Catharanthus Roseus Cell Cultures. *Phytochemistry* **1998**, *49*, 1627–1629, doi:10.1016/S0031-9422(98)00241-6.
156. Blaschke, G.; Kraft, H.P.; Fickentscher, K.; Köhler, F. Chromatographic separation of racemic thalidomide and teratogenic activity of its enantiomers. *Arzneimittelforschung* **1979**, *29*, 1640–1642.
157. Knoche, B.; Blaschke, G. Investigations on the in Vitro Racemization of Thalidomide by High-Performance Liquid Chromatography. *Journal of Chromatography A* **1994**, *666*, 235–

240, doi:10.1016/0021-9673(94)80385-4.
158. Tokunaga, E.; Yamamoto, T.; Ito, E.; Shibata, N. Understanding the Thalidomide Chirality in Biological Processes by the Self-Disproportionation of Enantiomers. *Scientific reports* **2018**, *8*, 1–7.
159. Nishimura, K.; Hashimoto, Y.; Iwasaki, S. (S)-Form of Alpha-Methyl-N(Alpha)-Phthalimidoglutarimide, but Not Its (R)-Form, Enhanced Phorbol Ester-Induced Tumor Necrosis Factor-Alpha Production by Human Leukemia Cell HL-60: Implication of Optical Resolution of Thalidomidal Effects. *Chemical & Pharmaceutical Bulletin* **1994**, *42*, 1157–1159, doi:10.1248/cpb.42.1157.
160. Jacques, V.; Czarnik, A.W.; Judge, T.M.; Van der Ploeg, L.H.; DeWitt, S.H. Differentiation of Antiinflammatory and Antitumorigenic Properties of Stabilized Enantiomers of Thalidomide Analogs. *Proceedings of the National Academy of Sciences* **2015**, *112*, E1471–E1479.
161. Reichel, C.; Brugger, R.; Bang, H.; Geisslinger, G.; Brune, K. Molecular Cloning and Expression of a 2-Arylpropionyl-Coenzyme A Epimerase: A Key Enzyme in the Inversion Metabolism of Ibuprofen. *Mol Pharmacol* **1997**, *51*, 576–582, doi:10.1124/mol.51.4.576.
162. Ikuta, H.; Kawase, A.; Iwaki, M. Stereoselective Pharmacokinetics and Chiral Inversion of Ibuprofen in Adjuvant-Induced Arthritic Rats. *Drug Metab Dispos* **2017**, *45*, 316–324, doi:10.1124/dmd.116.073239.
163. Kaiser, D.G.; Vangiessen, G.J.; Reischer, R.J.; Wechter, W.J. Isomeric Inversion of Ibuprofen (R)-enantiomer in Humans. *Journal of Pharmaceutical Sciences* **1976**, *65*, 269–273, doi:10.1002/jps.2600650222.
164. Akiko, I.; Yumi, A.; Kayoko, S. The Third Report of Epidemiology Based on a Nationwide Survey of Rhododenol-Induced Leukoderma in Japan. *Jpn J Dermatol* **2015**, *125*, 2401–2414, doi:10.14924/dermatol.125.2401.
165. Nurul Islam, M.; Downey, F.; Ng, C.K.Y. Comparative Analysis of Bioactive Phytochemicals from Scutellaria Baicalensis, Scutellaria Lateriflora, Scutellaria Racemosa, Scutellaria Tomentosa and Scutellaria Wrightii by LC-DAD-MS. *Metabolomics* **2011**, *7*, 446–453, doi:10.1007/s11306-010-0269-9.
166. Han, J.; Ye, M.; Xu, M.; Sun, J.; Wang, B.; Guo, D. Characterization of Flavonoids in the Traditional Chinese Herbal Medicine-Huangqin by Liquid Chromatography Coupled with Electrospray Ionization Mass Spectrometry. *Journal of Chromatography B* **2007**, *848*, 355–362, doi:10.1016/j.jchromb.2006.10.061.
167. Sadasivam, K.; Kumaresan, R. A Comparative DFT Study on the Antioxidant Activity of Apigenin and Scutellarein Flavonoid Compounds. *Molecular Physics* **2011**, *109*, 839–852, doi:10.1080/00268976.2011.556576.
168. Sung, N.Y.; Kim, M.-Y.; Cho, J.Y. Scutellarein Reduces Inflammatory Responses by Inhibiting Src Kinase Activity. *Korean J Physiol Pharmacol* **2015**, *19*, 441–449, doi:10.4196/kjpp.2015.19.5.441.
169. Hamada, H.; Hiramatsu, M.; Edamatsu, R.; Mori, A. Free Radical Scavenging Action of Baicalein. *Archives of Biochemistry and Biophysics* **1993**, *306*, 261–266, doi:10.1006/abbi.1993.1509.
170. Hong, S.-J.; Kim, K.-J. Scutellaria baicalensis Georgi(SBG) inhibits Melanin Synthesis in Mouse B16 Melanoma Cells. *The Journal of Korean Medicine Ophthalmology and*

Otolaryngology and Dermatology **2009**, *22*, 104–117.
171. Stanojević, M.; Stanojević, Z.; Jovanović, D.; Stojiljković, M. Ultraviolet Radiation and Melanogenesis. *Archive of Oncology* **2004**, *12*, 203–205.
172. D'Mello, S.A.N.; Finlay, G.J.; Baguley, B.C.; Askarian-Amiri, M.E. Signaling Pathways in Melanogenesis. *International Journal of Molecular Sciences* **2016**, *17*, 1144, doi:10.3390/ijms17071144.
173. Smit, N.; Vicanova, J.; Pavel, S. The Hunt for Natural Skin Whitening Agents. *International Journal of Molecular Sciences* **2009**, *10*, 5326–5349, doi:10.3390/ijms10125326.
174. Li, J.; Tian, C.; Xia, Y.; Mutanda, I.; Wang, K.; Wang, Y. Production of Plant-Specific Flavones Baicalein and Scutellarein in an Engineered E. Coli from Available Phenylalanine and Tyrosine. *Metabolic Engineering* **2019**, *52*, 124–133, doi:10.1016/j.ymben.2018.11.008.
175. Shi, X.; Chen, G.; Liu, X.; Qiu, Y.; Yang, S.; Zhang, Y.; Fang, X.; Zhang, C.; Liu, X. Scutellarein Inhibits Cancer Cell Metastasis in Vitro and Attenuates the Development of Fibrosarcoma in Vivo. *International Journal of Molecular Medicine* **2015**, *35*, 31–38, doi:10.3892/ijmm.2014.1997.

Acknowledgment

First of all, I would like to sincerely thank my mentor, Professor Kazuhisa Maeda, for his continuous support and help in my doctoral research. Without his guidance or help when my experiment encounters a bottleneck, this paper may never be completed. I would also like to thank Professor Akio Fujisawa for his careful guidance on the operation of LC–MS, and for giving me many opinions and references when I submitted the paper.

Then I would also like to thank Professor Wanping Zhang from Shanghai Institute of Technology for allowing me to participate in an internship when I was unable to return to Japan due to the Covid-19 epidemic, and to make my knowledge reserve more comprehensive through teaching.

I would also like to thank the members of the Maeda Research Office who have graduated and have not yet graduated. Their kindness and friendship have made a strong mark in my life.

At the same time, I also want to thank my wife Dai Liyun for supporting me like a dawn in my most difficult moments.

Finally, I want to thank my parents for their continuous financial support and encouragement during the process of writing my doctoral dissertation.